REPORT NO.
UCB/EERC-84/20
NOVEMBER 1984

EARTHQUAKE ENGINEERING RESEARCH CENTER

DYNAMIC RESPONSE BEHAVIOR OF QUAN SHUI DAM

by

R. W. CLOUGH
K.-T. CHANG
H.-Q. CHEN
R. M. STEPHEN
Y. GHANAAT
J.-H. QI

Report to the National Science Foundation on
Research conducted under the U.S.-China Protocol for
Scientific and Technical Cooperation in Earthquake Studies

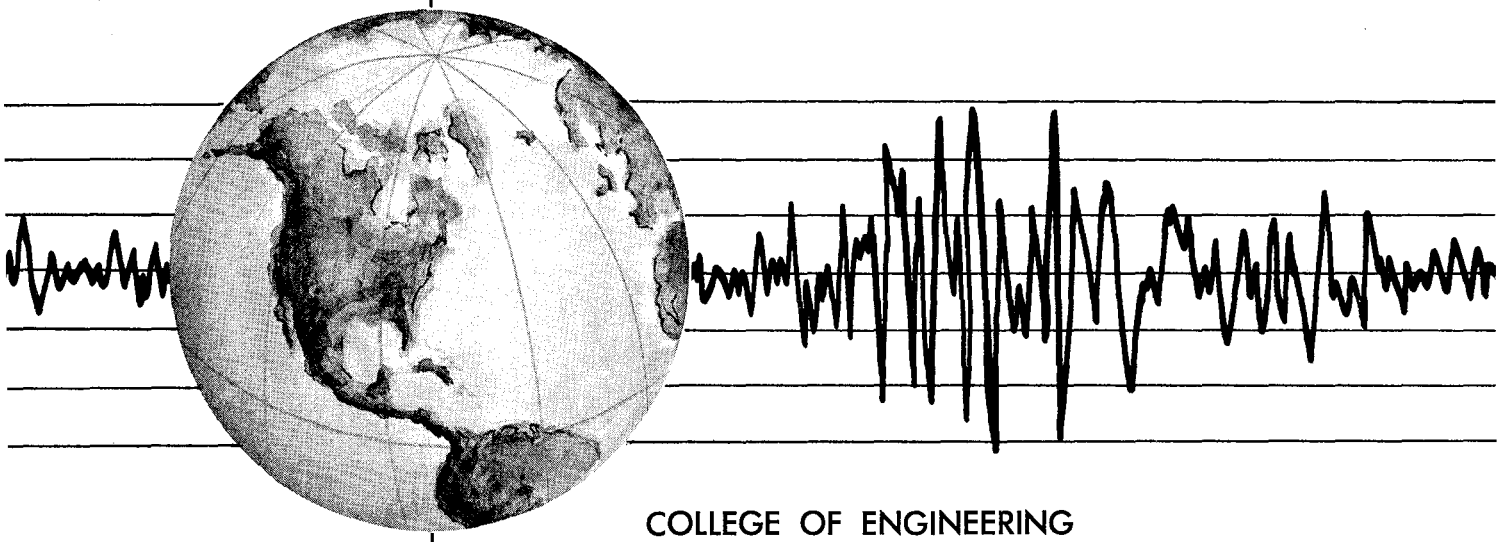

COLLEGE OF ENGINEERING

UNIVERSITY OF CALIFORNIA · Berkeley, California

DISCLAIMER

Any opinions, findings, and conclusions or recommendations expressed in this publication are those of the authors and do not necessarily reflect the view of the National Science Foundation or the Earthquake Engineering Research Center, University of California, Berkeley.

50272-101

REPORT DOCUMENTATION PAGE	1. REPORT NO. NSF/CEE-84028	2.	3. Recipient's Accession No. PB86 115177/AS
4. Title and Subtitle: Dynamic Response Behavior of Quan Shui Dam			5. Report Date: November 1984
			6.
7. Author(s): R. W. Clough, K.-T. Chang, H.-Q. Chen, R. M. Stephen, Y. Ghanaat and J.-H. Qi			8. Performing Organization Rept. No. UCB/EERC-84/20
9. Performing Organization Name and Address: Earthquake Engineering Research Center, University of California, Berkeley, 1301 So. 46th Street, Richmond, Calif. 94804			10. Project/Task/Work Unit No.
			11. Contract(C) or Grant(G) No. (C) (G) CEE-8214198
12. Sponsoring Organization Name and Address: National Science Foundation, 1800 G Street, N.W., Washington, D.C. 20550			13. Type of Report & Period Covered
			14.

15. Supplementary Notes

16. Abstract (Limit: 200 words)

This study of Quan Shui Dam is the second phase of a U.S.-China cooperative project on "Interaction Effects in the Seismic Response of Arch Dams," and was carried out by the Scientific Research Institute of Water Conservancy and Hydroelectric Power and Tsinghua University, Beijing, and the Earthquake Engineering Research Center, University of California, Berkeley.

The same experimental and analytical procedures were used as for the Xiang Hong Dian Dam; the essential difference between the two studies is that Quan Shui Dam is a thin-shell doubly curved arch, whereas the first structure is a single curvature gravity arch. Thus, the interaction effects due to both reservoir and foundation are significantly different in the two cases, as are the basic vibratory properties.

The basic conclusions drawn previously about the mathematical modeling of the interacting system still seem to be valid; the volume of rock and of the reservoir that should be modeled seems to be similar for both types of structures. However, the analytical correlation obtained in the study of Quan Shui Dam is significantly less satisfactory than in the first study and further study is needed to determine the reason for this, preferably considering a thin shell arch not having such solid spillway sections. It is believed that the difference in quality of the results is due mainly to the complexity of the doubly curved dam geometry, particularly to the effect of the gravity spillway sections that are combined with the thin shell system.

17. Document Analysis a. Descriptors

b. Identifiers/Open-Ended Terms

c. COSATI Field/Group

18. Availability Statement: Release Unlimited	19. Security Class (This Report)	21. No. of Pages 130
	20. Security Class (This Page)	22. Price A07

(See ANSI-Z39.18) *See Instructions on Reverse* OPTIONAL FORM 272 (4-77) (Formerly NTIS-35) Department of Commerce

j.a

DYNAMIC RESPONSE BEHAVIOR OF QUAN SHUI DAM

by

Ray W. Clough, K.-T. Chang
Huo-Qun Chen, Roy M. Stephen
Yusof Ghanaat, J.-H. Qi

A Report on Research Conducted under the
U.S.-China Protocol
for Scientific and Technical Cooperation
in Earthquake Engineering

Report No. UCB/EERC-84/20
Earthquake Engineering Research Center
University of California
Berkeley, California

November 1984

ABSTRACT

This study of Quan Shui Dam is the second phase of the cooperative research project on "Interaction Effects in the Seismic Response of Arch Dams". It is a continuation of the work reported previously on the dynamic behavior of Xiang Hong Dian Dam. The entire project is being carried out under the U.S.-China Protocol for Scientific and Technical Cooperation in Earthquake Studies; the cooperating organizations are the Scientific Research Institute of Water Conservancy and Hydroelectric Power and Tsinghua University of Beijing, and the Earthquake Engineering Research Center of the University of California, Berkeley.

The experimental and analytical procedures employed in this study were the same as were used on the first dam; the essential difference between the two studies is that Quan Shui Dam is a thin-shell doubly curved arch, whereas the first test structure (Xiang Hong Dian Dam) is a single curvature gravity arch. Thus, the interaction effects due to both reservoir and foundation are significantly different in the two cases, as are the basic vibratory properties.

The basic conclusions that were drawn previously about the mathematical modeling of the interacting system still seem to be valid; the volume of rock and of the reservoir that should be modeled seems to be similar for both types of structures. However, the analytical correlation obtained in the study of Quan Shui Dam is significantly less satisfactory than was found in the first study. It is believed that the difference in quality of the results is due mainly to the complexity of the doubly curved dam geometry, particularly to the effect of the gravity spillway sections that are combined with the thin shell system. Further study will be needed, preferably considering a thin shell arch not having such solid spillway sections, to determine the reason for the lower quality correlation obtained in the investigation of Quan Shui Dam.

PUBLICATION NOTE

This report is being published simultaneously by the Scientific Research Institute for Water Conservancy and Hydroelectric Power of Beijing (in Chinese) and by the Earthquake Engineering Research Center of the University of California, Berkeley (in English). The report produced by each organization is provided with the standard cover for that organization.

TABLE OF CONTENTS

TABLE OF CONTENTS (Cont'd) Page

LIST OF TABLES

LIST OF TABLES (Cont'd) Page

Table

LIST OF FIGURES

LIST OF FIGURES (Cont'd)

LIST OF FIGURES (Cont'd)

LIST OF FIGURES (Cont'd)

Chapter 1

Introduction

1.1 Background

This report describes the second phase of the cooperative research project entitled "Interaction Effects in the Seismic Response of Arch Dams" administered under the U.S.-China Protocol for Scientific and Technical Cooperation in Earthquake Studies. In the first phase of the study, the vibration behavior of Xiang Hong Dian Dam, a single curvature gravity arch in Anhui Province, was studied analytically and experimentally. The report on that investigation[1] has been published in English by the University of California Earthquake Engineering Research Center (EERC), and the Chinese translation has been published by the Scientific Research Institute of Water Conservancy and Hydroelectric Power (SRIWCHP).

This second phase of the cooperative project involved a similar study of the dynamic properties of Quan Shui Dam, a double curvature, thin shell arch located in Guangdong Province. This second test structure was deliberately chosen because its thin shell geometry was expected to have significantly different vibration behavior than the single curvature thick arch studied first. The basic objectives of the research remained the same, however; to evaluate the influence of interaction of the reservoir and of the foundation rock on the dynamic response of the dam.

In general, the organization of the research effort in this phase was the same as in the first phase, involving the EERC of Berkeley and the SRIWCHP of Beijing as the cooperating institutions, with Vice President K. T. Chang of Tsinghua University and Professor R. W. Clough of the University of California acting as the Principal Investigators. Funding for the EERC part of the research was provided by the U.S. National Science Foundation; that for the SRIWCHP part came from the Ministry of Water Conservancy and Electric

Power of China.

1.2 Method and Scope

The procedures followed in this study were essentially the same as those applied in the investigation of Xiang Hong Dam. Therefore, only brief summaries of the methods are presented in this report; readers are referred to Reference 1 for complete details. In general, the work involved (a) field measurement of the vibration properties, using ambient as well as rotating mass excitation, (b) analysis of vibration properties using finite element models of dam, reservoir and foundation, (c) correlation of the experimental and analytical results, including adjustment of the assumed material properties, and (d) analysis of stresses and deflections expected from static and earthquake loads. This report is divided into four main chapters, one each on these four topics; a final chapter summarizes the principal conclusions drawn from the study up to this point. A final report based on additional analytical studies as well as the results of the two field investigations will present the final conclusions concerning consideration of interaction effects in the dynamic response analysis of arch dams.

1.3 Acknowledgements

As was the case with Xiang Hong Dian Dam, this study of Quan Shui Dam was a large team effort, and the specific contributions of many individuals must be recognized. Again in this study, the field work was done under the direct supervision of Mr. H.-Q. Chen, Vice-Head of Earthquake Engineering at SRIWCHP; he also supervised the reduction of data taken by the SRIWCHP team and preparation of a preliminary report. Also as before, Mr. R. M. Stephen, Principal Development Engineer at the University of California, Berkeley, directed the U.S. part of the field work for Quan Shui Dam as well as the reduction and processing of the U.S. data. The interest and cooperation of Mr. T.-M. Lee, Superintendent of the Quan Shui power plant contributed

greatly to the success of the field work. Mr. G.-L. Wang, working as a Visiting Research Engineer at EERC on leave from the Department of Hydraulic Structures of Tsinghua University, did the preliminary analyses on Quan Shui Dam, and his place on the EERC team was then taken by Mr. J.-H. Qi, on leave from SRIWCHP. Dr. Y. Ghanaat, Consultant to the project, supervised the analytical work and made the necessary program modifications. Finally, Mr. C.-H. Chang, Department of Hydraulic Structures of Tsinghua University made a significant contribution in carrying out a parallel study on foundation interaction, greatly enlarging the scope of this phase of the work.

Chapter 2

Experimental Investigation

2.1 Test Structure

The Quan Shui Dam[2], selected as the test structure for the second phase of this cooperative project, is a thin shell double curvature arch dam, located on the Nan Shui River in Ruyuan County, Guangdong Province as shown in Fig. 2.1. The dam, shown as viewed from downstream in Fig. 2.2, is located in a rather narrow canyon. The maximum height of the dam is 80 m, the crest length is 209 m and the base thickness is 9 m. The extrados is a single centered circular arc, while the intrados is a three-centered circular arc providing gradual thickening of the section toward the abutments; the central angle varies from 80° to 100°. As may be seen in the layout drawings of Fig. 2.3, the dam was constructed in 11 blocks separated by vertical contraction joints. It was completed in 1974, after two years of construction; first filling began in February, 1976, and normal water level was reached in 40 days.

A major structural feature of the dam is the spillway arrangement that may be seen in the photograph, Fig. 2.2; two spillways are provided at each end. Although the layout drawings of Fig. 2.3 do not indicate this fact, the spillway blocks are typical gravity overflow sections that make a drastic increase in stiffness compared with the thin shell stiffness properties. The photograph, Fig. 2.4, shows the overflow section of Block 8 at the left side of the dam; Block 2 near the right abutment was of similar form. The controlling influence of these thick blocks on the vibration mode shapes will be evident in later sections of the report.

As may be seen in the layout drawings and in the photograph the dam was built with four walkways across the downstream face, spaced at about 15 m increments of elevation. These walkways greatly facilitated the measurement

of the dam vibration mode shapes, as described later.

2.2 Test Equipment

Following the same procedures used in the first phase study, the vibration properties of Quan Shui Dam were measured using both ambient and rotating mass shaker excitation. Forced vibration motions of the dam were measured with velocity meters; sensitive Ranger accelerometers were used on the dam for ambient vibration measurements, and on the foundation rock for measuring the forced vibration response. In addition, pressure gages were used to measure the hydrodynamic pressures against the dam face as well as within the reservoir during the forced vibration tests. Because most of the equipment used at Quan Shui Dam has been described in the report on the Xiang Hong Dian Dam study[1], only the general features of the equipment and the significant differences from the previous test will be mentioned here.

2.2.1 Eccentric Mass Shakers

The rotating mass shakers used in this study were the same units used before. They were designed and built by SRIWCHP, have a force capacity of 4000 kg each and a speed range up to 25 Hz. The basic difference in the Quan Shui measurement procedure is that only two shaking units were used; it was concluded that this number would provide sufficient excitation for this relatively flexible thin shell structure. The force output characteristics of each shaker unit is shown in Fig. 2.5.

2.2.2 Measurement Systems

Transducers and recording systems used in the Quan Shui study were essentially the same as are described in the Xiang Hong Dian Dam report[1]. Velocity meters were used to measure the forced vibration response of the dam, and their output was recorded by photorecording oscillographs. Ranger seismometers were used for ambient vibration measurements of the dam and for

measuring foundation rock motions during the forced vibration tests. Output from these seismometers was recorded on magnetic tape by the Kinemetrics Digital Data System. Also recorded by this unit were the signals from the Kistler hydrodynamic pressure gages.

An additional measurement system, not used in the previous study, was provided for the Quan Shui tests by Tsinghua University, under the direction of C.-H. Chang. Transducers used by this group are designated type CD-7, and were coupled with amplifiers GE-5. Details of this supplementary study are presented in Reference [3] and will not be duplicated here. However, it should be noted that this supplementary study served to extend the range of the foundation interaction investigation and some of the results contained in Reference [3] will be mentioned later.

2.2.3 Locations of Shakers and Transducers

During the test, the two rotating mass shakers were positioned on the crest of the dam, oriented to exert their forces in the local radial direction. They were located symmetrically at a distance of 20 m on each side of the nominal centerline of the dam (center of Block 5) as shown in Fig. 2.6.

A total of 44 velocity transducer stations were established on the dam crest and on the four walkways. In general these were located at about the 1/3 and 2/3 span positions in Blocks 3, 4, 6 and 7 and at mid-span of the central Block 5, as shown in Fig. 2.6. Stations at the crest also were established on Blocks 2, 8, 9, and 10, as indicated in this figure.

The Ranger seismometer stations for measuring the interaction of the dam and the foundation rock were located on the foundation rock at the base of the dam face, and at stations 5 to 10 meters downstream from these locations. A few additional stations were established at greater distances from the dam. A total of 22 Ranger seismometer stations were used; locations of these are shown on Fig. 2.7. An additional six rock interaction measurement stations

were established in the river channel by the Tsinghua University supplementary measurement team as shown in Fig. 2.8.

Dynamic water pressures were measured at 29 stations across the face of the dam, and at 12 stations in the reservoir, on a plane normal to the face of the dam as shown in Fig. 2.9. In general, the stations at the face of the dam corresponded in lateral position to the stations of the velocity meters, and they were at a depth of 5, 15, 25, and 35 meters. The stations out in the reservoir were on the vertical plane normal to station 6L, at distances of 10, 20, 30, and 40 meters from the dam face, and at depths of 5, 15, and 25 meters. The pressure gages used in the Xiang Hong Dian study were modified to avoid the problems with water leakage that developed in that study, and an additional gage was obtained. Thus a total of 4 pressure gages was used in this test, and no difficulties were encountered with any of them.

Because there were far more stations for measuring rock acceleration and water pressures than there were Ranger seismometers and pressure gages, it was necessary to repeat the tests several times, moving the transducers from station to station between tests.

2.3 Experimental Procedures and Results

The fundamental dynamic properties of any dam are its vibration frequencies, mode shapes, and damping ratios; also, the most direct indication of the reservoir interaction mechanism is the distribution of water pressures during harmonic excitations. All of these quantities were evaluated for Quan Shui Dam, following the procedures described in the Xiang Hong Dian report[1]. Only the essential details of the procedures are repeated here, together with the results obtained for Quan Shui Dam.

2.3.1 Vibration Frequencies

Ambient vibration measurements were made with the Ranger Seismometers at

13 stations across the crest of the dam and also at stations on the rock adjacent to each end of the dam. In one series of ambient tests, two seismometers located at the centers of Blocks 5 and 7, were wired together so that the sum or the difference of their signals could be recorded. Because of the essentially symmetric location of these stations relative to the dynamic center of the dam, the sum of the signals represents the symmetric vibration response while the difference indicates the antisymmetric response amplitude. Fourier amplitude spectra calculated from the two different types of ambient vibration signals are plotted in Fig. 2.10; frequency peaks representing the first six modal vibration frequencies are indicated on the plots and also are listed in the third column of Table 2.1. For most modes the significant frequency is easily identified; in fact, essentially the same frequency is seen in both the symmetric and the antisymmetric response curves. However, in some cases the designation of the frequency and mode number is rather arbitrary.

Frequency response curves showing the amplitude of response measured at the crest in Blocks 4 and 5 during the harmonic excitation of the dam are presented in Figs. 2.11a and 2.11b; the two shaking machines were operated out-of-phase and in-phase, respectively, to obtain the results shown in these two plots. The frequency peaks shown in these plots are identified with mode numbers and the frequency value; these results also are listed in column 4 of Table 2.1. It is apparent in this table that the vibration frequencies obtained by the ambient and the harmonic excitation techniques are reasonably consistent, but a significant difference is seen for mode 5. As a matter of fact, the ambient vibration frequency curve does not have a strong peak for this mode, so it is not surprising that the frequency is uncertain.

2.3.2 Mode Shapes

Following the procedure used for Xiang Hong Dian Dam, the Quan Shui vibration mode shapes were determined by operating the two shakers at frequencies associated with peak response amplitudes. During the forced vibration tests, six modal frequencies were identified, as indicated in Table 2.1, four produced by symmetrical (in-plane) operation and two by anti-symmetrical (out-of-phase) operation. Slightly different frequencies were used in the mode shape measurements, as shown in column 5 of Table 2.1, because these were found to give peak responses at that time.

The radial displacement amplitudes due to excitation at these frequencies measured at 39 stations on the crest and the walkway levels are listed in Tables 2.2 (a-f) while the corresponding tangential displacements are listed in Tables 2.3 (a-f) and the vertical displacements are given in Tables 2.4 (a-f). Plots of the shapes represented by these data are shown in Figs. 2.12 (a-f). It will be noted that a separate curve is included in each graph for the radial, tangential, and vertical displacement amplitudes, and also that a separate graph depicts the motions at the crest and at each of the walkway levels. A different view of the forced response displacement patterns is presented in Fig. 2.13 (a-f), where each displacement component is plotted on selected vertical sections in the central part of the dam.

Vibration mode shapes at the crest also were derived for Quan Shui Dam from the ambient vibration measurements, following the procedures described in the Xiang Hong Dian report [1]. In summary, the Fourier amplitude at each of the designated frequencies was calculated from the signal measured at each station across the crest. The relative values of these displacement amplitudes then represented the shape of the motion induced at the designated frequencies. Plots of these ambient mode shapes are presented later in comparison with both the forced vibration mode shapes as well as the

analytically predicted vibration mode shapes.

2.3.3 Modal Damping Ratios

Damping ratios were determined from the forced vibration frequency response curves (Figs. 2.11a and 2.11b), using the half-power method as described in the Xiang Hong Dian report[1]. The specific curves used for this purpose are those labeled with the mode number. As was discussed in Reference [1], this procedure for evaluating damping ratios is not entirely valid for structures with more than one degree of freedom, so the results presented in Table 2.5 must be viewed accordingly. Further information on the modal damping ratios is presented in Chapter 4, in connection with the correlation of analytical and experimental results.

2.3.4 Hydrodynamic Pressures

Dynamic water pressures were measured at each of the pressure gage stations shown in Fig. 2.9 while the vibration exciters were operating at each of the selected test frequencies. The measured pressure data are listed in Table 2.6. Plots of these measured values correlated with the analytically predicted pressures are presented in Chapter 4.

2.3.5 Base Rock Displacement Response

Vibration amplitudes were measured by the Ranger seismometers during the rotating mass shaker excitation at each of the stations indicated in Fig. 2.7. In addition, motions were measured by the velocity meters at the PRC stations indicated on this figure. Table 2.7 lists the measured displacement amplitudes obtained at the various stations. Plots of Ranger results are presented in Chapter 4, where they are compared with analytically predicted results; further discussion of the base rock motions is deferred to that chapter.

However, the results obtained by C.-H. Chang[3], shown in Fig. 2.14, are worth mentioning here. This figure shows the reduction of amplitude of the measured response with increasing distance downstream from the dam. Distances of the six measurement stations are indicated on the horizontal axis of the graph, and the amplitude of motion relative to that measured at the base of the dam is shown as the abscissa for the four excitation frequencies which produced the greatest foundation response. It is significant that at a distance of 80 m, equal to the height of the dam, the relative motion is well over 50 percent at all four frequencies; thus it is clear that the assumed foundation model does not include all of the foundation rock that is subjected to interaction. This fact demonstrates what is discussed later in this report: determination of the relative modulus for the foundation rock is influenced by the size of the assumed finite element model. Providing limiting boundaries of the rock requires that the corresponding modulus of elasticity be relatively lower than would be the case if a larger foundation zone were considered.

Chapter 3

Analytical Study

3.1 ADAP Computer Program

The analytical study of Quan Shui Dam was carried out using the same computer program used in the study of Xiang Hong Dian Dam: ADAP (Arch Dam Analysis Program). The element types used in modeling the concrete dam body were the special elements developed for arch dam studies: "thickshell" (THKSHL) and "3D-shell (3DSHEL). The foundation rock was modeled with eight node "brick" elements, and the reservoir was modeled with the sixteen node "3D-shell" elements.

In the analysis, the original program capabilities were employed: static response analysis due to gravity and water load effects, eigenproblem solution to obtain mode shapes and frequencies, and mode superposition dynamic analysis by both response spectrum and time history procedures. In addition, the extended capabilities developed for the Xiang Hong Dian Dam study were used. These include: (1) the finite element incompressible liquid modeling of the reservoir -- reducing its effect to an added mass matrix to be combined with the concrete mass for the nodes at the face of the dam, (2) the steady state forced response analysis, to determine the vibrations induced by the rotating mass shakers at the dam crest, and (3) the hydrodynamic pressures at the dam face induced by the harmonic excitation of the dam. The reservoir interaction program was further modified in the Quan Shui study to increase the number of nodes that could be included in the reservoir model, and to evaluate hydrodynamic pressures at nodes within the reservoir as well as at the dam face.

3.2 Idealization of Quan Shui Dam

3.2.1 Dam Body

The mesh generator capability was used to obtain a basic idealization of the Quan Shui Dam, first defining the "reference surface", a vertical cylinder passing through the upstream edge of the dam crest, and then projecting radially from that surface to locate the nodes on the upstream and downstream faces of this basic thin shell model. Vertical edges of the elements were established to coincide with the vertical monolith contraction joints, except that a node line was established at the center of the central monolith (Block 5) which was substituted for the joints between Blocks 4-5 and Blocks 5-6. Horizontal mesh lines were established at five levels within the dam in addition to the crest.

This basic thin shell model was then supplemented by adding "3D-shell" elements on the downstream faces of Blocks 2 and 8 to provide the thick spillway profile of these blocks. Figure 3.1 shows a perspective view from downstream of the finite element model of the concrete dam body. Exterior surfaces of the elements added to model the spillway sections are shaded to show how this model has been changed from the basic thin shell geometry provided by the mesh generator. Figure 3.2 presents a projection of the upstream face of the dam (viewed from upstream) on the X-Z plane (cross-canyon plane coordinates). The thin shell basic model includes 18 "thickshell" elements in the central body of the dam and 24 "3D-shell" elements in the regions adjacent to the foundation rock. An additional eight "3D-shell" elements were used to model the spillway sections, five in Block 2 and three in Block 8.

3.2.2 Foundation Rock

The foundation mesh generator was used to establish the basic foundation rock model. As described in the Xiang Hong Dian report, this program defines

planes cut into the rock in the direction normal to the dam-rock contact surface at the interface node locations. Figure 3.3 shows the traces of these planes in view from downstream. The locations of the upper two planes generated automatically on each side of the canyon (shown dashed in Figure 3.3) were modified in the finite element mesh used for study of Quan Shui Dam. These planes were rotated up to the solid line locations in the figure so that the true ground surface on both sides of the canyon could be represented while maintaining reasonable element shapes in the rock. As shown, six planes were provided in the foundation rock on each side of the canyon, in addition to the vertical plane at the middle of the canyon.

Boundary nodes of the foundation elements associated with these planes cut into the canyon wall all lie on a semicircle. The horizontal edge of the semicircle coincides with the canyon wall, so the basic assumption of this foundation model is that the canyon has a prismatic form in the upstream-downstream direction. However, the topography of the Quan Shui canyon differed considerably from a simple prism form, and it was considered important to include the major topographic features of the rock in the finite element model. Therefore, an additional layer of surface elements was established, with nodal coordinates taken from the topographic map. Figure 3.4 is an isometric view of the foundation element mesh on the right side of the canyon, with the vertical mid-section shown shaded. The added layer of elements defining the true canyon geometry is clearly visible superposed on the generated elements. The rock beyond the elements in this foundation model was assumed to be rigid, so all the boundary nodes of the foundation block were fixed in position. Of course, the rock on the left side of the canyon was modeled similarly.

3.2.3 Reservoir Model

The reservoir formed behind Quan Shui dam has a sharp bend to the right immediately upstream from the dam, and a fairly accurate representation of this geometry was adopted in the finite element modeling of the reservoir because no information was available on how such topographic effects might influence the reservoir interaction. Figure 3.5 is a topographic map of the canyon immediately upstream from the dam; also shown are the straight line segments adopted to define the finite element approximation of the reservoir boundaries. Nodes of the reservoir elements lay on vertical planes located at distances upstream from the dam face of 30m, 80m, and 160m measured along the river channel (also shown on Fig. 3.5); these nodes correspond with the concrete nodes at the upstream face of the dam. A perspective view of the reservoir element mesh is shown in Fig. 3.6.

For comparison purposes, an additional model of the reservoir was formed using the reservoir mesh generator option. This model was of prismatic form and extended 300m in the upstream direction; the nodes all lay on lines projected upstream from the corresponding nodes on the face of the dam. The upstream end of all reservoir models was assumed to be a rigid face, as was the bottom surface of all cases.

3.2.4 Material Properties

Material properties used in preliminary studies of the dynamic dam behavior were supplied by SRIWCHP, as follows. For the dam concrete, the Young's modulus used in static analysis was $E_s = 2.0 \times 10^6$ T/m^2 (2.84×10^6 psi) and for the preliminary vibration studies the dynamic value was taken to be $E_c = 4.0 \times 10^6$ T/m^2 (5.68×10^6 psi). The modulus of the foundation rock for static analyses and for preliminary vibration analyses was set at $E_c = 4.0 \times 10^6$ T/m^2 (5.68×10^6 psi). Poisson's ratio of both concrete and rock was assumed to be 0.2. The unit weight of the concrete was 2.4 T/m^3

(150 pcf) and this same value was used for foundation rock extending above the basic cylindrical canyon wall (as described in Section 3.2.2) below that surface, the rock was assumed to be massless. Unit weight of the reservoir water was taken to be 1.0 T/m^3 (62.4 pcf) and it was assumed to be incompressible, as mentioned earlier.

3.3 Results of Preliminary Analyses

3.3.1 General Comments

As was done in the Xiang Hong Dian study, a series of preliminary analyses were carried out on the Quan Shui dam and reservoir model in order to establish the basic characteristics of the system. For this purpose, it was assumed that the vibration frequencies would provide a good indicator of the quality of the finite element model, and the frequency analysis was carried out for a variety of model systems. Results of these studies are discussed in the following sections.

3.3.2 Basic Effects of Reservoir and Foundation Interaction

The first series of vibration analyses were done to demonstrate the basic influences of reservoir inertia and foundation flexibility on the frequencies of vibration. First an analysis was made using a foundation modulus of 10^9 T/m^2, and not including any added mass from the reservoir; with this foundation modulus set at 250 times that of the concrete, the foundation system is essentially rigid, so neither foundation nor reservoir interaction was developed in this analysis. Frequencies calculated for the first 8 modes of vibration for this case without interaction are listed in the 2nd column of Table 3.1. In a second analysis, the foundation modulus was taken to be the same as the concrete 4×10^6 T/m^2, but again no reservoir mass was considered. Frequencies calculated for this case are shown in the third column of Table 3.1; as expected the inclusion of foundation flexibility causes a reduction in the vibration frequencies, but the change amounts to no more than 2 or 3 percent for most modes.

The influence of the reservoir was examined in a third analysis, in which the finite element model of Fig. 3.6 was considered with water depth taken to be 74.5m (reservoir level = 444.5m). Results for this case are shown in the fourth column of Table 3.1, and it is clear that the added mass of the water reduces the frequencies considerably, by an average of about 17% in the lower modes. As expected, the reservoir interaction is much more significant for this thin shell dam than it was in the Xiang Hong Dian gravity arch - where the average frequency change due to the reservoir was only 5 percent. The fifth column of Table 3.1 shows the vibration frequencies used in the forced vibration tests; this gives a qualitative comparison with these basic cases. Comments will be made on the correlation of measured and calculated frequencies later.

3.3.3 Effects of Reservoir Geometry

In order to determine how much of the reservoir had to be included in the finite element reservoir model to adequately represent the reservoir interaction, a series of analyses were carried out considering differing lengths of the reservoir. In all cases the surface level of the reservoir remained the same at 444.5m, and the standard foundation and concrete models were used.

Three different reservoir lengths were considered using the actual canyon topography, designated 30m, 80m, and 160m in Fig. 3.5. The first of these models had only two layers of elements in the upstream direction, with nodes located on vertical planes at 15 and 30m from the dam face. The second of these models had a third layer of elements, with nodes on a vertical plane at 80m from the dam face. In the third model the 15m nodal section was omitted, and the upstream nodal plane was located at 160m from the dam face, leading to three layers of elements with nodes at the sections shown in Fig. 3.5.

As mentioned earlier, it was assumed that the upstream face of all these finite element models was a rigid vertical plane. The vibration frequencies for the three cases, listed in columns 2, 3, and 4 of Table 3.2, show that the added mass of the reservoir decreases with increasing length, as expected. In other words, the inertial resistance exerted by the water on the dam face is increased by the proximity of the rigid face at the upstream end of the reservoir because it forces the flow into the lateral and vertical directions.

Two other cases also were considered in this study to determine whether the upstream boundary was far enough removed from the dam. In the first of these, the upstream face was a rigid surface sloping upward at an angle of 45° away from the dam; the river channel intersection of this slope was at the 160m line shown in Fig. 3.5. Results from this analyses (Column 5 of Table 3.2) are almost identical with those from the rigid vertical face (Col. 4), hence it may be concluded that no significant pressure constraint results from the vertical face at this distance. The second added case considered a prismatic reservoir with the dam rock interface geometry projected upstream for a distance of 300m to a vertical rigid plane boundary. Three layers of elements were used in the upstream direction; frequency results for this case (Column 6 of Table 3.2) show only slight differences from those of the model representing the true curved river canyon topography. From this result it may be concluded that there is no need to consider curvature of the river channel in modeling the reservoir; however, the general characteristics of the side wall topography should be simulated.

3.3.4 Effects of Reservoir Depth

It is well known that the reservoir depth directly influences the added mass to be applied at the dam face, so a series of analyses was performed using different water surface levels to determine the depth effect for Quan

Shui dam. Table 3.3 lists the frequencies of the lowest 8 modes of vibration determined for the reservoir with 160m length and with depths ranging from 0 (empty) to 80m (full). It should be noted that these results were obtained considering the foundation rock modulus of elasticity to be half that of the dam concrete; thus these results are not directly comparable with those in Tables 3.1 and 3.2.

The frequency variations with depth represented by the data in Table 3.3 have been plotted in Figures 3.7a and 3.7b to give a graphic view of the reservoir depth effect. It is apparent in this figure that the reservoir has little interaction effect for any mode until it reaches about half the height of the dam; then the frequency is seen to drop rapidly as the water level rises above mid-height. Modes 4 and 8 are somewhat anomalous in that a significant frequency reduction is induced by the water below the mid-height level; on the other hand, Mode 5 shows relatively little frequency change due to the water acting against the upper half of the dam. These peculiarities of specific modes undoubtedly are related to the vibration shapes of those modes; however, no detailed study has been made of this factor. It is worth noting that the reservoir water level varied between 443.6 and 446.0m (i.e., 92% to 95% of full) during the test program. The horizontal lines drawn in Fig. 3.7 at these levels show that small but noticeable frequency changes did result from this effect during the testing of the dam.

Chapter 4

Correlation of Analytical and Experimental Results

4.1 Preliminary Comments

The parametric studies described in Chapter 3 demonstrated that the finite element reservoir model is large enough and of suitable geometric form to adequately represent the reservoir interaction mechanism. No similar study was made of the foundation rock model because the Xiang Hong Dian dam study[1] had demonstrated that the basic foundation mesh gave reasonable results. For the thin shell Quan Shui dam, the mass of the dam is relatively less significant than it was for the previous gravity-arch investigation, so the basic model should be adequate here as well.

However, comparison of the measured vibration frequencies with the calculated results, as shown in Tables 3.1 and 3.2, indicates that further adjustment is needed for the finite element models -- specifically in selecting the moduli of elasticity of the foundation rock and of the dam concrete. The procedure followed in making this selection for Quan Shui dam is the same as that described in the Xiang Hong Dian report[1]: first, correlation of the analytical and measured forced vibration displacements at the rock-dam interface is used as the basis for selecting the modulus ratio of rock to concrete, then the concrete modulus is selected to optimize the correlation of the lower mode frequencies of vibration.

These procedures are described in the following sections of this chapter; then after the material properties have been established the results obtained with the final mathematical model are compared with the measured vibration properties.

4.2 Foundation Rock-Concrete Modulus Ratio

In the preliminary vibration studies described in the preceding chapter, the foundation rock and dam concrete both were given a Young's modulus of

4.0×10^6 T/m^2; thus it was assumed that both materials had the same elastic stiffness. The validity of this assumption was checked by repeating the analyses, using the same finite element idealization but modifying the foundation rock modulus. Ratios of foundation to concrete modulus were taken to be E_f/E_c = 1.5, 0.5, 0.25 and 0.10 in addition to the original E_f/E_c ratio of 1.0.

The influence of the foundation/concrete modulus ratio was studied by plotting the calculated displacements of the rock-concrete interface induced by operation of the shaking machines located on the dam crest. Figures 4.1a through 4.1e show the variation of radial displacements across the base of the dam calculated for modulus ratios of 1.0 and 0.5 with the exciters operating at the nominal frequencies of the first five modes. Also plotted and identified by asterisks at the data points are the corresponding rock displacements measured by the Ranger seismometers during the shaking tests. Figures 4.2a-e similarly show the tangential displacements calculated for the same modulus ratios together with the measured values. Similar plots also were made for the other modulus ratios used in the analyses, but are omitted here for reasons of brevity.

Study of these plots first reveals that the measured and calculated motions at the base of the dam are generally quite similar -- certainly the gross feature of the calculated curves resemble similar features in the measured plots. The principal discrepancies are seen in the vicinity of the spillway blocks, and these regions clearly are difficult to model reliably. As expected, the calculated displacements change nearly in inverse proportion to the assumed modulus of the rock, thus a softer foundation is subjected to greater motions. The relationship between the measured and calculated displacement amplitudes is not constant -- it varies from mode to mode with the measured values at some locations for some frequencies exceeding the calculated values based on either modulus and at other points in other modes

the reverse relationship was found. On the average, however, it was concluded that the calculated results with the modulus ratio $E_f/E_c = 0.5$ gave the best correlation with the measured data, and this ratio was adopted in all subsequent calculations.

It should be emphasized here that the assumed value of rock modulus should be considered together with the assumed size of the foundation zone in the modeling process. A larger volume of rock will give increased displacements for a given modulus of elasticity. Thus it may be recognized that the modulus ratio indicated by this correlation is somewhat low as a consequence of compensating for the finite foundation zone included in the analysis. It also must be remembered that the foundation rock is assumed to have zero mass in this analysis, in order to avoid problems with wave propagation in the foundation; this assumption also tends to lead to a reduced value for the assumed Young's modulus, but it probably is not a significant factor here.

4.3 Young's Modulus of the Concrete

Having established the relative value of the Young's moduli for foundation rock and dam concrete to be 0.5, it was possible to choose the value of the modulus for the concrete to give the best possible correlation between the measured and calculated frequencies of the dam. For this purpose, the Young's modulus of the concrete required to obtain the measured frequency for each mode of vibration was determined by simple proportion from the frequency calculated using $E_f = 2.0 \times 10^6$ T/m^2 and $E_c = 4.0 \times 10^6$ T/m^2, using the formula

$$E_i = 4.0 \times 10^6 \quad (\omega_i{}^M/\omega_i)^2 \tag{4.1}$$

where

E_i = concrete modulus required to obtain the measured frequency for mode "i"

ω_i^M = frequency measured in mode "i"

ω_i = frequency calculated in mode "i" using $E_c = 4.0 \times 10^6$ T/m^2.

The calculations involved in the adjustment of the concrete modulus are presented in Table 4.1. The measured frequencies listed in the second column are those that were determined from the forced vibration frequency response curves as listed in the fourth column of Table 2.1. The calculated frequencies indicated in the third column of Table 4.1 were obtained with the modulus ratio $E_f/E_c = 0.5$ and the reservoir depth of 74.5m, as presented in the third column of Table 3.3. The concrete modulus required to adjust the calculated frequency of column 3 to the measured value of column 2, using Eq. 4.1, is listed in column 4. Because these modulus values change from mode to mode, it is clear that no single concrete modulus will lead to perfect correlation of the experimental and analytical results. For the purpose of this study, it was decided that the average of the first three mode values of column 4 would be most appropriate to use in subsequent calculations. Choosing this value of the concrete modulus and still applying the modulus ratio $E_f/E_c = 0.5$ led to the adjusted modal frequencies ω_i^* listed in the fifth column of Table 4.1, using the following equation:

$$\omega_i^* = \omega_i \sqrt{E_c^*/E_c} \tag{4.2}$$

where $E_c^* = 3.788 \times 10^6$ T/m^2 (avg. of Modes 1- 3 in Table 4.1) and the other terms are as defined earlier. The final result of this frequency correlation effort is presented in Table 4.2, in which the measured frequency for each mode (from Col. 2 of Table 4.1) is presented in column 2, and the adjusted calculated frequency (from Col. 5 of Table 4.1) is listed in column 3. The

percent difference between the calculated and measured results is shown in Column 4. It is evident that the difference is rather large for the two highest modes. However, it must be remembered for these modes that the measured and calculated values may not even apply to the same mode; the mode shapes also are quite different.

4.4 Modal Damping Ratios

Using the established finite element model incorporating the above determined Young's modulus values for concrete and foundation rock, it was possible to calculate the modal damping ratio for the system that best simulated the measured performance. For this purpose, the mathematical model was subjected to forced vibration representing the effect of the rotating mass shakers mounted at the crest of the dam. Adjusting the intensity and frequency of the exciting forces to match those employed in the forced vibration tests, the resulting displacement amplitudes at the crest nodes of the finite element model were calculated based on an assumed modal damping ratio. Then because the response is inversely proportional to the damping ratio, it was a simple matter to determine the damping ratio that provided a peak analytical response to match the measured peak response displacement.

The analytically determined frequency response curves obtained with modal damping ratios established in this way are plotted in Figs. 4.3a-d; also shown on these plots are the experimentally determined frequency response curves, replotted to appropriate scales from Figs. 2.11a,b. The first mode frequency response curves are plotted in Fig. 4.3a. The analytical correlation is excellent because the modulus has been adjusted to match the experimental frequency and the damping ratio has been adjusted to give the experimental amplitude. The significant difference between analysis and experiment is in the value of the damping ratio; a value of

3.5% was found by the half-power method from the experimental curve, while it was necessary to reduce the analytical damping ratio to only 1.3% to obtain the desired response amplitude. The reason for this discrepancy is indicated by the second peak on the analytical response curve at about 4.13 Hz. This shows the contribution of the second mode to the first mode response curve. The test procedure was not sensitive enough to identify the second peak in the response curve, but the second mode led to a broadening of the response curve which was interpreted as increased damping by the half-power method analysis.

The corresponding problem is seen in Fig. 4.3b, where the first mode analytical peak is seen to the left of the second mode peak. Again the half-power method merely recognizes this effect as a broadening of the second mode response curve, indicating correspondingly increased damping. The problem is even worse with the third and fourth modes shown in Fig. 4.3c, because the third mode contribution is so small that no analytical peak is obtained even though a small peak was identified experimentally. Similar behavior is shown for modes 5 and 6 in Fig. 4,3d, where the experimental peaks for mode 5 is not obtained analytically. The significant frequency discrepancy between the analytical and experimental results for these modes casts doubt on the ability of the analytical model to simulate the physical system behavior in these higher modes, so little weight has been given in this study to the analytical performance beyond mode 4.

Based on this discussion, the most reasonable estimates of the modal damping ratios are a combination of values obtained by the half-power method from the experimental data and by analytical adjustment of the forced vibration response amplitude, with the final results as shown in Table 4.2.

4.5 Vibration Mode Shapes

Using the same mathematical model employed in the damping ratio correlation, it was possible to make a variety of comparisons of the calculated vibration mode shapes with those determined experimentally, presented in Figs. 2.12 and 2.13. In principle, the most obvious comparison of the experimental shapes would be with the modal eigenvectors obtained from solution of the undamped eigenproblem associated with the finite element mass and stiffness matrices, and this type of correlation is presented in Fig. 4.4. In this figure, the radial displacements of the dam crest are shown. The solid lines depict the displacements measured during the forced vibration tests at the first four excitation frequencies; these are the same curves shown for elevation 450m in Figs. 2.12a, b, c, and d. The dash-dot lines depict the shapes of the Fourier amplitude obtained at these frequencies from the ambient vibrations measured at the crest, while the dashed lines indicate the crest mode shapes (eigenvectors) determined by solving the undamped eigenproblem.

Comparing the results of the harmonic and the ambient vibration measurements first, it is clear that the shapes of these normalized curves are similar but that they have significant differences; presumably this is due to the different manner of excitation which led to different degrees of interference from the adjacent modes. The calculated eigenvectors show the only pure mode shapes, so the differences in both sets of experimental curves represent contributions from other modes.

It should be remembered that the experimental results were obtained for frequencies that differ somewhat from the calculated (eigenvalue) frequencies, so this factor also contributes to the shape discrepancies shown in Fig. 4.4. A more detailed analytical study of this factor is presented in Figs. 4.5a-e, where the eigenvector shapes are compared with the shapes

calculated from harmonic excitation applied at the crest. These figures give results respectively for the first five test excitation frequencies (in dashed lines) and for the first five eigenvectors (solid lines); the curves depict radial displacements at five levels on the downstream face. These results clearly show that adjacent modes make a significant contribution to the forced vibration shapes at frequencies of 6.85 and 8.83 Hz, which explains why the analytical frequency response curves (Figs. 4.3c and d) do not show any peaks at these frequencies.

The final mode shape correlation is presented in Figs. 4.6a-e, in which the radial vibration shapes measured at the selected excitation frequencies are compared with the forced vibration shapes calculated at these same frequencies. The measured results presented in solid lines are the same as those shown by solid lines in Figs. 2.12a-e; the calculated results shown by dashed lines are the same as those shown by dashed lines in Figs. 4.5a-e. This correlation in Fig. 4.6 gives the best indication of the quality of the mathematical model, because the analysis attempts to fully simulate the conditions of the field vibration measurements. In general it may be concluded from these results that the mathematical model gives a reasonable approximation of the field conditions; however, the discrepancies from the measured results are somewhat disappointing. Clearly this rather complicated structure in a very irregular canyon represents a difficult modeling problem. The major constraint provided by the spillway blocks is apparent at all test frequencies, but it also is evident that the left spillway block was forced to respond significantly at the fifth frequency (Fig. 4.6e).

4.6 Hydrodynamic Pressures

As was mentioned in Chapter 2, the problem encountered with leakage of the pressure gages during the Xiang Hong Dian Dam tests was solved by improving

the waterproofing system, so an extensive measurement program was carried out of the hydrodynamic pressures induced during forced vibration testing of Quan Shui Dam. Then the pressure analysis subroutine of the extended ADAP computer program (described in Reference 1) was used to calculate the pressures generated during the forced vibration tests. The measured and calculated pressures obtained at the five test frequencies are compared here in Figs. 4.7 through 4.11; in each figure, the pressures developed at the face of the dam are shown in sheet "a", and the pressures within the reservoir on a vertical section extending in the radial direction from station 6L on the dam crest are shown in sheet "b". The locations of the pressure measurement stations are shown in Fig. 2.9, as described earlier.

Study of Figs. 4.7 through 4.11 reveals that the calculated and measured hydrodynamic pressures developed at each excitation frequency are of the same order of magnitude, and that the variations across the face of the dam and within the reservoir have similar shapes. However, a very obvious difference in magnitude exists; the measured pressures are found to be consistently higher than the calculated values, at all frequencies. In general, the correlation suggests that the pressures are indeed induced by the accelerations of the dam face in the direction normal to the face, as the analytical theory assumes, but it appears that a scaling discrepancy may exist between the measured and calculated values. This discrepancy could be related to the pressure gage calibration or to the data acquisition and reduction procedure, or it might be related to some scale factor entering the procedure for calculating the forced vibration pressure response. The curious fact about this discrepancy is that it did not appear in the correlation of the pressure data measured on Xiang Hong Dian Dam[1], where excellent correlation was obtained for the relatively few pressure measurements that were made. Obviously, further study must be made of this

question because it suggests that the analytical procedure for representing reservoir interaction may not be adequate.

Chapter 5

Static Load and Earthquake Response Behavior

5.1 General Comments

The ultimate purpose of this research project is to evaluate and make improvements on the mathematical models used to calculate the stresses and deflections induced in arch dams by seismic loads. Therefore it is appropriate to use the mathematical model of Quan Shui dam that has been discussed and developed in the preceding chapters of this report for the analysis of stresses and deflections to be expected in the structure when it is subjected to earthquake excitation. The purpose of the analysis that is described in this chapter is merely to demonstrate the expected behavior of the dam in a qualitative way. It is not intended to account for all static loading effects that might influence the dam -- such as temperature changes or uplift pressures of water acting in the foundation rock or in cracks in the dam, nor has any effort been made to determine the characteristics of the largest earthquake that might occur at this location. For these reasons, the results of these analyses should not be used to judge the safety of the dam; however, it is reassuring to note that there is nothing in these analytical results which suggests the dam is unsafe.

5.2 Static Load Analysis

The mathematical model of Quan Shui Dam that has been formulated in this study is equally suitable for analysis of response to static or to dynamic loads; it is necessary only to utilize the appropriate dynamic or static modulus of elasticity of the materials. In the present analysis it has been assumed that the static modulus of elasticity is half of the dynamic value, and the stresses and deflections resulting from the two types of static load (gravity acting on the concrete mass and hydrostatic pressures acting on the

face of the dam) have been calculated by the standard ADAP static analysis procedure.

The deflections caused by these static loads are shown in Fig. 5.1; the displacements in the horizontal (x-y) plane of points on the crest are shown in sketch "a", while the displacements in the vertical (y-z) plane of points on the mid-section (crown cantilever) are indicated in sketch "b". In each sketch the displacements due to gravity alone are shown by the dashed line, while the combined effect of gravity and the hydrostatic pressure is indicated by the solid line. These results clearly show the significant downstream thrust caused by the water load; the reservoir depth was assumed to be 74.5m (elev. - 444.5) in these calculations, the same as it was during the field test program. Also it is clear that the spillway blocks cause a major constraint to the downstream movement. The stresses due to these static loads will be discussed later together with the results of the earthquake response analysis.

5.3 Combined Static and Earthquake Response

As was the case in the study of Xiang Hong Dian Dam[1], there are no records of earthquakes that have occurred in the vicinity of Quan Shui Dam. Consequently, it was decided to use the same earthquake input in this study as was used in Reference 1 -- the earthquake record obtained at Hsin Feng Jiang dam in Kwangdong Province multiplied by a factor of 5 to obtain a peak acceleration of 0.225g. The acceleration history of this amplified earthquake record is shown in Fig. 5.2, together with the velocity and displacement history obtained by integration of the acceleration record. The response spectrum of this ground motion is included in Reference 1, but it is not presented here because only time-history analyses were carried out in this case.

As was done in Reference 1, a step-by-step analysis of the response of Quan Shui dam to this earthquake applied in the upstream-downstream was carried out for the first six modes of vibration, using a time step of 0.01 sec. and 2 percent critical damping in each mode (which is reasonably representative of the measured values). The calculated upstream-downstream displacement response at the crest of the dam mid-section is shown in Fig. 5.3. The fundamental mode period of about 1/4 second is clearly evident in this response, but significant higher mode effects also are present. Figure 5.4a shows the corresponding maximum variation of arch stress on the upstream face near the mid-section crest, while Fig. 5.4b shows the maximum cantilever stress component calculated at point "x" in Figs. 5.6(b and d). Of particular interest in these figures is the fact that the arch stresses relate closely to the fundamental mode response -- similarly to the displacement history. On the other hand, the cantilever stress variation shows a dominant frequency of about 11.5 Hz, which is associated with the short thin shell section to the right of the right spillway block.

Before the practical significance of this dynamic response analysis can be established, it must be combined with the results due to the static loads. Of course, the static stresses and displacements are acting continuously, so these dynamic results must be added or subtracted from the static values according to the history of the dynamic response. To illustrate the combination of stresses, Tables 5.1 and 5.2 have been prepared, considering four instants of time when maximum dynamic stress components were developed, and combining these dynamic stresses with the static stresses. Tables 5.1a and b show the arch stresses at vertical sections A-A and B-B, respectively, at times $t = 0.89$ and $t = 1.03$ seconds, when the highest arch stresses reached their positive and negative peaks. Similarly, Tables 5.2a and b show the cantilever stresses at the same sections, at times $t = 0.90$ and $t = 0.94$ when the cantilever stresses became maximum.

Study of these tables clearly shows that the static stresses dominate the arch action in the central part of the dam. Tensile arch stresses are found only near the crest of the dam and they have relatively small values, well within the expected tensile strength of the concrete. The cantilever stresses also are dominated by the static effects, and they are even smaller than the arch stress values.

A more comprehensive view of the stress state induced by the static and dynamic loads is presented in Figs. 5.5 and 5.6 by means of stress contours. The distributions of the arch stress component at the two instants of peak arch stress are presented in Figs. 5.5a through d. Stress contours at time t = 0.89 sec.are shown in Figs. 5.5a and b for the upstream and downstream faces, respectively, while the corresponding results at time t = 1.03 secs. are shown in Figs. 5.5c and d. It is interesting to note in these figures that tensile stresses due to the combined static plus seismic loads are developed only on the downstream face and only in small zones near the top and base of the central part of the dam. The maximum tensile arch stresses of about 15-20 kg/cm^2 are well within the expected capacity of the concrete.

Figures 5.6a through d similarly portray the distribution of the cantilever stress components at the two instants of time when the peak values are developed. The stress contours at time t = 0.90 sec. are shown in Figs. 5.6a and b for the upstream and downstream faces, respectively; similarly Figs. 5.6c and d show the corresponding results at time t = 0.94 sec. It should be noted that the dynamic stresses on the downstream face changed from maximum tension to maximum compression during the 0.04 second interval between these two sets of figures, reflecting the high frequency of the modal response associated with these peak stresses. However, it is apparent in Table 5.2 that the static load is the dominant factor in producing

tensile stress on the downstream face; the additional tension due to the earthquake is relatively unimportant. Also, the combined static plus dynamic stress is within the tensile capacity of the concrete.

Chapter 6

Summary and Conclusions

6.1 Summary

This study of Quan Shiu Dam is the second phase of the cooperative research project on "Introduction Effects in the Seismic Response of Arch Dams" being carried out under the U.S.-China Protocol for Scientific and Technical Cooperation in Earthquake Studies. The principal objective of this second phase was to correlate the analytically predicted vibratory properties of a thin shell doubly curved arch dam with the properties measured in the field using a rotating mass shaking system. The basic difference from the phase one study was in the type of arch dam considered; the gravity arch structure studied first is much more massive and thus interacts differently with the reservoir and foundation than does this thin shell system.

One of the first facts discovered in this study is that the Quan Shui Dam is not truly a thin shell structure. The massive spillway sections located at each end of the curved arch structure have a major influence on the static and dynamic behavior of the dam. The vibratory properties of this dam involve a combination of thin shell and gravity section deformations; this fact complicates both the analytical and experimental evaluation of the properties. The result is that the agreement between analysis and experiment is much less satisfactory than it was with Xiang Hong Dian Dam, the simple curved gravity structure tested in the first phase of the study. Because of the relatively poor agreement obtained here between analysis and experiment, it is difficult to draw conclusions on the mathematical modeling procedures. However, a few observations are made in the next section concerning the Quan Shui test results. In addition, a summary of the findings from both experimental studies will be presented in the phase 3 final report on this research

program.

6.2 Conclusions from the Quan Shui Study

(1) It appears that a relatively coarse mesh model of the concrete dam can simulate the dynamic behavior of the structure, and that the spillway blocks can be modeled effectively by adding solid elements on the downstream face of the thin shell structure created by the mesh generator program.

(2) The foundation interaction associated with the spillway blocks is quite different from that associated with the thin shell structure. It appears that a more refined foundation model will be required to simulate this interaction mechanism.

(3) The finite element reservoir model can effectively represent the river canyon topography, but it appears that there is no need to simulate the topography at upstream distances greater than the dam height; an idealized prismatic channel extending in a straight line three times the dam height is adequate.

(4) Pressure transducers again were found to provide an effective means to study reservoir interaction, at distances as great as 40m from the dam face. However, the significantly greater value of the measured pressures as compared with the calculated values requires further study. It is not clear whether the discrepancy is due to an erroneous assumption in the analysis (such as the assumed incompressibility, perhaps) or to some type of experimental error (perhaps in calibration).

(5) These analytical results clearly show that Quan Shui Dam is not very sensitive to the type of earthquake motion considered in this study; the static stresses significantly exceed the dynamic component. However, that static tensile stresses on the downstream face seem higher than is usual, and it is assumed that this is a consequence of the constraint

imposed by the spillway blocks. Clearly, this complicated "hybrid" type of structure requires special care in selecting its shape in order to obtain optimum performance.

References

1. "Dynamic Response Behavior of Xiang Hong Dian Dam" by R. W. Clough, K. T. Chang, H.-Q. Chen, R. M. Stephen, G.-L. Wang and Y. Ghanaat, University of California Earthquake Engineering Research Center Report No. UCB/EERC-84/02, April 1984.

2. "Analysis and Observation Data of Quanshui Arch Dam and Estimation of its Strength Safety Factor", by H.-N. Chu, W.-Y. Yu, Z.-B. Huang, W.-Y. Chen and R.-X. Liu. Proceedings, 13th Congress on Large Dams, New Delhi, India, 1979, pp. 509-526.

3. "Field Measurement and Analysis on Dynamic Behavior of Quanshui Arch Dam" by C.-H. Chang and W.-X. Li, Tsinghua University, Beijing, May 1984.

Table 2.1 Measured Vibration Frequencies

Mode	Type*	Ambient Excit.	Harmonic Excit.	Mode Shape Test Frequency
1	AS	3.95	3.85	3.96
2	S	4.0	4.10	4.30
3	S	6.90	6.80	6.85
4	S	7.52	7.60	7.75
5	AS	8.20	8.80	8.83
6	S	9.29	9.05	9.25

*Symmetry or Anti Symmetry as indicated by mode of recording (ambient) or mode of excitation (shakers).

Table 2.2 Forced Vibration Radial Displacement

(a) Antisymmetric Excitation at 3.96 Hz

Exciting Force = 627.3 Kg											
Elevation (M)	Displacements (m x 10^{-6}) Block Number										
	3	3'	4	4'	5	6	6'	7	7'	9	10
450.0	18.82	33.51	45.21	44.52	4.64	-40.36	-32.55	-21.52	-42.03		
434.5	11.35	20.59	35.70	31.67	8.25	33.50	-25.70	-18.50	-26.95		
419.5	6.00	10.34	17.06	18.25	3.93	-18.34	-10.01	-6.35	-12.29		
404.5	-1.00	-0.38	5.01	5.23	1.87	-6.22	-5.45				
392.0			1.23	1.69	0.55	-1.28	-1.57				

(b) Symmetric Excitation at 4.30 Hz

Exciting Force = 739.6 Kg											
Elevation (M)	Displacements (m x 10^{-6}) Block Number (Radial)										
	3	3'	4	4'	5	6	6'	7	7'	9	10
450.0	-1.57	-0.90	4.51	11.30	10.78	0.77	15.06	-0.36	3.67		
434.5	-1.24	-0.72	2.62	8.00	12.85	7.15	10.78	-0.27	1.71		
419.5	-0.63	-0.74	1.08	3.68	6.93	3.51	5.98	0.58	0.56		
404.5	0.19	0.11	0.31	2.25	2.90	1.13	2.12				
392.0			0.05	0.39	0.90	0.08	0.61				

Table 2.2 Forced Vibration Radial Displacement (Cont'd)

(c) Symmetric Excitation at 6.85 Hz

Exciting Force = 1876.9 Kg											
Elevation (M)	Displacements ($m \times 10^{-6}$) Block Number (Radial)										
	3	3'	4	4'	5	6	6'	7	7'	9	10
450.0	3.00	5.66	7.88	6.88	2.13	8.05	6.90	4.81	6.34		
434.5	1.27	1.79	1.82	0.38	-2.85	1.19	-0.94	1.80	2.27		
419.5	-0.35	-1.02	-0.80	-2.17	-3.87	-1.91	-2.79	-0.39	-1.02		
404.5	-0.09	-0.07	-0.39	-0.77	-0.19	-0.94	-1.43				
392.0			-0.13	-0.37	-0.59	-0.06	-0.35				

(d) Symmetric Excitation at 7.75 Hz

Exciting Force = 2402.5 Kg											
Elevation (M)	Displacements ($m \times 10^{-6}$) Block Number (Radial)										
	3	3'	4	4'	5	6	6'	7	7'	9	10
450.0	20.84	44.64	51.13	46.25	14.13	51.27	39.08	42.26	58.69		
434.5	9.59	17.95	21.60	13.00	-7.50	16.00	3.69	17.35	23.95		
419.5	0.10	4.98	2.94	-7.18	-23.50	5.22	-11.17	3.52	4.34		
404.5	1.14	0.34	0.89	-3.45	-12.35	-3.19	-8.63				
392.0			-0.16	-1.48	-3.71	-0.60	-2.87				

Table 2.2 Forced Vibration Radial Displacement (Cont'd)

(e) Antisymmetric Excitation at 8.83 Hz

Exciting Force = 3118.8 Kg											
Elevation (M)	Displacements ($m \times 10^{-6}$) Block Number										
	3	3'	4	4'	5	6	6'	7	7'	9	10
450.0	8.93	22.03	28.75	29.38	3.36	-28.74	-24.72	-8.22	-22.89		
434.5	-2.54	-3.54	-4.95	-5.17	0.83	5.35	5.15	1.89	1.95		
419.5	-4.46	-7.61	-10.36	-10.36	1.45	8.93	7.68	3.84	6.52		
404.5	0.80	-0.42	-4.97	-5.36	-0.84	6.14	6.38				
392.0			-1.53	-1.88	-0.12	1.74	2.55				

(f) Symmetric Excitation at 9.25 Hz

Exciting Force = 3422.5 Kg											
Elevation (M)	Displacements ($m \times 10^{-6}$) Block Number (Radial)										
	3	3'	4	4'	5	6	6'	7	7'	9	10
450.0	11.67	15.72	8.13	7.19	4.27	5.75	6.90	12.91	6.16		
434.5	3.93	5.20	4.10	-3.74	-2.85	4.84	4.30	3.75	3.25		
419.5	1.18	1.34	-1.23	-4.12	-5.48	2.71	-2.00	0.64	1.51		
404.5	-0.84	-0.29	-0.83	-1.71	-3.36	0.92	-1.64				
392.0			-0.12	-0.63	-1.07	0.40	0.69				

Table 2.3 Forced Vibration Tangential Displacement

(a) Antisymmetric Excitation at 3.96 Hz

Exciting Force = 627.3 Kg											
Elevation (M)	Displacements (m x 10^{-6}) Block Number										
	3	3'	4	4'	5	6	6'	7	7'	9	10
450.0	2.36	4.33	6.63	7.88	9.47	10.73	9.34	4.51	4.96		
434.5	-2.52	-2.42	1.04	9.46	15.72	6.74	12.56	-2.15	-0.73		
419.5	-2.37	-2.60	0.37	4.79	8.54	3.31	6.22	-2.01	-10.65		
404.5			0.14	0.93	3.95	0.92	1.62				
392.0			-0.24	0.50	1.15	-0.17	0.60				

(b) Symmetric Excitation at 4.30 Hz

Exciting Force = 739.6 Kg											
Elevation (M)	Displacements (m x 10^{-6}) Block Number										
	3	3'	4	4'	5	6	6'	7	7'	9	10
450.0	-2.00	-2.46	-1.70	-1.73	-1.50	0.22	0.76	1.76	2.03		
434.5	-0.67	-0.76	-3.11	-2.78	-1.28	2.32	1.80	1.53	2.63		
419.5	-0.56	-1.05	-1.70	-1.76	-0.74	1.58	1.52	0.90	1.37		
404.5			-0.55	-0.69	-0.33	0.74	0.65				
392.0			-0.34	-0.35	-0.12	0.34	0.39				

Table 2.3 Forced Vibration Tangential Displacement (Cont'd)

(c) Symmetric Excitation at 6.85 Hz

Exciting Force =											
Elevation (M)	Displacements (m x 10^{-6}) Block Number										
	3	3'	4	4'	5	6	6'	7	7'	9	10
450.0	-0.48	-0.45	0.60	0.34	-0.25	-0.10	-0.28	0.28	-0.37		
434.5	-0.29	-0.11	0.53	0.99	0.37	-0.67	-0.98	0.41	0.19		
419.5	0.20	0.43	0.68	0.78	0.25	-0.67	-0.75	-0.19	-0.38		
404.5			0.36	0.43	0.27	-0.45	-0.43				
392.0			0.20	0.22	0.08	-0.23	-0.26				

(d) Symmetric Excitation at 7.75 Hz

Exciting Force = 2402.5 Kg											
Elevation (M)	Displacements (m x 10^{-6}) Block Number										
	3	3'	4	4'	5	6	6'	7	7'	9	10
450.0	0.59	2.43	3.08	0.68	0.36	-7.47	-1.96	-3.24	-0.73		
434.5	-3.79	-3.50	0.80	5.49	1.84	-5.18	-5.21	4.50	1.32		
419.5	-1.27	0.90	2.44	5.16	1.98	-4.65	-5.11	0.83	-1.31		
404.5			1.85	2.72	1.40	-2.69	-2.43				
392.0			0.93	0.39	0.66	1.31	1.40				

Table 2.3 Forced Vibration Tangential Displacement (Cont'd)

(e) Symmetric Excitation at 8.83 Hz

Exciting Force = 3118.8 Kg											
Elevation (M)	Displacements (m x 10^{-6}) Block Number										
	3	3'	4	4'	5	6	6'	7	7'	9	10
450.0	-1.93	-1.67	-1.17	-1.47	-1.87	-1.62	-1.26	-1.93	-2.48		
434.5	-1.76	-2.45	-2.86	-2.33	-1.31	-2.49	-1.49	-2.24	-4.41		
419.5	1.66	1.48	-0.25	-3.20	-5.24	-2.03	-3.44	0.82	0.18		
404.5			-0.09	-0.89	-4.26	-0.48	-1.43				
392.0			0.31	-0.69	-1.40	-0.55	0.65				

(f) Symmetric Excitation at 9.25 Hz

Exciting Force = 3422.5 Kg											
Elevation (M)	Displacements (m x 10^{-6}) Block Number										
	3	3'	4	4'	5	6	6'	7	7'	9	10
450.0	-1.05	1.70	1.37	1.08	-1.15	-1.05	-0.90	2.54	1.85		
434.5	-0.71	0.66	1.92	1.75	-0.47	1.16	-0.67	1.28	1.93		
419.5	-1.28	0.40	1.42	1.14	-0.90	-0.90	-1.50	0.51	0.59		
404.5			0.58	0.71	-0.58	-0.71	-0.98				
392.0			0.29	0.32	-0.15	-0.32	-0.46				

Table 2.4 Forced Vibration Vertical Displacement Response

(a) Antisymmetric Excitation at 3.96 Hz

Exciting Force = 627.3 Kg											
Elevation (M)	Displacements (m x 10^{-6}) Block Number										
	3	3'	4	4'	5	6	6'	7	7'	9	10
450.0	-1.22	0.89	8.97	2.90	0.79	0.10	-0.22	1.86	0.45		
434.5	1.89	0.70	0.27	2.64	0.72	-1.68	-1.23	-0.76	-1.25		
419.5	0.46	0.57	1.00	1.15	0.26	-1.16	-0.04	-0.86	-1.27		
404.5			0.17	0.60	0.08	-0.32	-0.09				
392.0			0.12	0.10	-0.09	-0.13	-0.06				

(b) Symmetric Excitation at 4.30 Hz

Exciting Force = 739.6 Kg											
Elevation (M)	Displacements (m x 10^{-6}) Block Number										
	3	3'	4	4'	5	6	6'	7	7'	9	10
450.0	-0.06	-0.27	-2.56	0.41	0.95	0.15	0.14	-0.28	-0.31		
434.5	0.13	0.14	0.21	0.78	0.87	0.55	0.61	-0.17	0.17		
419.5	-0.19	-0.11	0.05	0.15	0.44	0.18	0.08	0.03	-0.06		
404.5			-0.12	-0.05	0.01	-0.04	-0.08				
392.0			-0.07	-0.09	0.16	-0.13	-0.13				

Table 2.4 Forced Vibration Vertical Displacement Response

(c) Symmetric Excitation at 6.85 Hz

Exciting Force = 1876.9 Kg											
Elevation (M)	Displacements ($m \times 10^{-6}$) Block Number										
	3	3'	4	4'	5	6	6'	7	7'	9	10
450.0	0.16	0.44	0.65	1.02	0.95	0.58	0.69	0.19	0.51		
434.5	0.38	0.56	0.92	1.15	1.32	1.00	0.99	0.41	0.63		
419.5	0.11	0.10	0.08	0.22	-0.46	0.10	0.26	0.08	0.10		
404.5			-0.13	-0.26	-0.38	-0.09	-0.26				
392.0			-0.08	-0.12	-0.08	-0.04	-0.11				

(d) Symmetric Excitation at 7.75 Hz

Exciting Force = 2402.5 Kg											
Elevation (M)	Displacements ($m \times 10^{-6}$) Block Number										
	3	3'	4	4'	5	6	6'	7	7'	9	10
450.0	-0.50	2.88	3.66	4.74	2.35	1.82	1.72	-2.00	1.76		
434.5	2.39	3.33	4.87	6.70	5.66	5.38	4.63	2.94	4.60		
419.5	1.10	1.36	1.14	0.62	-1.41	0.38	0.17	0.87	1.21		
404.5			-0.64	-1.59	-2.79	-0.30	-1.94				
392.0			-0.43	-0.90	-0.86	-0.49	-1.09				

Table 2.4 Forced Vibration Vertical Displacement Response

(e) Antisymmetric Excitation at 8.83 Hz

Exciting Force = 3118.8 Kg											
Elevation (M)	Displacements ($m \times 10^{-6}$) Block Number										
	3	3'	4	4'	5	6	6'	7	7'	9	10
450.0	0.51	1.21	-1.45	2.88	0.74	-0.97	-0.68	-0.30	-0.97		
434.5	1.25	2.24	3.78	4.38	0.97	-3.35	-2.21	-1.02	-2.41		
419.5		-0.35	-0.46	-0.35	0.06	0.33	0.58	0.46	0.59		
404.5			-1.21	-1.67	-0.30	0.72	0.80				
392.0			-0.76	-0.82	0.015	0.81	0.65				

(f) Symmetric Excitation at 9.25 Hz

Exciting Force = 3422.5 Kg											
Elevation (M)	Displacements ($m \times 10^{-6}$) Block Number										
	3	3'	4	4'	5	6	6'	7	7'	9	10
450.0	-0.80	0.05	1.76	1.11	1.00	0.98	0.76	1.96	1.16		
434.5	0.52	0.79	0.91	1.72	1.67	1.01	0.99	0.42	0.57		
419.5	0.21	0.29	0.63	0.89	0.73	0.74	0.46	0.50	0.67		
404.5			-0.51	-0.85	-0.86	0.23	-0.15				
392.0			-0.25	-0.44	-0.23	-0.17	-1.07				

Table 2.5 Modal Damping Ratios

(Derived from Figs. 2.11a,b by the half-power method)

Mode	Frequency	Damping Ratio
1	3.85	3.5%
2	4.10	3.9%
3	6.80	2.7%
4	7.60	2.4%
5	8.80	1.3%
6	9.05	4.3%

Table 2.6 Hydrodynamic Pressures during Forced Vibration Response

(a) Pressures on Dam Face ($T/m^2 \times 10^{-2}$)

Freq. (Hz)	Depth (M)	Location across Dam Face (Fig. 2.9)								
		Block 7R	Block 7L	Block 6R	Block 6L	Block 5	Block 4R	Block 4L	Block 3R	Block 3L
3.96	5	0.942			1.371	0.429	1.374	1.224	1.169	0.788
	15	1.222	1.737		1.575	0.544	1.822	1.838	1.522	1.550
	25	1.363	1.772		1.413	0.413	1.808	1.556		
	35	1.483	1.405		1.010					
4.30	5	0.142	0.284	0.616	0.801	0.955			0.360	
	15		0.462	0.937	1.259	0.987			0.458	
	25		0.638	0.570	0.839	0.963				
	35		0.452	0.765	1.580					
6.85	5	0.328	0.396	0.412	0.212	0.405	0.509	0.600	0.311	
	15	0.422	0.337	0.665	0.660	0.875		1.027		0.533
	25	0.475	0.591	0.759	1.167	0.979	1.117	1.240		
	35	0.626	0.551	1.032	1.160					
7.75	5	3.488	4.350	3.386	1.132	1.033	2.290	3.445	3.416	2.075
	15	3.132	3.048	0.896	2.359	4.713	1.431	2.205	2.831	
	25	2.054	1.440	2.313	4.897	6.884	1.772	0.636		
	35	1.386	0.812	2.694	4.682					
8.83	5	0.965	0.505	1.288	1.257	0.554	1.613	1.001	0.928	0.835
	15	3.101	2.603	2.463	1.566	0.609	3.023	3.831	3.213	3.031
	25	5.16	5.078	5.410	4.193	0.609	4.529	4.830		
	35	6.10	5.883	5.760	4.555					
9.25	5		0.870	1.363	1.150	0.896			1.361	1.258
	15		0.788	1.392	0.962	1.489			1.206	1.202
	25	0.664	0.958	1.144	1.011	2.159				
	35		1.163	1.044	0.967					

Table 2.6 Hydrodynamic Pressures during Forced Vibration Response Cont'd

(b) Pressures in Reservoir on Radial Section 6L ($T/m^2 \times 10^{-2}$)

Freq. (Hz)	Depth (M)	10m	20m	30m	40m
	5	0.359			
3.96	15	0.841	0.539		
	25	1.571	1.268	0.238	
	5	0.198			
4.30	15	0.473	0.477	0.119	
	25	0.650	0.914	0.225	
	5				
6.85	15	0.363		0.244	
	25	0.449		0.290	
	5	0.299	0.411		0.385
7.75	15	1.742	1.299		0.608
	25	1.280	1.485	1.380	0.859
	5		0.279		
8.83	15	1.088	0.795	0.433	0.308
	25	0.559	0.723	0.902	0.413
	5				
9.25	15		0.274	0.368	
	25	1.099	0.892	0.232	

Table 2.7 Forced Vibration Displacements of the Foundation Rock

(a) Radial Motions ($m \times 10^{-6}$)

Survey Station		Frequency (Hz)											
		3.96		4.28		6.85		7.75		8.83		9.25	
U.C.	P.R.C.	U.C.	P.R.C.	U.C.	P.R.C.	U.C.	P.R.C.	U.C.	P.R.C.	U.C.	P.R.C.	U.C.	P.R.C.
1	C	0.102	0.077	0.036	0.021	0.015	0.004	0.097	0.101	0.110	0.104	0.079	0.096
2	Q	0.113	0.097	0.056	0.029	0.037	0.017	0.193	0.182	0.234	0.156	0.306	0.288
3	E	0.394	0.296	0.108	0.060	0.194	0.030	0.796	0.747	0.496	0.460	1.125	1.034
4		1.117		0.020		0.075		1.291		1.310		1.000	
5	P_R''	0.379	0.635	0.034	0.220	0.026	0.085	0.348	1.140	0.542	0.120	0.205	0.410
6	O	0.296	0.081	0.109	0.021	0.032	0.162	0.337	0.446	0.348	0.490	0.043	0.118
8	I	0.208	0.098	0.034	0.038	0.009	0.017	0.100	0.082	0.296	0.093	0.035	0.017
8'	H	0.107	0.051	0.055	0.024	0.018	0.022	0.226	0.031	0.288	0.093	0.092	0.023
7'		0.137		0.048		0.018		0.150		0.303		0.074	
6'	P	0.217	0.090	0.064	0.063	0.028	0.023	0.184	0.141	0.443	0.148	0.166	0.089
5'	P_L''	0.451		0.123		0.069		0.406		0.448		0.296	
5''		0.0261		0.142		0.021		0.063		0.182		0.131	
1'	B	0.0661	0.069	0.041	0.028	0.017	0.012	0.105	0.127	0.064	0.086	0.067	0.089

Table 2.7 Forced Vibration Displacements of the Foundation Rock (Cont'd)

(b) Tangential Motions ($m \times 10^{-6}$)

Survey Station		Frequency (Hz)											
		3.96		4.28		6.85		7.75		8.83		9.25	
U.C.	P.R.C.	U.C.	P.R.C.	U.C.	P.R.C.	U.C.	P.R.C.	U.C.	P.R.C.	U.C.	P.R.C.	U.C.	P.R.C.
1	C	0.085	0.062	0.238	0.131	0.033	0.005	0.148	0.102	0.141	0.124	0.071	0.023
2	Q	0.099	0.072	0.289	0.226	0.086	0.033	0.176	0.150	0.331	0.199	0.083	0.026
3	E	0.325	0.245	0.516	0.207	0.085	0.022	1.204	0.362	0.160	0.069	1.283	0.443
4		0.719		0.241		0.068		1.441		0.327		0.829	
5	P_R''	0.342	0.635	0.129	0.220	0.017	0.085	0.515	1.140	0.463	0.120	0.134	0.410
6	O	0.692	0.053	0.300	0.178	0.048	0.062	0.817	0.256	1.813	0.064	0.282	0.081
8	I	0.133	0.050	0.119	0.101	0.022	0.039	0.282	0.206	0.472	0.055	0.109	0.038
8'	H		0.062	0.044	0.038	0.008	0.025	0.010	0.107	0.271	0.017	0.046	0.024
7'				0.106		0.047		0.206		0.397		0.058	
6'	P		0.154	0.153	0.095	0.069	0.137	0.155	0.080	0.619	0.019	0.040	0.036
5'	P_L''		0.545	0.147	0.110	0.085	0.095	0.518	0.554	0.260	0.325	0.264	0.310
5''		0.290		0.237		0.037		0.427		0.170		0.264	
1'	B		0.105	0.150	0.147	0.026	0.016	0.125	0.147	0.081	0.078	0.065	0.085

Table 2.7 Forced Vibration Displacements of the Foundation Rock (Cont'd)

(c) Vertical Motions ($m \times 10^{-6}$)

Survey Station		Frequency (Hz)											
		3.96		4.28		6.85		7.75		8.83		9.25	
U.C.	P.R.C.	U.C.	P.R.C.	U.C.	P.R.C.	U.C.	P.R.C.	U.C.	P.R.C.	U.C.	P.R.C.	U.C.	P.R.C.
1	C		0.002		0.000		0.002		0.004		0.003		0.003
2	Q		0.009		0.064		0.183		0.497		0.315		0.488
3	E		0.032		0.015		0.027		0.247		0.037		0.209
4													
5	P_R''		0.400		0.090		0.080		0.910		0.340		0.490
6	O		0.050		0.027		0.020		0.250		0.135		0.072
8	I		0.070		0.065		0.006		0.067		0.048		0.006
8'	H	0.039	0.057	0.096	0.062	0.015	0.006	0.333	0.049	0.080	0.029	0.098	0.030
7'		0.041		0.130		0.020		0.158		0.276		0.088	
6'	P	0.011	0.050	0.061	0.046	0.013	0.008	0.051	0.050	0.330	0.146	0.072	0.041
5'	P_L''	0.251	0.060	0.088	0.080	0.035	0.040	0.275	0.310	0.096	0.100	0.113	0.110
5''		0.009		0.037		0.026		0.198		0.052		0.067	
1'	B	0.016	0.011	0.024	0.014	0.013	0.007	0.064	0.063	0.028	0.031	0.016	0.013

Table 3.1 Calculated Basic System Frequencies of Vibration (Hz)

Interaction Considered:				
Foundation	No(1)	Yes(2)	Yes	
Reservoir	No	No	Model-(3) (160 meter)	Test Frequency
Mode 1	4.54	4.44	4.04	3.96
Mode 2	5.49	5.33	4.24	4.30
Mode 3	8.85	8.73	7.45	6.85
Mode 4	10.12	9.90	8.34	7.75
Mode 5	11.29	10.83	10.51	8.83
Mode 6	11.59	11.40	10.77	9.25
Mode 7	12.97	12.58	17.07	
Mode 8	14.99	14.24	12.31	

(1) Rigid Foundation; $E_f/E_c = 250$

(2) Flexible Foundation; $E_f/E_c = 1.0$

(3) Reservoir Depth = 74.5 meters

Table 3.2 Influence of Reservoir Configuration on Vibration Frequency

Reservoir Configuration						
Boundary Length	Natural 30m	Natural 80m	Natural 160m	Natural 160m w/Slope	Straight 300m	Test Frequency
Mode 1	3.89	3.98	4.04	4.04	4.04	3.96
Mode 2	4.07	4.17	4.24	4.24	4.28	4.30
Mode 3	6.99	7.35	7.45	7.45	7.64	6.85
Mode 4	8.19	8.21	8.34	8.34	8.27	7.75
Mode 5	10.36	10.40	10.51	10.51	10.50	8.83
Mode 6	10.65	10.66	10.77	10.77	10.73	9.25
Mode 7	11.67	11.90	12.06	12.07	12.21	
Mode 8	12.23	12.24	12.31	12.31	12.33	

Basic Assumptions

$E_f/E_c = 1.0$; $E_c = 4 \times 10^6\ T/m^2$; Reservoir Depth = 74.5m

Table 3.3 Influence of Reservoir Depth on Calculated Frequencies

Surface Elev.	450	444.5	440	430	420	410	370
Depth	80	74.5	70	60	50	40	0
1	3.63	3.96	4.12	4.30	4.35	4.36	4.36
2	3.84	4.11	4.36	4.88	5.10	5.17	5.19
3	6.93	7.22	7.35	7.69	8.32	8.54	8.57
4	7.87	8.25	8.42	8.58	8.73	9.30	9.70
5	9.87	10.13	10.22	10.27	10.30	10.32	10.33
6	10.41	10.52	10.56	10.82	11.08	11.19	11.19
7	11.36	11.58	11.68	12.06	12.16	12.19	12.20
8	11.67	11.78	11.93	12.33	12.73	12.93	13.42

Basic Assumptions

$E_f/E_c = 0.5$; $E_c = 4 \times 10^6$; Reservoir Length = 160m

Table 4.1 Adjustment of Concrete Modulus

Mode No.	Measured Frequency ω_i^M (Hz)	Calculated Frequency with $E_c = 4 \times 10^6$ ω_i (Hz)	Modulus to obtain Measured Frequency $E_i (T/m^2)$	Calculated Frequency with $E_c = 3.788$ ω_i^* (Hz)
1	3.85	3.96	3.781×10^6	3.85
2	4.10	4.11	3.981	4.00
3	6.80	7.22	3.601	7.03
4	7.60	8.25	3.395	8.03
5	8.80	10.13	3.039	9.86
6	9.05	10.52	3.093	10.24

Table 4.2 Comparison of Measured and Final Calculated Frequencies

Mode No.	Measured Freq. (Hz)	Calculated Freq. (Hz)	Difference %
1	3.85	3.85	0.0
2	4.10	4.00	-2.4
3	6.80	7.03	+3.3
4	7.60	8.03	+5.7
5	8.80	9.86	+12.0
6	9.05	10.24	+13.1

Table 4.3 Best Estimates of Modal Damping Ratios

Mode No.	Damping Ratio	Method
1	1.3%	Analyt.
2	1.3%	Analyt.
3	2.7%	Half-Power
4	2.4%	Half-Power
5	1.3%	Half-Power
6	4.3%	Half-Power

Table 5.1 Arch Stresses at Instants of Peak Stress (Kg/cm^2)

(a) Section A-A (see Figs. 5.5) (Tension = Positive)

Height (M)	Upstream Face					Downstream Face				
	Gravity and Hydro-static	t = 0.89 sec.		t = 1.03 sec.		Gravity and Hydro-static	t = 0.89 sec.		t = 1.03 sec.	
		Earth-quake	Total	Earth-quake	Total		Earth-quake	Total	Earth-quake	Total
78.20	-18.89	5.66	-13.23	-5.30	-24.19	6.23	-3.07	3.16	0.18	6.41
73.30	-26.54	4.74	-21.80	-4.24	-30.78	3.49	-4.12	-0.63	-1.40	2.09
70.44	-30.31	3.68	-26.63	-3.28	-33.59	1.32	-3.89	-2.57	1.49	2.81
67.56	-33.99	2.73	-31.26	-2.41	-36.40	-1.33	-3.29	-4.62	1.28	-0.05
63.44	-39.65	1.90	-37.75	-1.53	-41.18	-6.14	-2.90	-9.04	1.42	-4.72
55.06	-48.09	0.98	-47.11	-0.74	-48.83	-13.41	-1.82	-15.23	1.22	-12.19
49.78	-51.49	1.36	-50.13	-1.24	-52.73	-15.19	-0.94	-16.13	0.81	-14.38
43.72	-52.70	1.77	-50.93	-1.78	-54.48	-16.81	-0.59	-17.40	0.79	-16.02
41.50	-43.14	1.15	-41.99	-1.58	-44.72	-25.56	0.83	-24.73	-0.41	-25.97
29.75	-30.2	1.37	-28.83	-1.37	-31.57	-21.49	0.93	-20.56	-0.45	-21.94
18.00	-9.80	0.59	-9.21	-0.51	-10.31	-14.94	0.62	-14.32	-0.36	-15.30

Table 5.1 Arch Stresses at Instants of Peak Stress (Kg/cm^2) (Cont'd)

(b) Section B-B (see Figs. 5.5) (Tension = Positive)

Height (M)	Upstream Face					Downstream Face				
	Gravity and Hydrostatic	t = 0.89 sec.		t = 1.03 sec.		Gravity and Hydrostatic	t = 0.89 sec.		t = 1.03 sec.	
		Earthquake	Total	Earthquake	Total		Earthquake	Total	Earthquake	Total
78.20	-18.81	12.13	-6.68	-12.06	-30.87	6.74	-9.38	-2.64	5.88	12.62
73.30	-26.28	11.39	-14.89	-10.82	-37.10	4.26	-11.04	-6.78	7.76	12.02
70.44	-29.93	9.99	-19.94	-9.29	-39.22	1.81	-10.69	-8.88	7.72	9.53
67.56	-33.81	8.69	-25.12	-7.85	-41.66	-1.57	-10.06	-11.63	7.40	5.83
63.44	-39.54	6.85	-32.69	-5.92	-45.46	-6.39	-7.92	-14.31	5.81	-0.58
55.06	-48.07	4.45	-43.62	-3.29	-51.36	-13.30	-4.95	-18.25	3.63	-9.67
49.78	-51.29	3.79	-47.50	-2.51	-53.80	-16.04	-3.80	-19.84	2.80	-13.24
43.72	-52.48	3.72	-48.76	-2.49	-54.97	-17.61	-2.10	-19.71	1.41	-16.20
41.50	-43.14	2.32	-40.82	-1.28	-44.42	-25.79	-0.36	-26.15	0.14	-25.65
29.75	-30.18	2.28	-27.90	-1.79	-31.97	-21.22	0.95	-20.27	-1.09	-22.31
18.00	-9.95	1.00	-8.95	-0.93	-10.88	-16.28	1.25	-15.03	-1.23	-17.51

Table 5.2 Cantilever Stresses at Instants of Peak Stress (Kg/cm^2)

(a) Section A-A (see Figs. 5.6) (Tension = Positive)

Height (M)	Upstream Face					Downstream Face				
	Gravity and Hydro-static	t = 0.90 sec.		t = 0.94 sec.		Gravity and Hydro-static	t = 0.90 sec.		t = 0.94 sec.	
		Earth-quake	Total	Earth-quake	Total		Earth-quake	Total	Earth-quake	Total
78.20	-0.80	0.22	-0.58	-0.14	-0.94	-0.05	-0.27	-0.32	0.16	0.11
73.30	-4.10	-0.54	-4.64	1.08	-3.02	0.79	0.11	0.90	-0.76	0.03
70.44	-6.66	-1.31	-7.97	2.11	-4.55	2.30	1.02	3.32	-2.03	0.27
67.56	-10.21	-2.42	-12.63	3.31	-6.90	4.01	1.75	5.76	-3.00	1.01
63.44	-15.90	-3.25	-19.15	4.31	-11.59	6.28	2.23	8.51	-3.76	2.52
55.06	-22.46	-3.74	-26.20	4.17	-18.29	7.95	2.50	10.45	-3.54	4.41
49.78	-23.27	-2.33	-25.60	2.01	-21.26	6.76	1.76	8.52	-2.10	4.66
43.72	-22.06	-0.19	-22.25	-0.81	-22.87	4.53	-0.43	4.10	0.79	5.32
41.50	-20.61	1.63	-18.98	-2.65	-23.26	-1.76	-1.65	-3.41	2.42	0.66
29.75	-9.57	0.83	-8.74	-1.59	-11.16	-7.05	-1.46	-8.51	1.81	-5.24
18.00	4.70	-0.74	3.96	-0.11	4.59	-21.13	-0.24	-21.37	0.52	-20.61

Table 5.2 Cantilever Stresses at Instants of Peak Stress (Kg/cm^2) (Cont'd)

(b) Section B-B (see Figs. 5.6) (Tension = Positive)

Height (M)	Upstream Face					Downstream Face				
	Gravity and Hydro-static	t = 0.90 sec.		t = 0.94 sec.		Gravity and Hydro-static	t = 0.90 sec.		t = 0.94 sec.	
		Earth-quake	Total	Earth-quake	Total		Earth-quake	Total	Earth-quake	Total
78.20	-0.78	0.31	-0.47	-0.77	-1.55	-0.09	-0.53	-0.62	0.29	0.20
73.30	-4.04	0.27	-3.77	0.25	-3.79	0.97	-0.73	0.24	0.16	1.13
70.44	-6.96	-0.31	-7.27	1.01	-5.95	2.27	-0.56	1.71	-0.22	2.05
67.56	-10.35	-0.73	-11.08	1.68	-8.67	3.85	-0.37	3.48	-0.66	3.19
63.44	-15.15	-2.35	-17.50	3.63	-11.52	6.18	1.13	7.31	-2.54	3.64
55.06	-21.78	-2.74	-24.52	3.71	-18.07	8.03	1.98	10.01	-3.14	4.89
49.78	-22.53	-1.80	-24.33	2.02	-20.51	6.89	0.77	7.66	-1.27	5.62
43.72	-21.49	-0.63	-22.12	0.22	-21.27	4.62	0.04	4.66	0.03	4.65
41.50	-20.29	1.35	-18.94	-2.11	-22.40	1.42	-1.50	-0.08	2.17	3.59
29.75	-8.10	0.48	-7.62	-1.23	-9.33	-6.78	-1.03	-7.81	1.43	-5.35
18.00	6.25	-1.08	5.17	0.08	6.33	-21.84	0.18	-21.66	0.15	-21.69

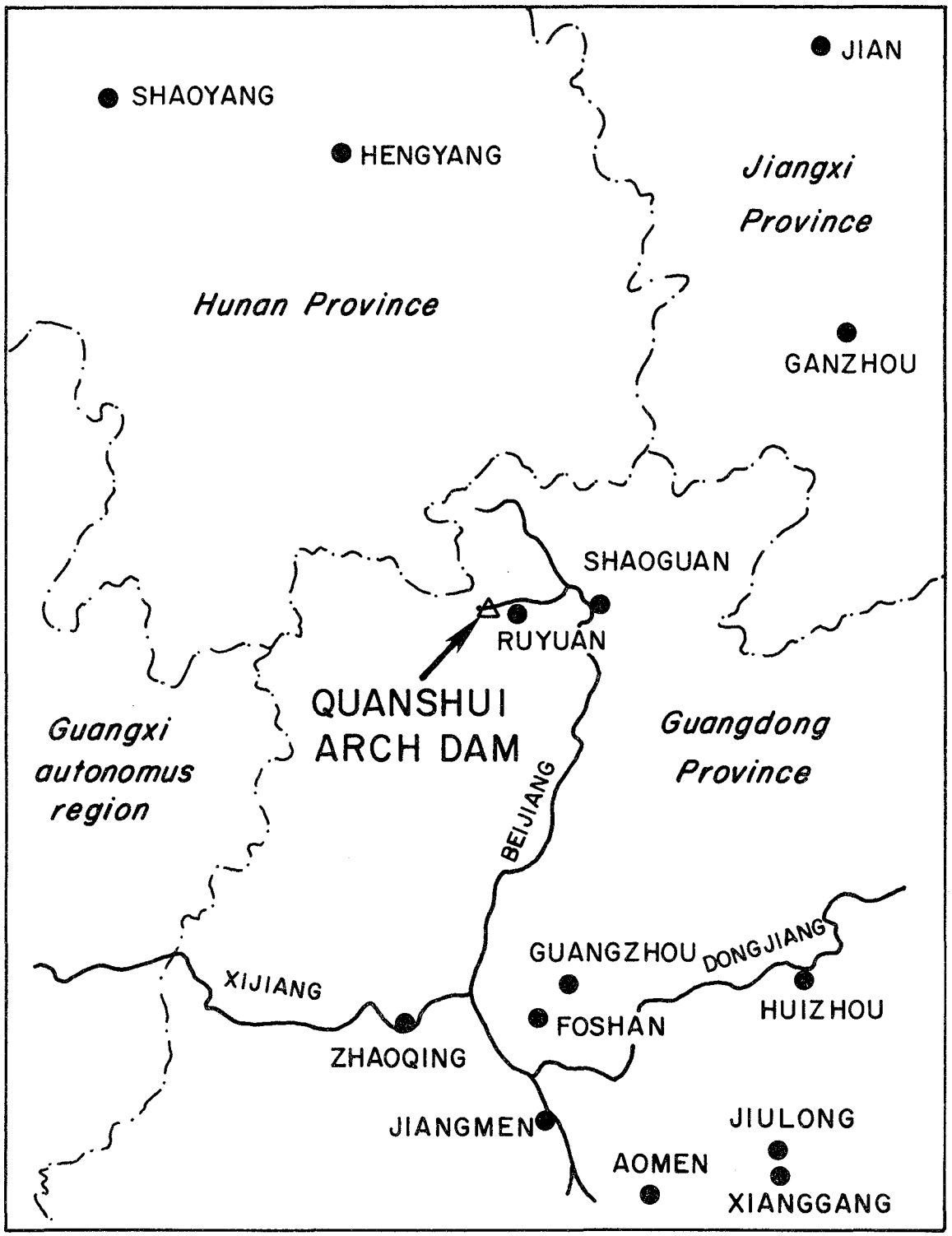

FIG. 2.1 LOCATION OF QUAN SHUI DAM IN GUANGDONG PROVINCE

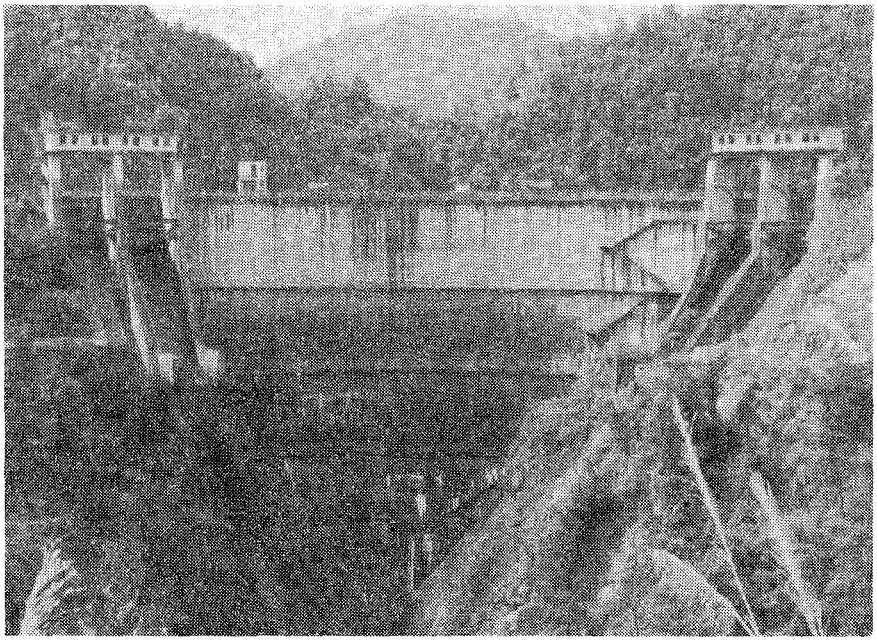

FIG. 2.2 VIEW OF QUAN SHUI DAM FROM DOWNSTREAM

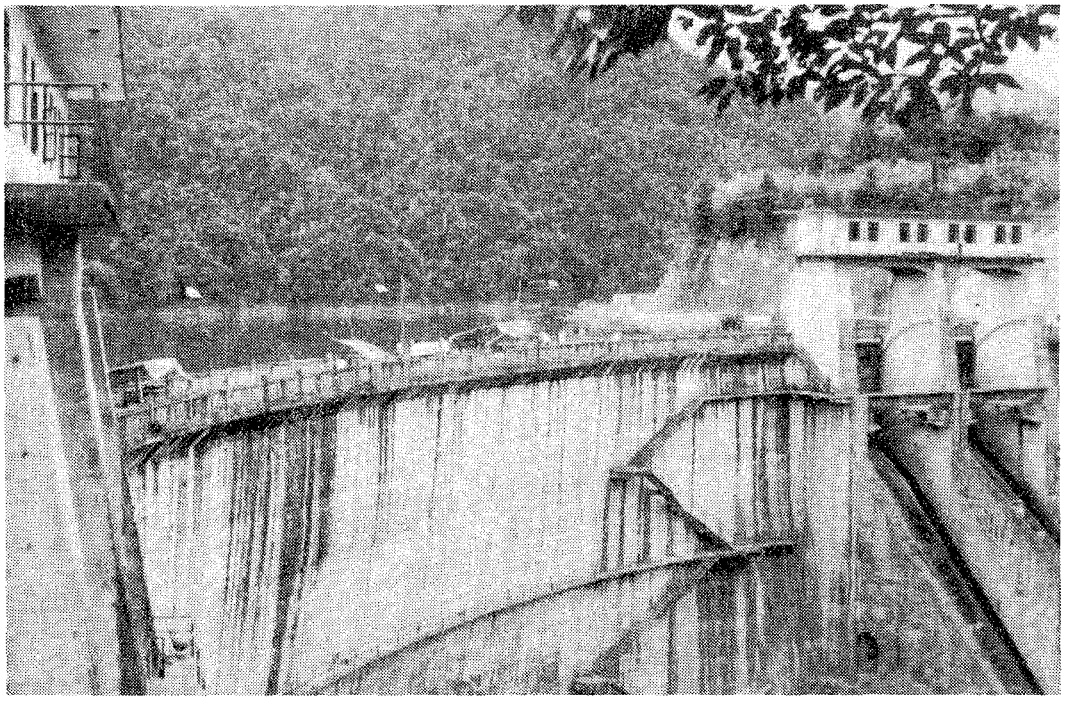

FIG. 2.4 VIEW SHOWING LEFT SPILLWAY BLOCK AND GATE STRUCTURE

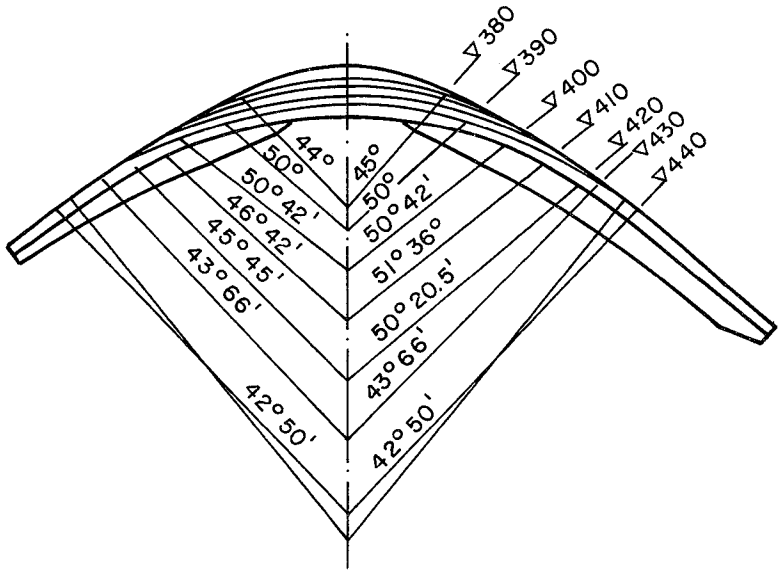

PLAN

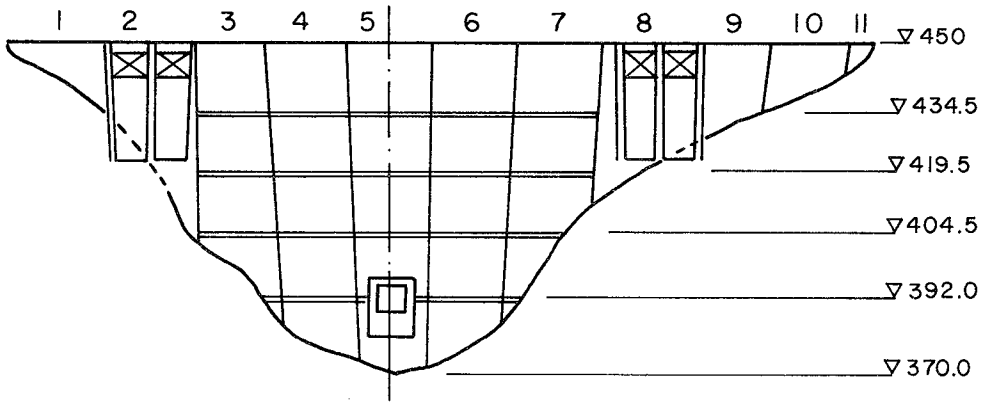

PROFILE (LOOKING FROM DOWNSTREAM)

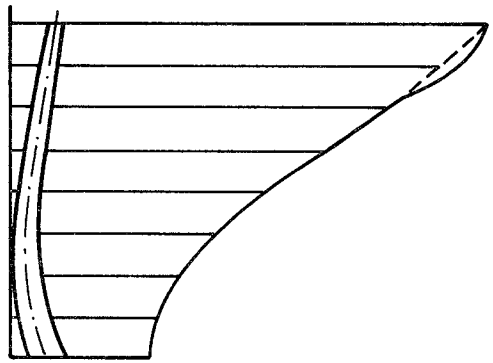

CENTRAL SECTION

FIG. 2.3 LAYOUT OF QUAN SHUI DAM

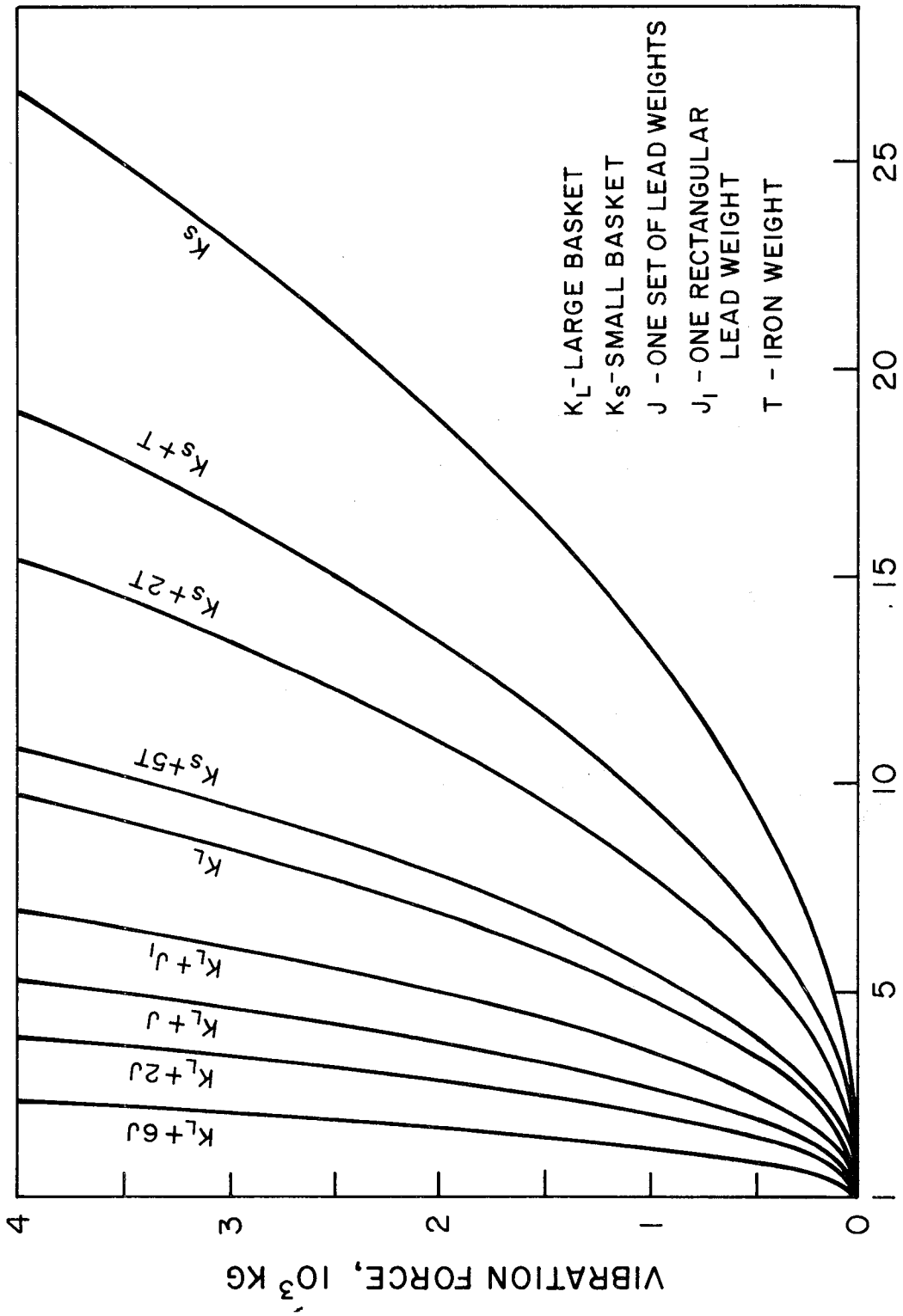

FIG. 2.5 HARMONIC FORCE APPLIED BY SINGLE SHAKER

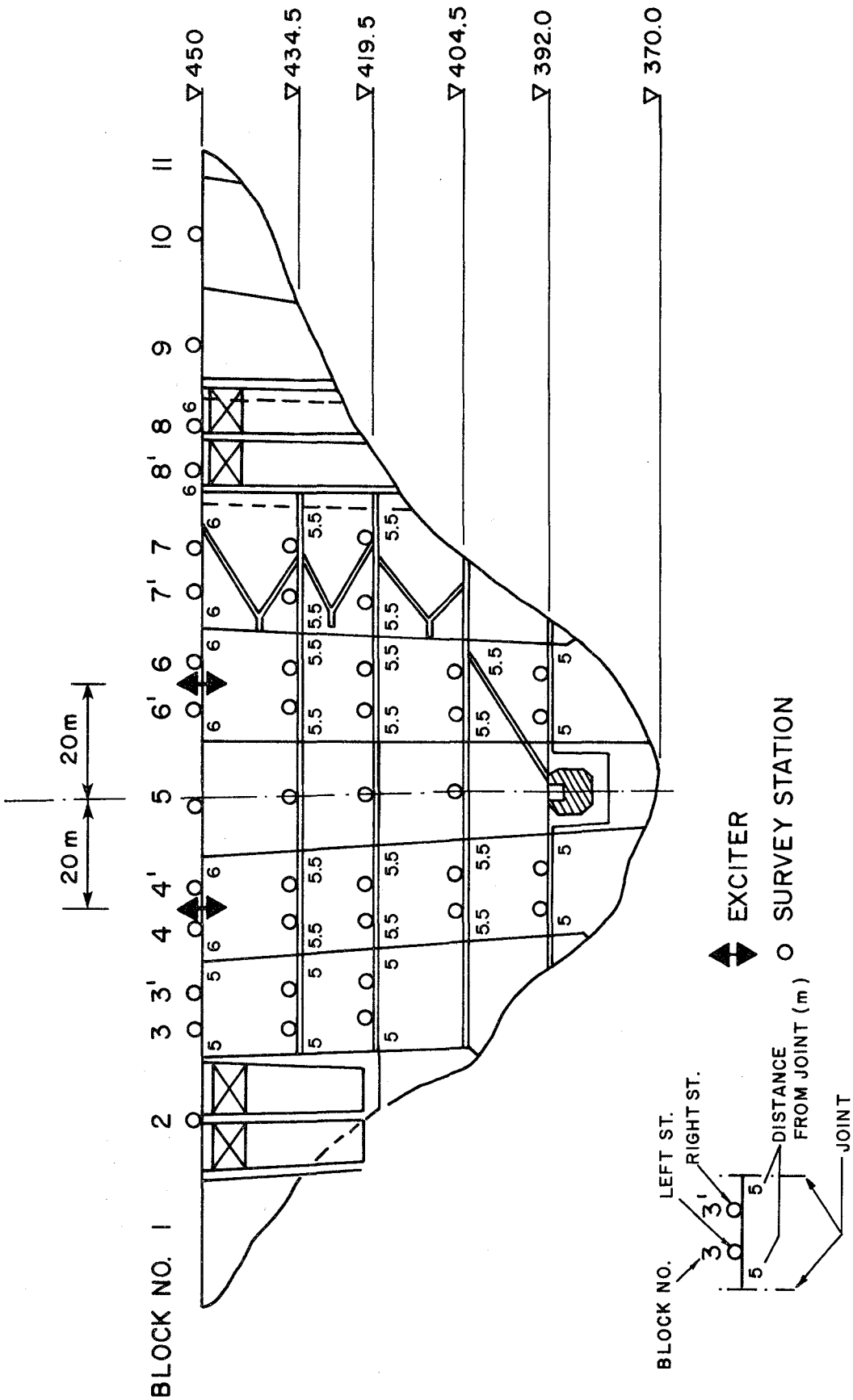

FIG. 2.6 LOCATIONS OF SHAKING MACHINES AND VELOCITY TRANSDUCERS

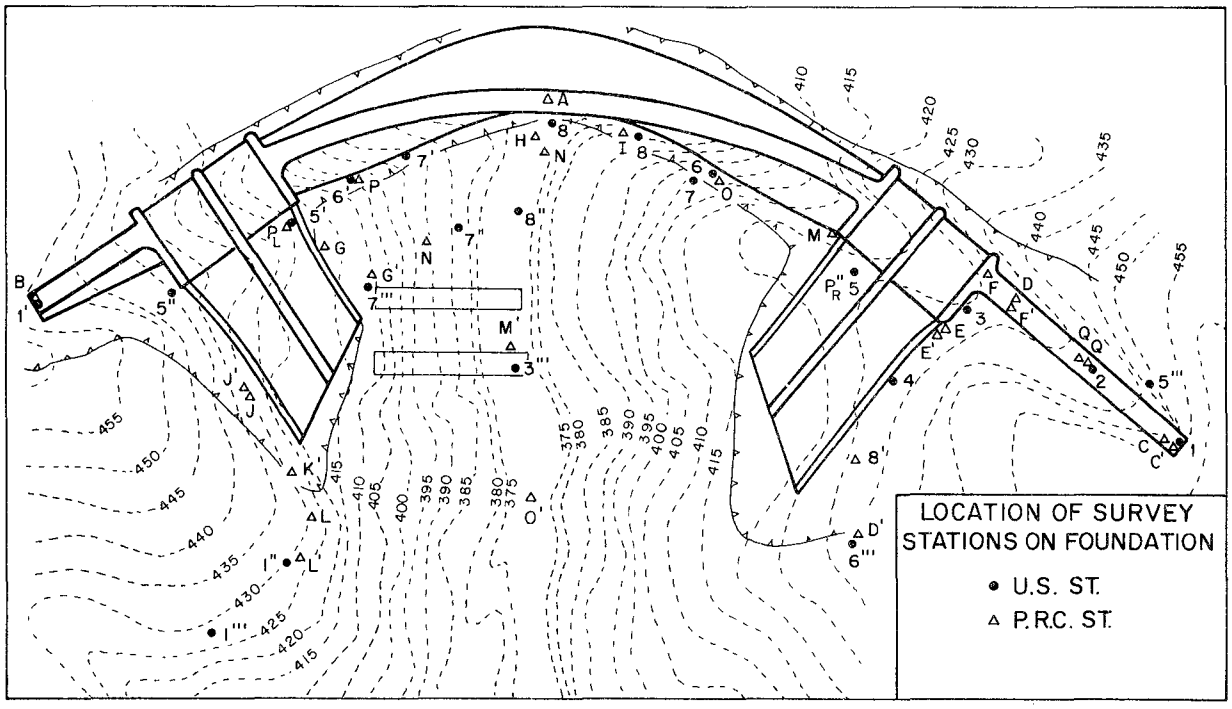

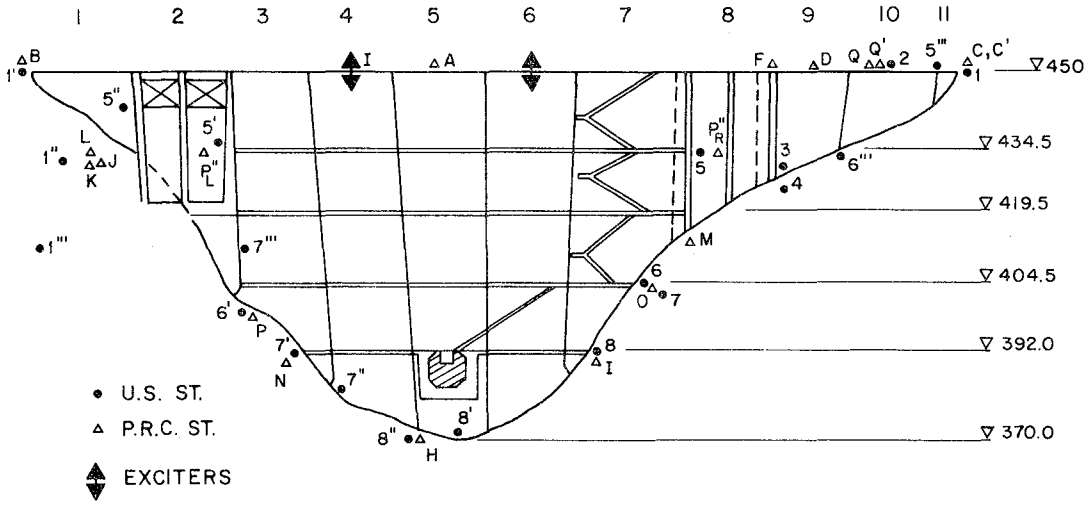

FIG. 2.7 LOCATIONS OF RANGER SEISMOMETERS ON FOUNDATION

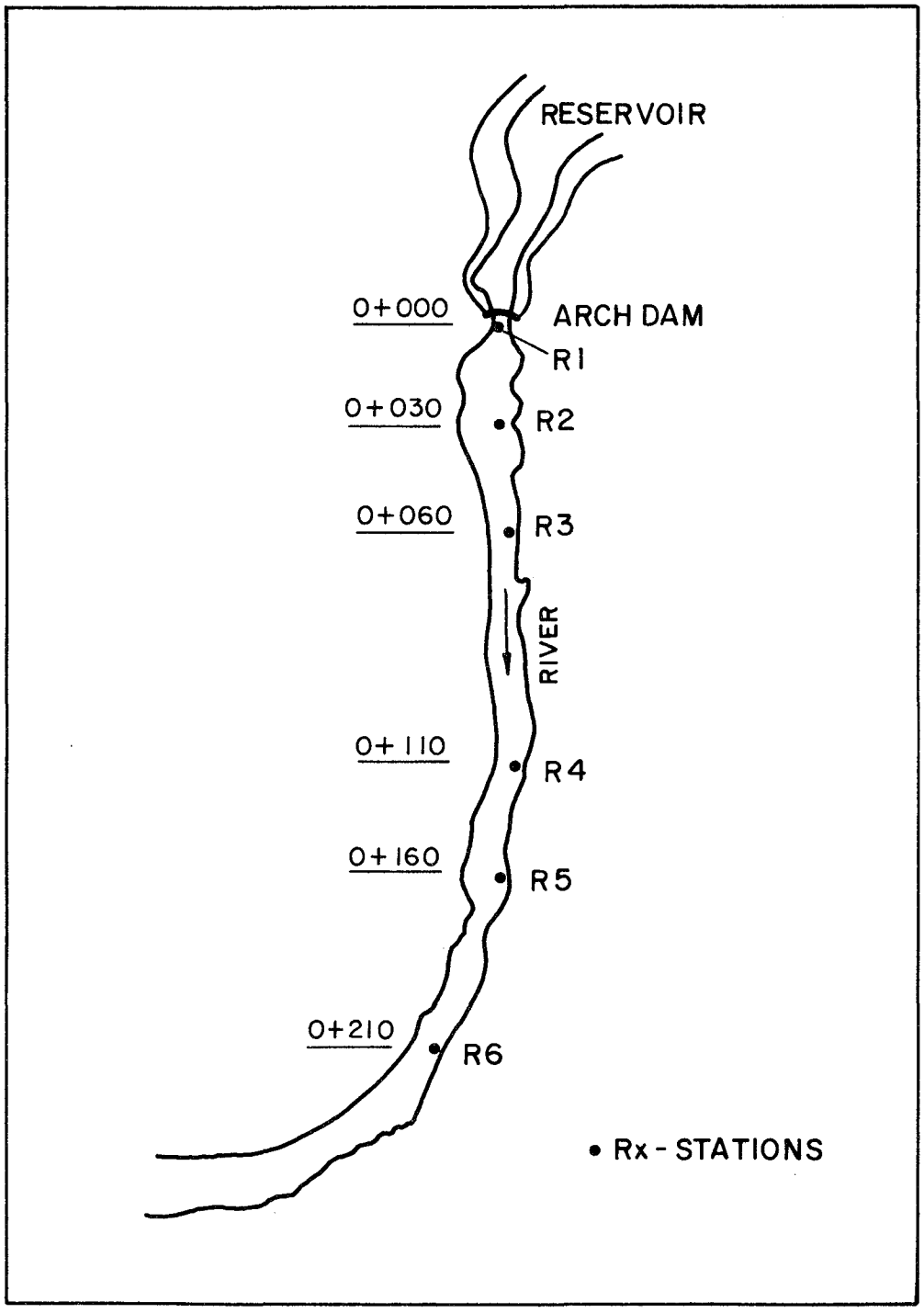

FIG. 2.8 VIBRATION MEASUREMENT STATIONS ALONG THE RIVER
(from Ref. 3 by C.-H. Chang)

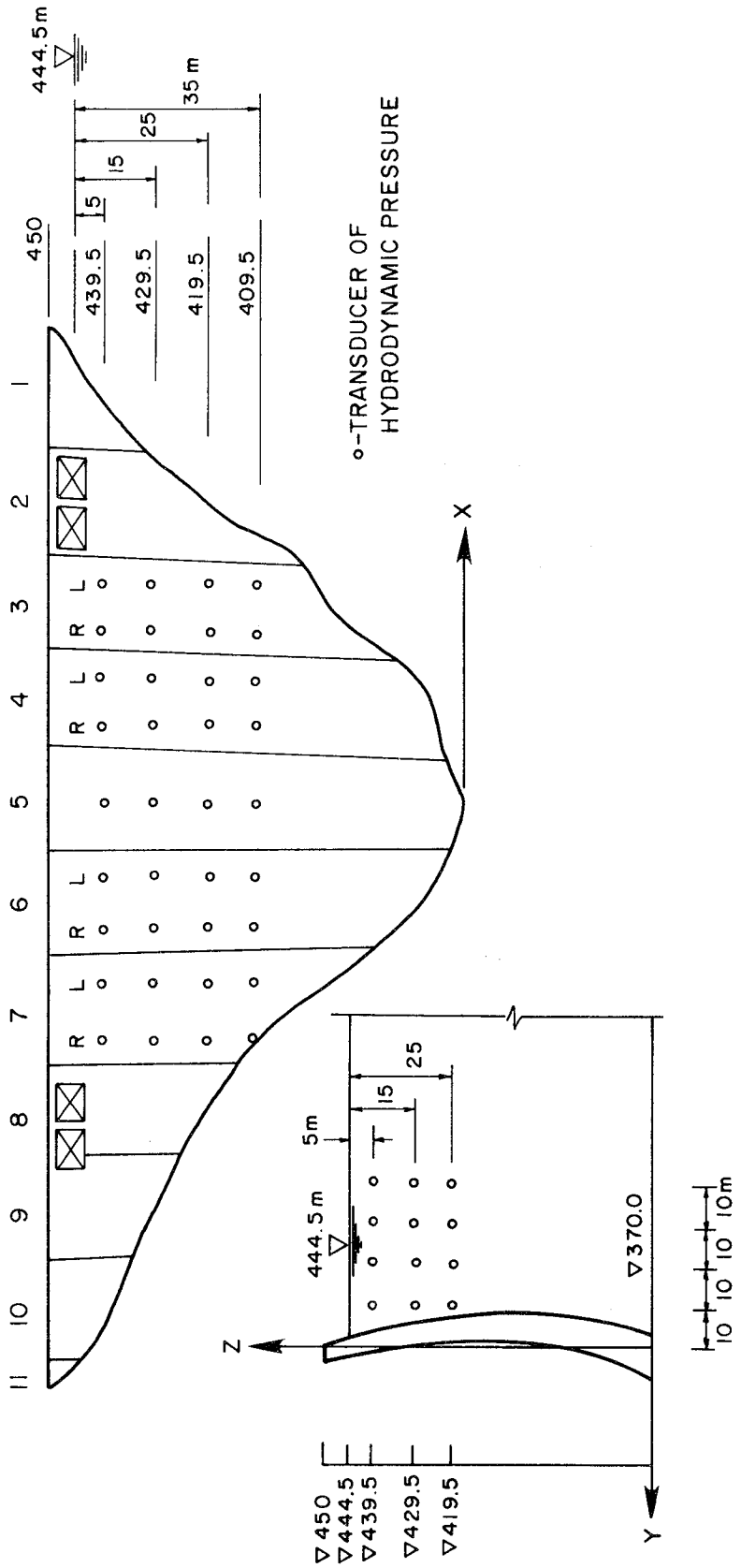

FIG. 2.9 LOCATIONS OF HYDRODYNAMIC PRESSURE GAGES

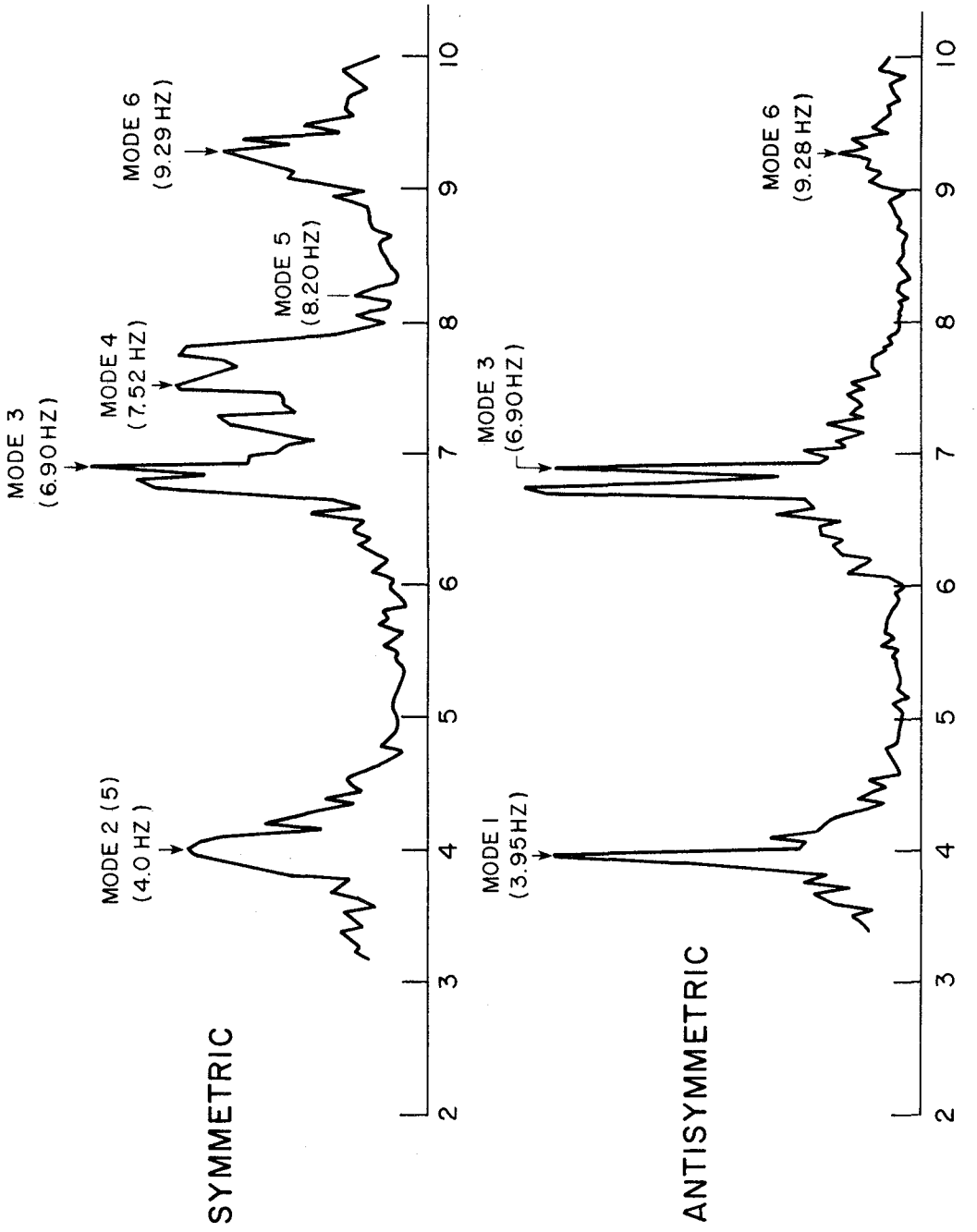

FIG. 2.10 FOURIER AMPLITUDE SPECTRA OF AMBIENT VIBRATION RESPONSE

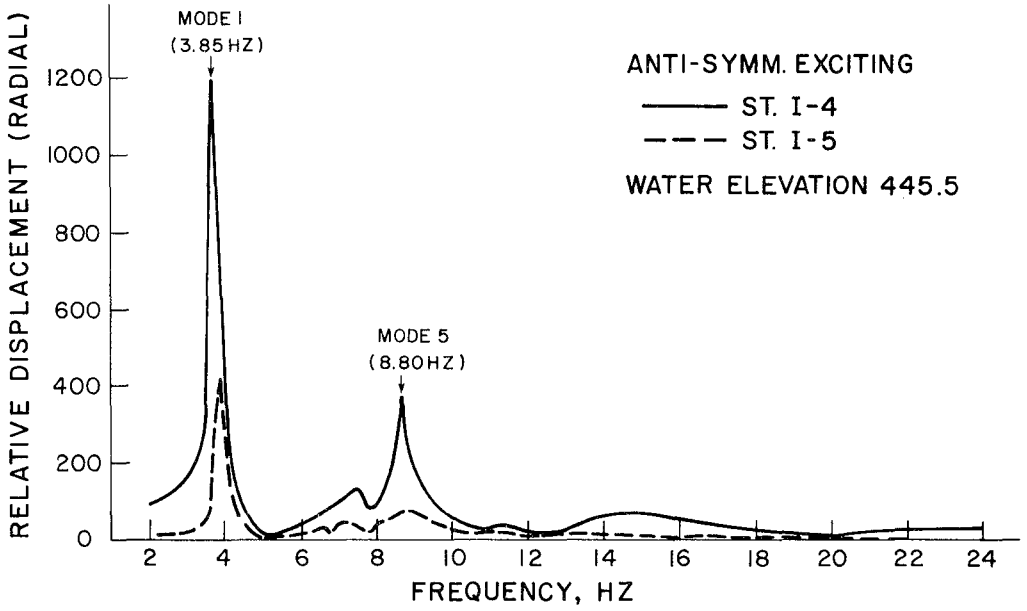

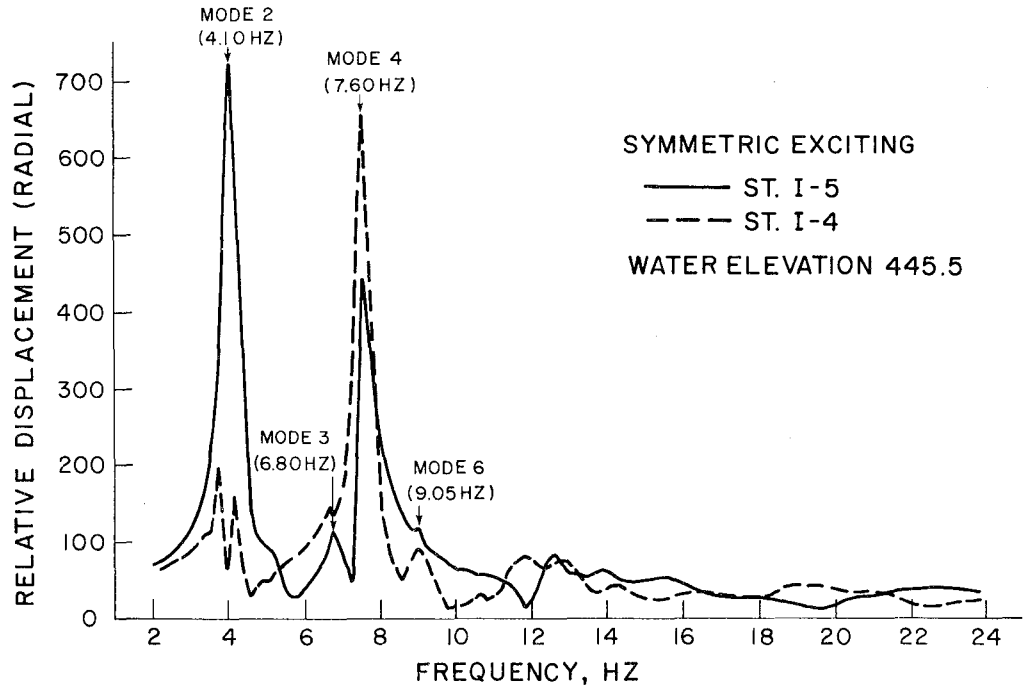

FIG. 2.11 FREQUENCY RESPONSE CURVES

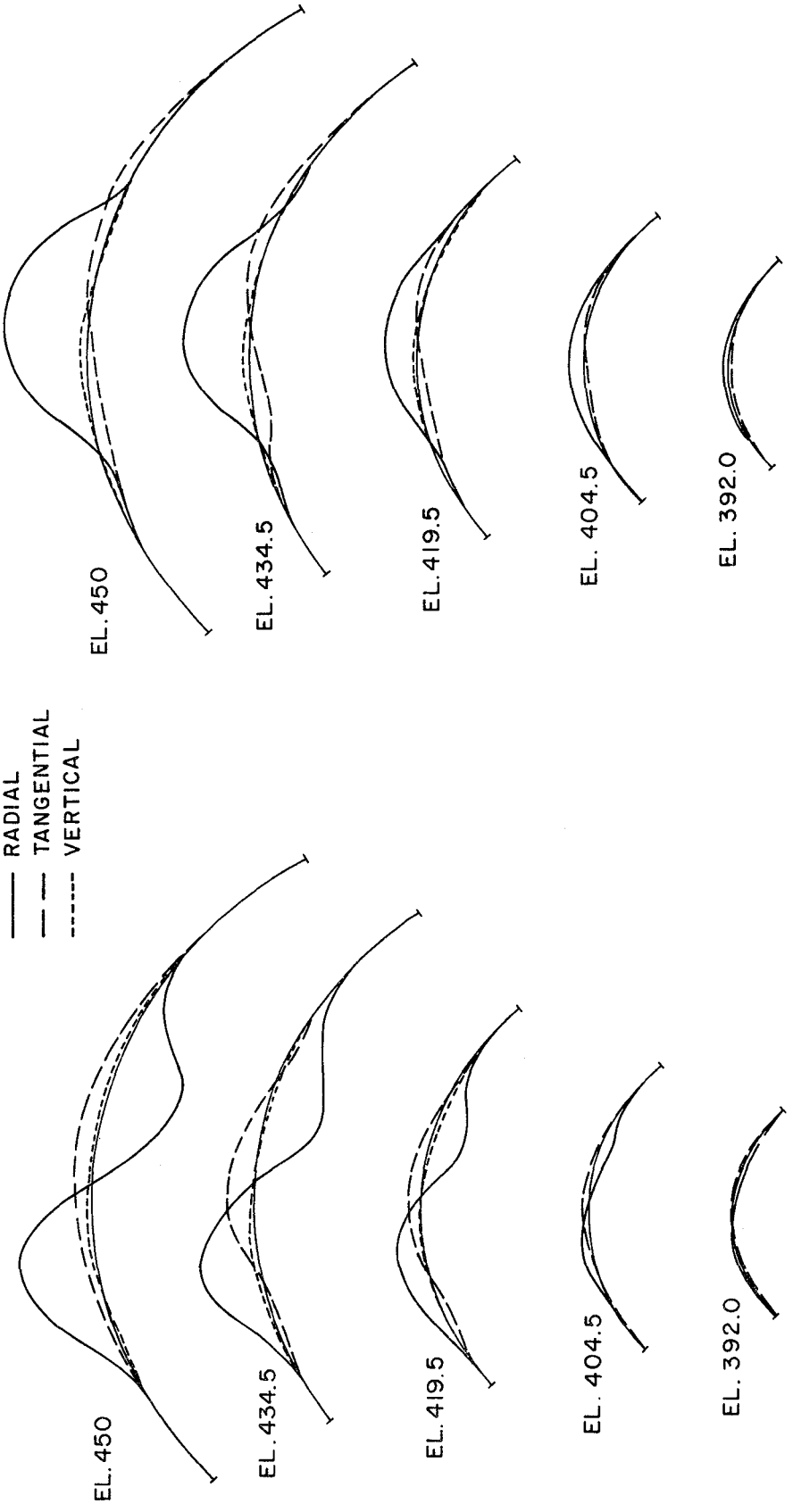

FIG. 2.12(a) FORCED VIBRATION RESPONSE AT 3.96 HZ

FIG. 2.12(b) FORCED VIBRATION RESPONSE AT 4.30 HZ

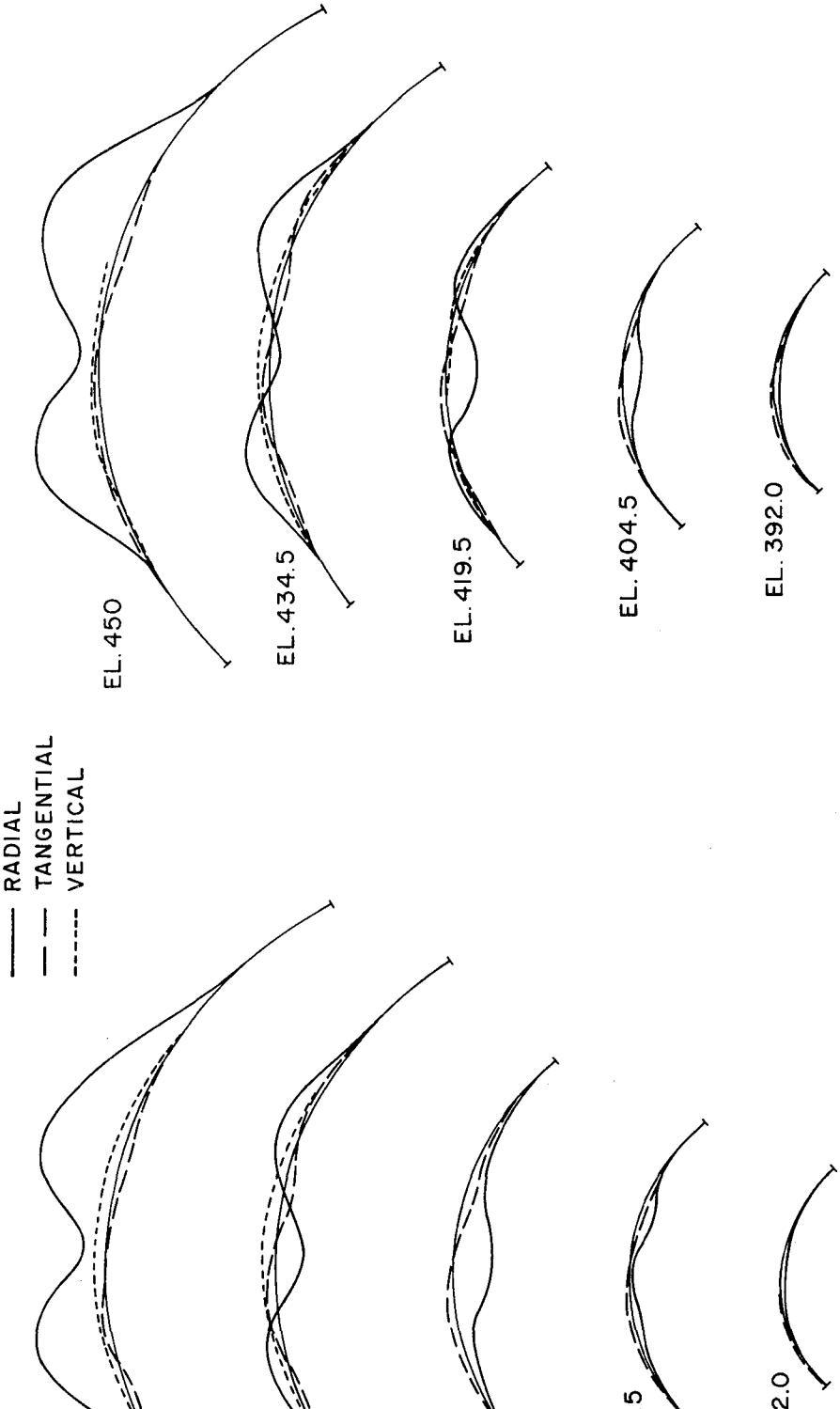

FIG. 2.12(c) FORCED VIBRATION RESPONSE AT 6.85 HZ

FIG. 2.12(d) FORCED VIBRATION RESPONSE AT 7.75 HZ

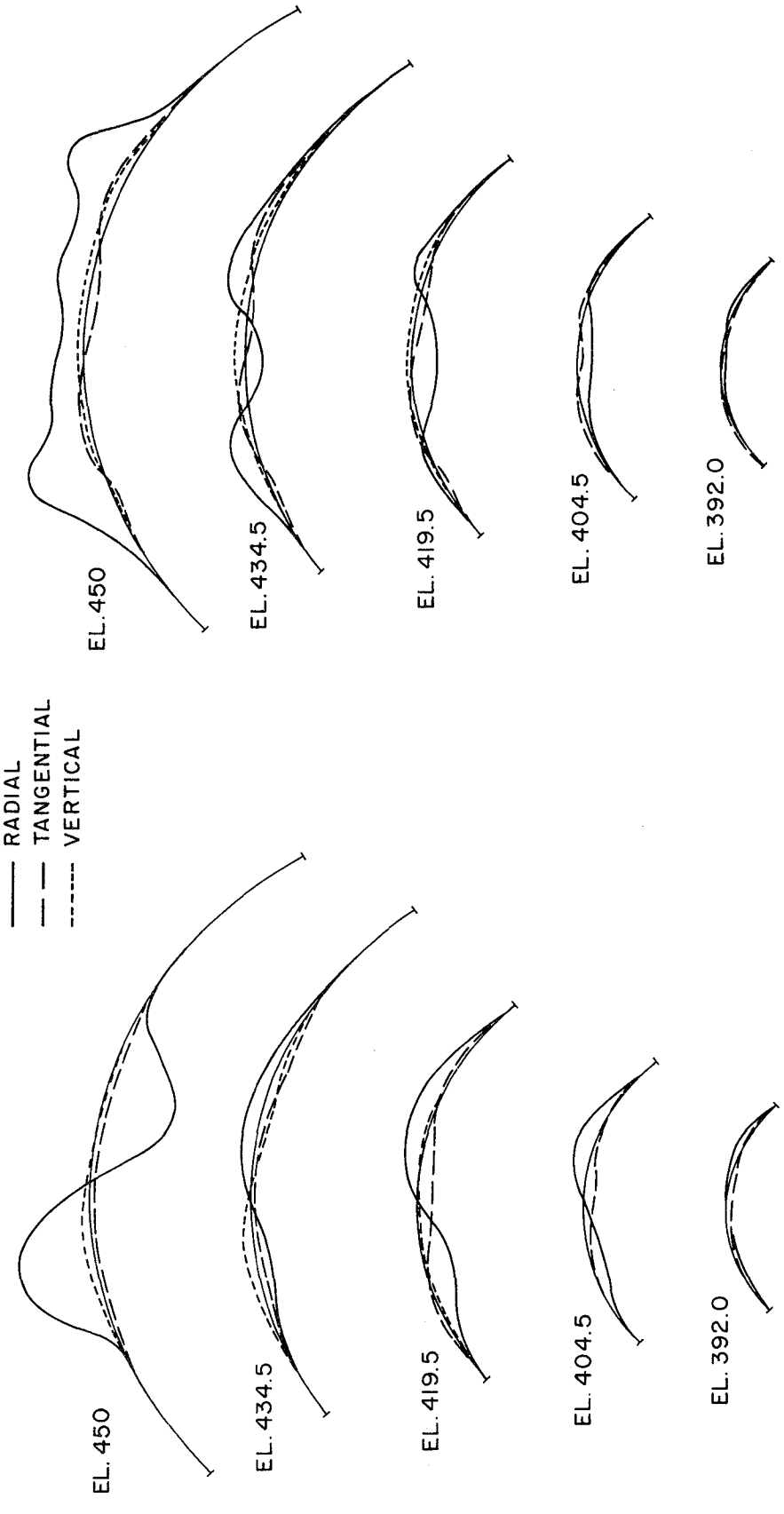

FIG. 2.12(e) FORCED VIBRATION RESPONSE AT 8.83 HZ

FIG. 2.12(f) FORCED VIBRATION RESPONSE AT 9.25 HZ

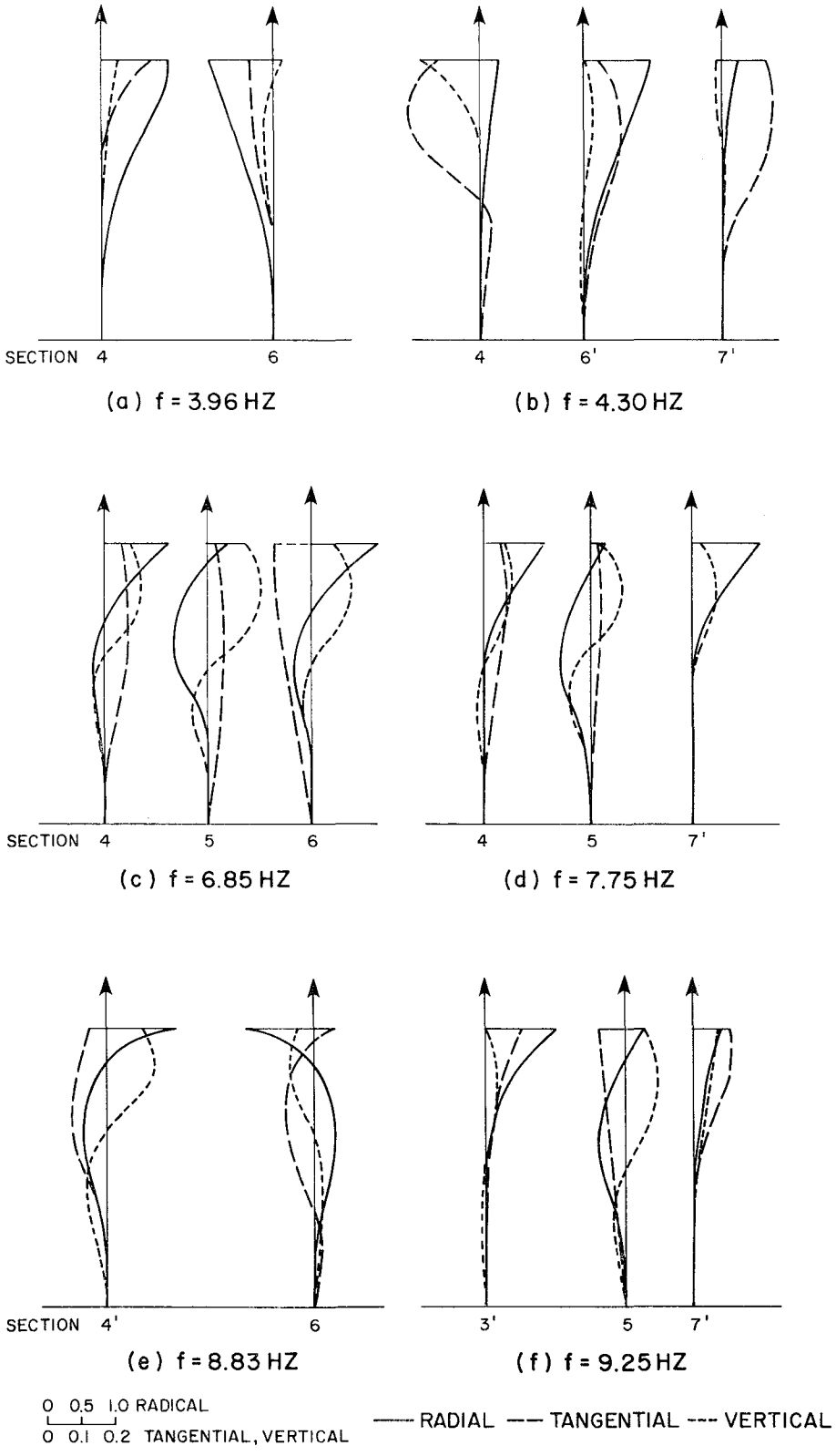

FIG. 2.13 FORCED VIBRATION RESPONSE ON VERTICAL SECTIONS (from Ref. 3 by C.-H. Chang)

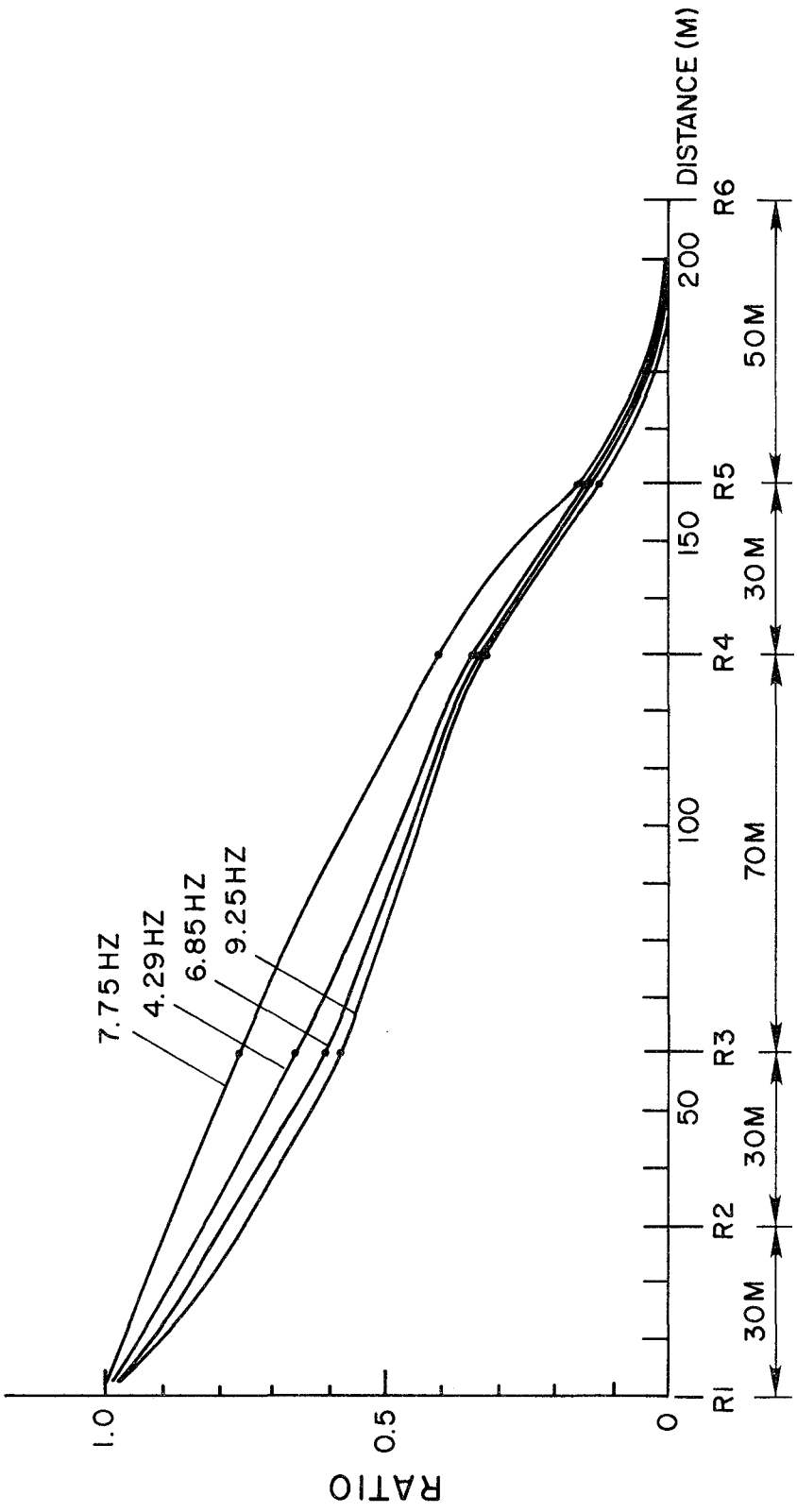

FIG. 2.14 RELATIVE FORCED DISPLACEMENT AMPLITUDE ALONG RIVER CHANNEL
(from Ref. 3 by C.-H. Chang)

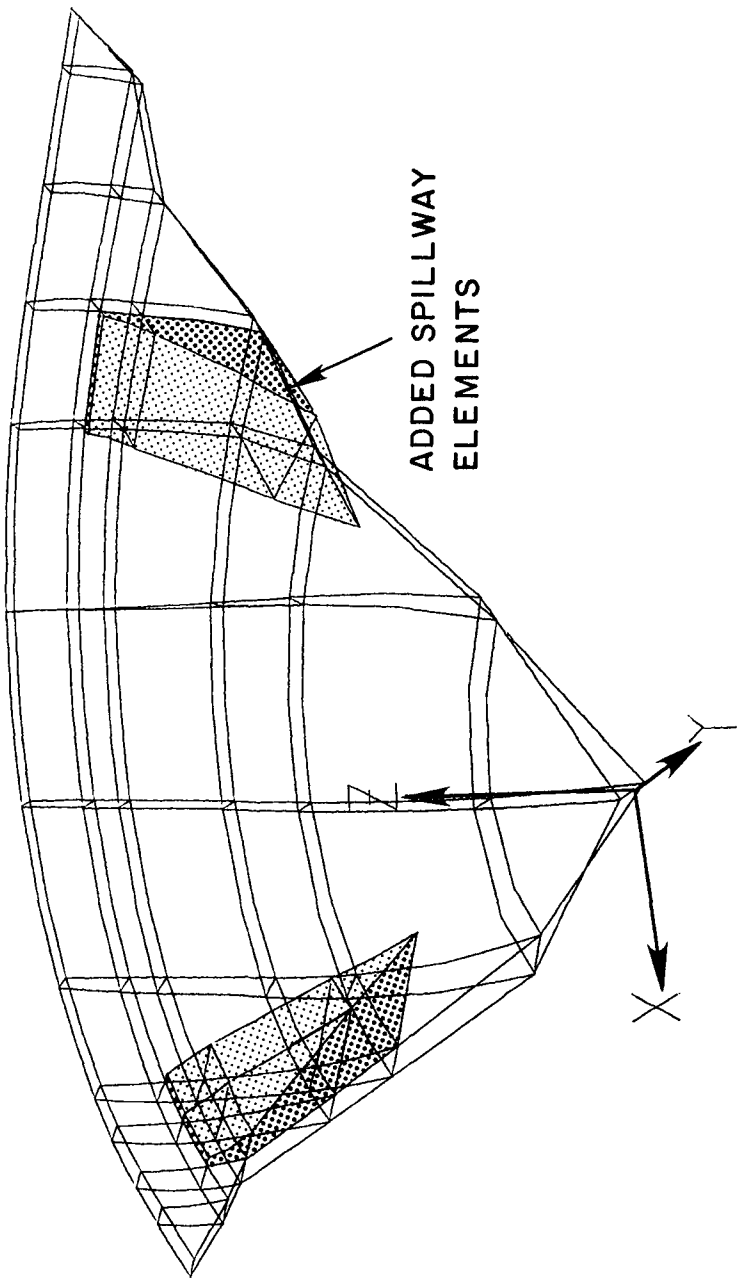

FIG. 3.1 FINITE ELEMENT MODEL OF DAM BODY, VIEWED FROM DOWNSTREAM

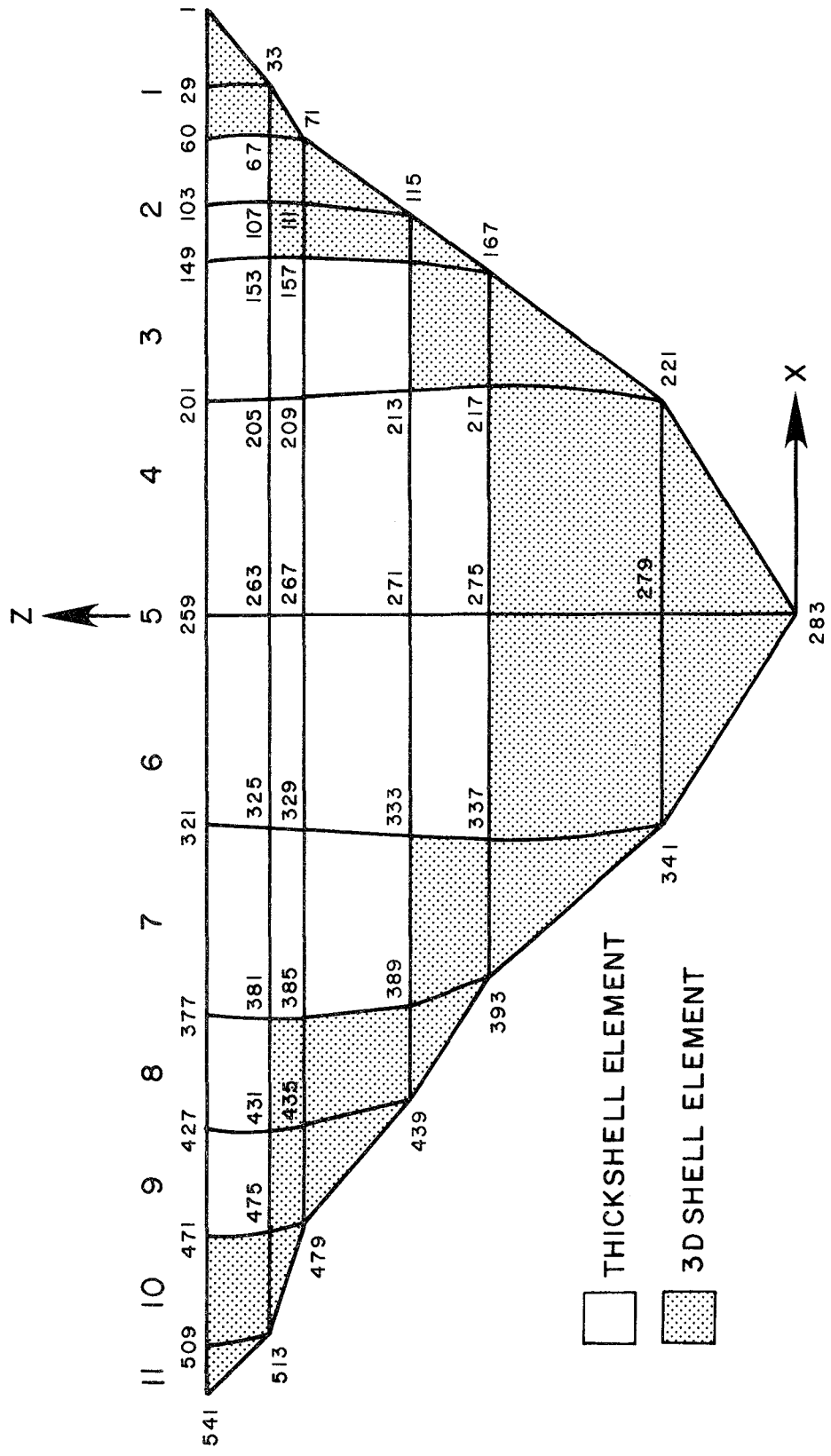

FIG. 3.2 PROJECTION OF UPSTREAM FACE OF DAM ON X-Z PLANE

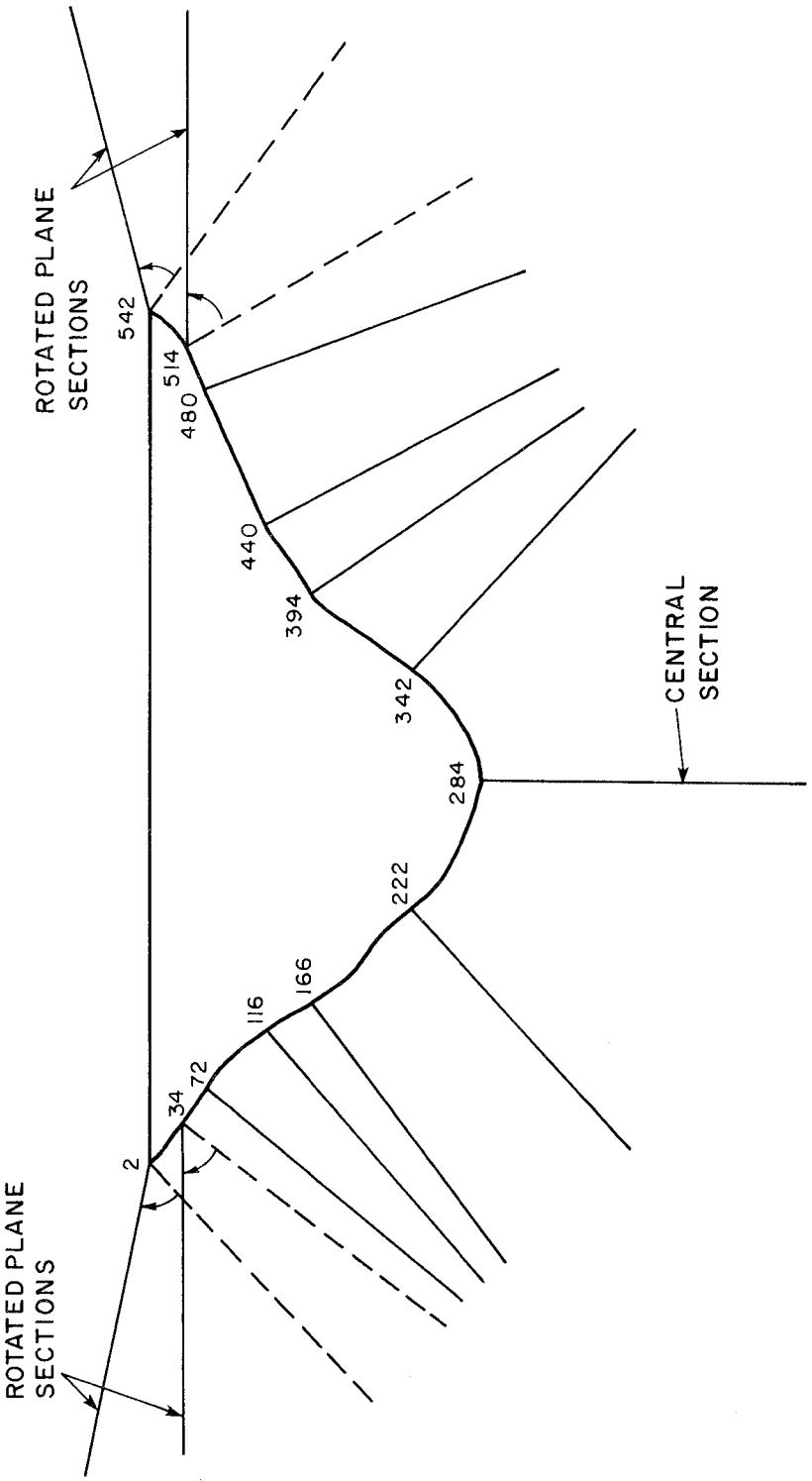

FIG. 3.3 VIEW FROM DOWNSTREAM OF FINITE ELEMENT PLANES IN FOUNDATION

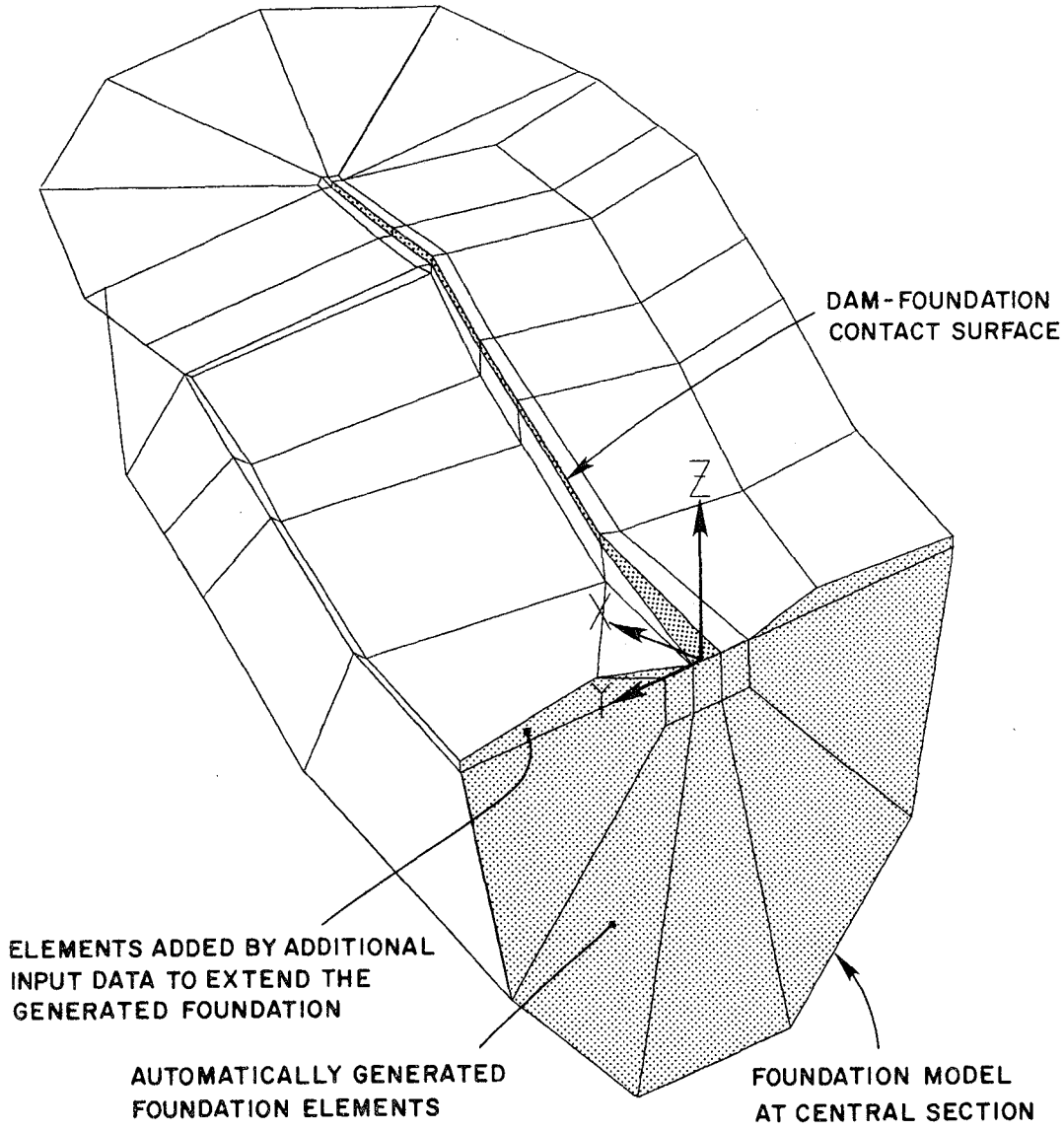

FIG. 3.4 ISOMETRIC VIEW OF FOUNDATION ELEMENTS - RIGHT SIDE OF CANYON

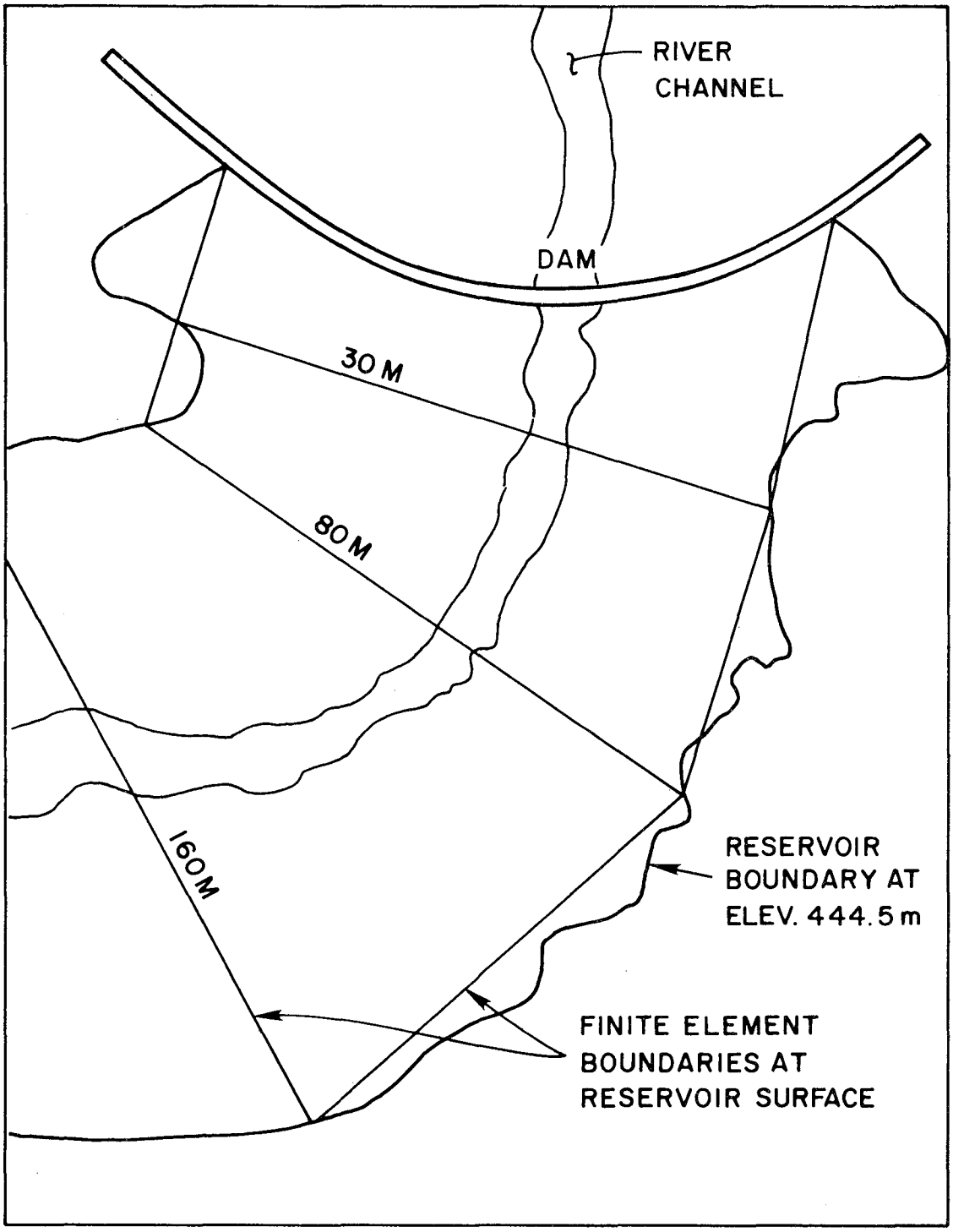

FIG. 3.5 MAP OF QUAN SHUI RESERVOIR

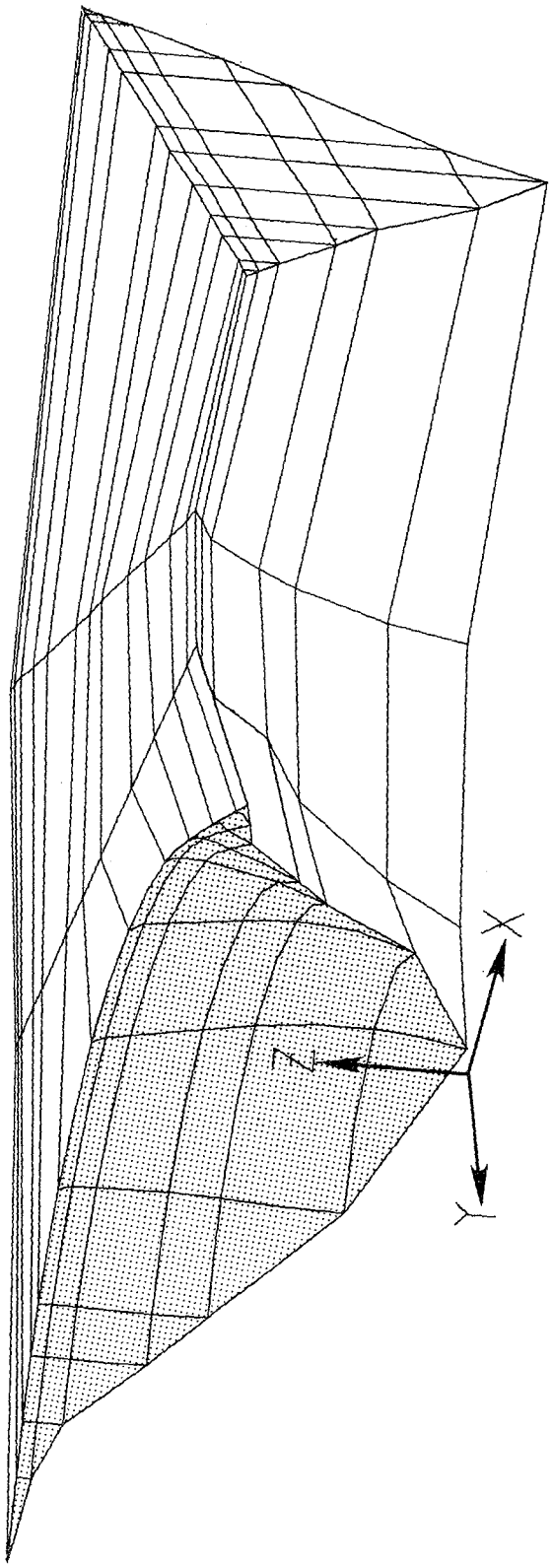

FIG. 3.6 ISOMETRIC VIEW OF FINITE ELEMENT RESERVOIR MODEL

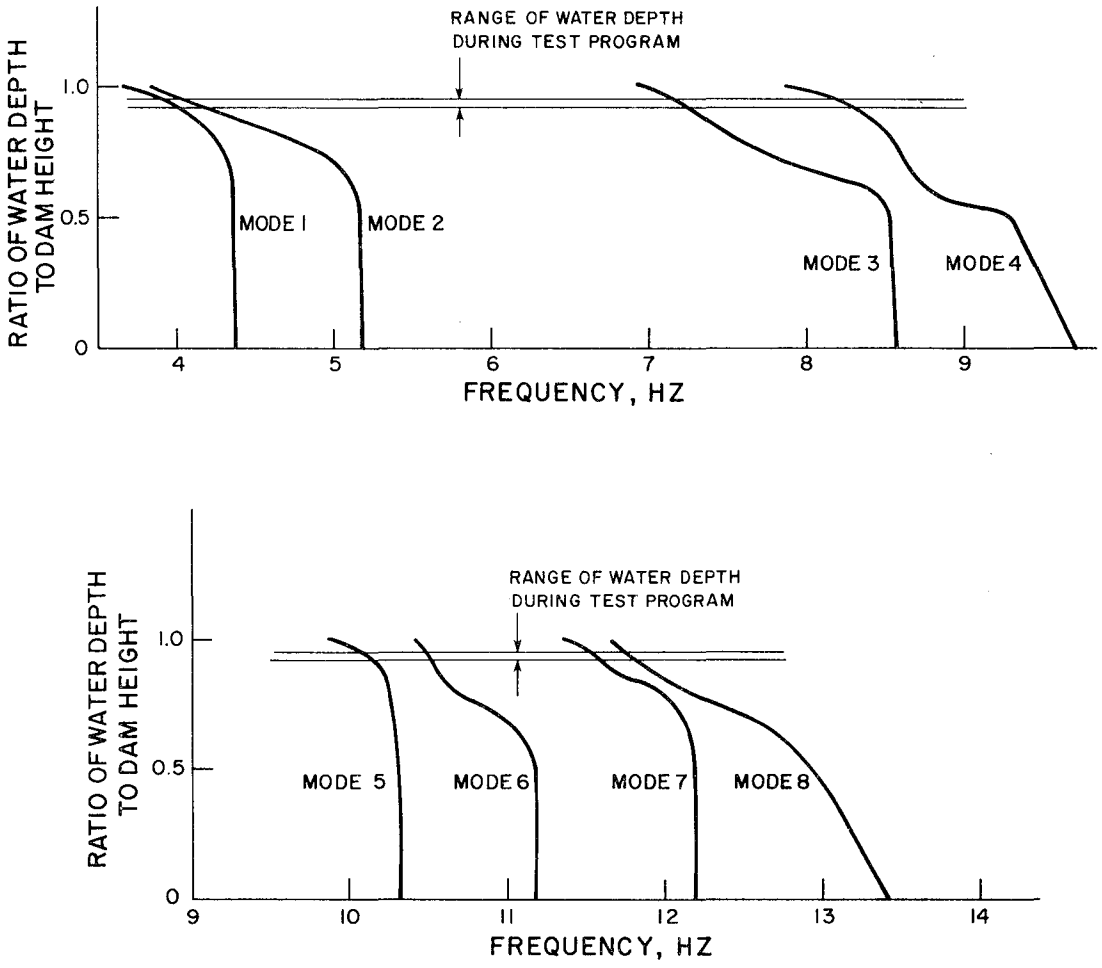

FIG. 3.7 VARIATION OF CALCULATED VIBRATION FREQUENCIES WITH RESERVOIR DEPTH

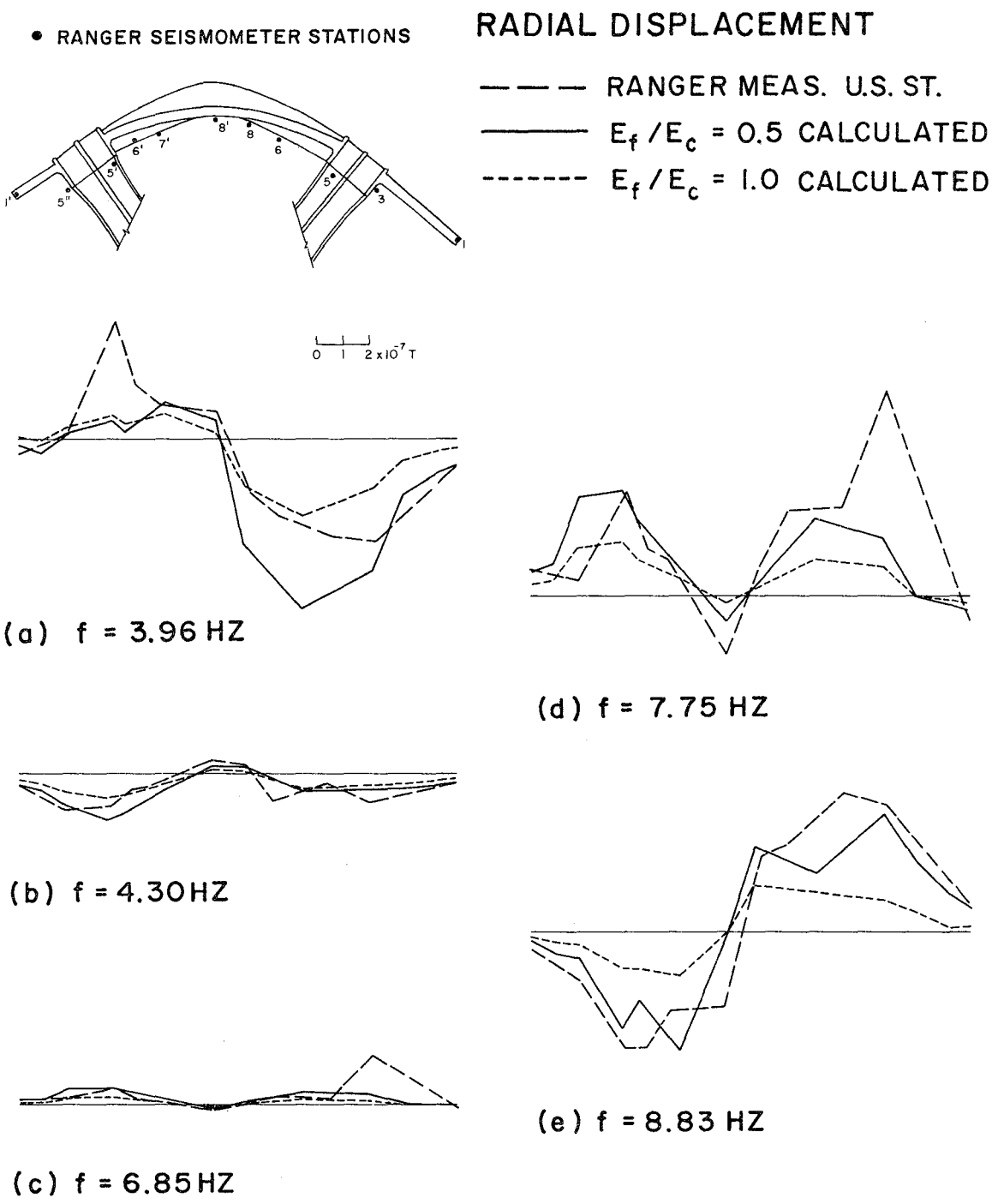

FIG. 4.1 CORRELATION OF RADIAL FORCED VIBRATION MOTIONS AT DAM BASE

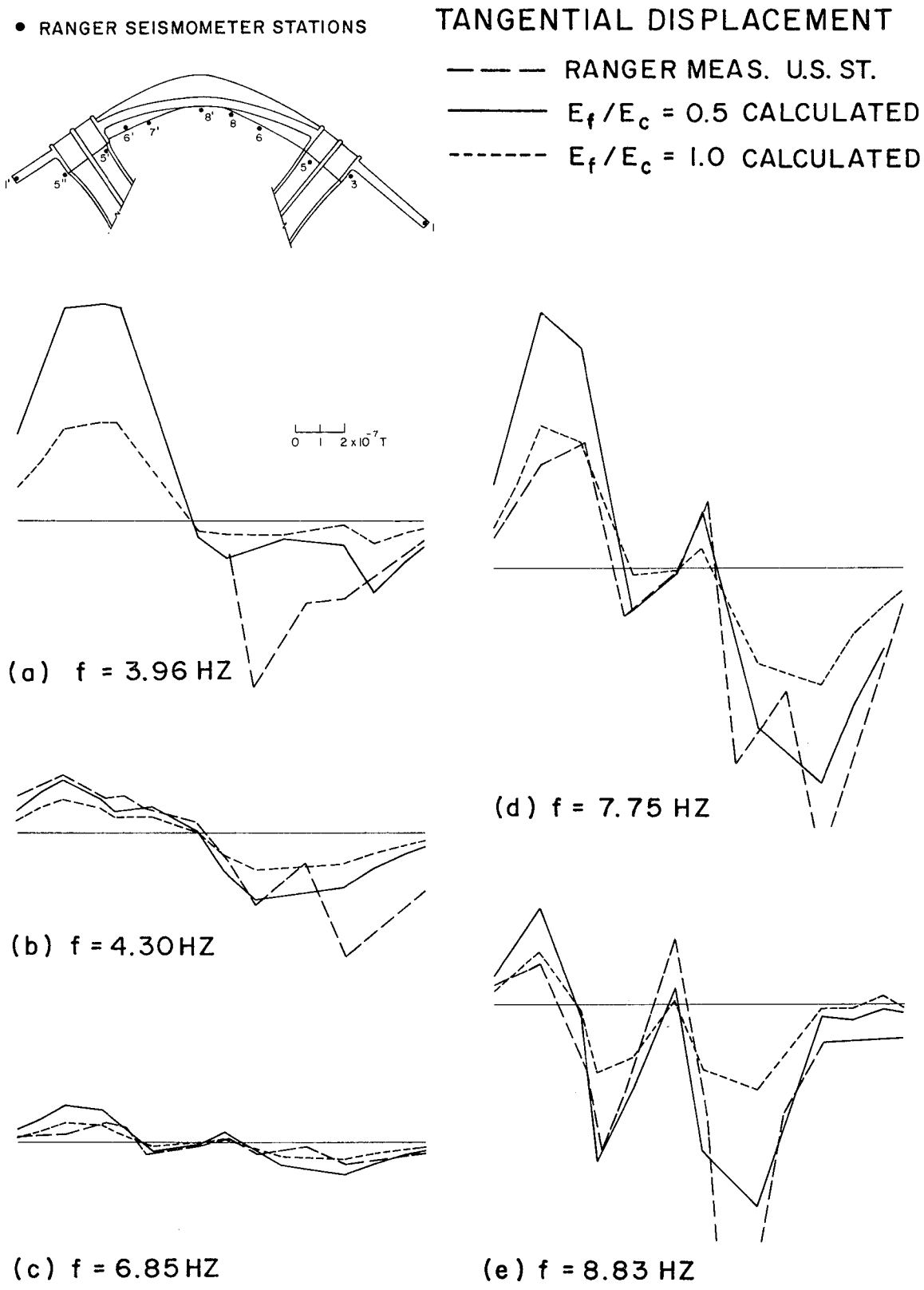

FIG. 4.2 CORRELATION OF TANGENTIAL FORCED VIBRATION MOTIONS AT DAM BASE

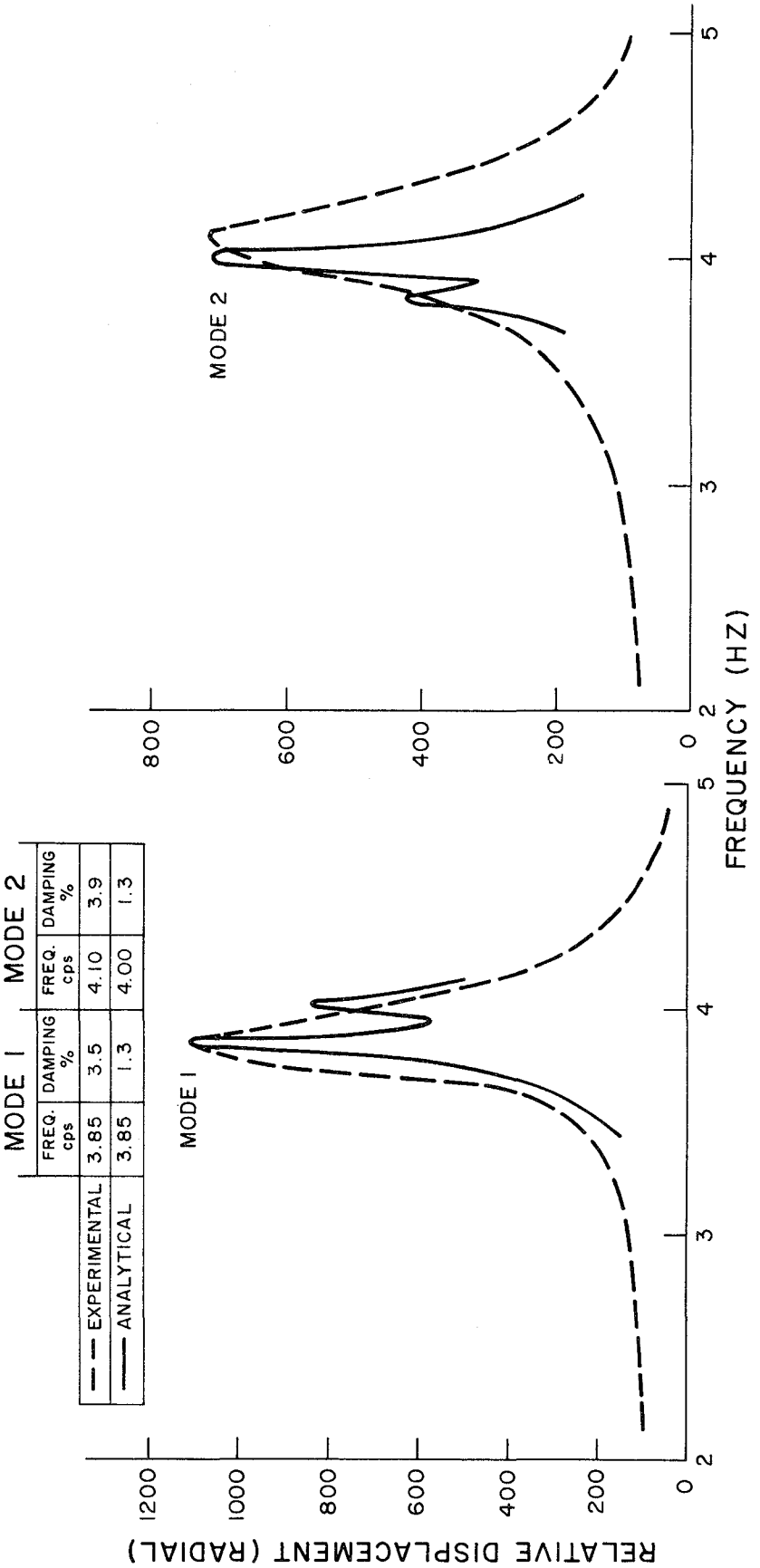

FIG. 4.3 CORRELATION OF FREQUENCY RESPONSE CURVES

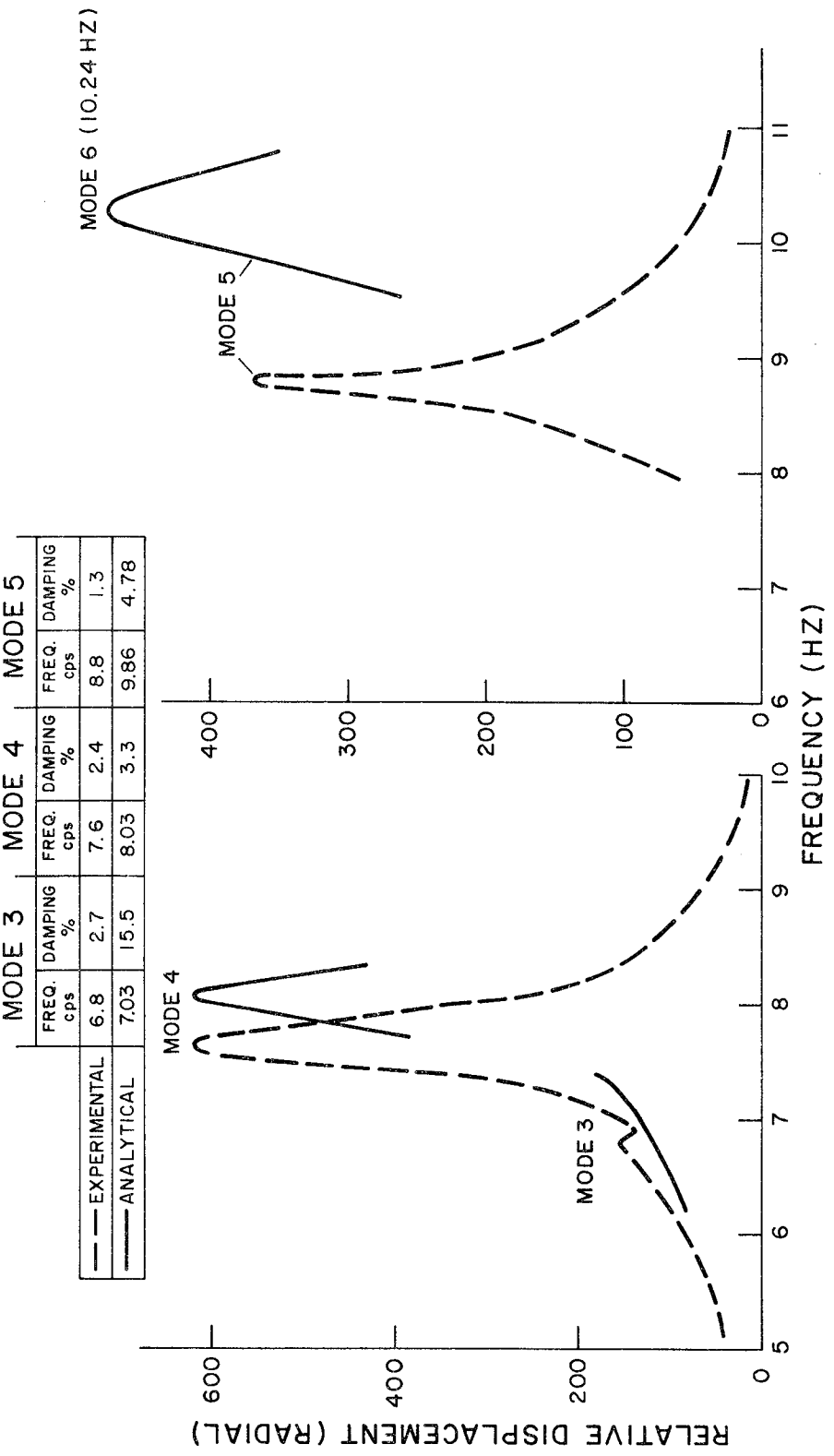

	MODE 3		MODE 4		MODE 5	
	FREQ. cps	DAMPING %	FREQ. cps	DAMPING %	FREQ. cps	DAMPING %
EXPERIMENTAL	6.8	2.7	7.6	2.4	8.8	1.3
ANALYTICAL	7.03	15.5	8.03	3.3	9.86	4.78

FIG. 4.3 (Cont'd)

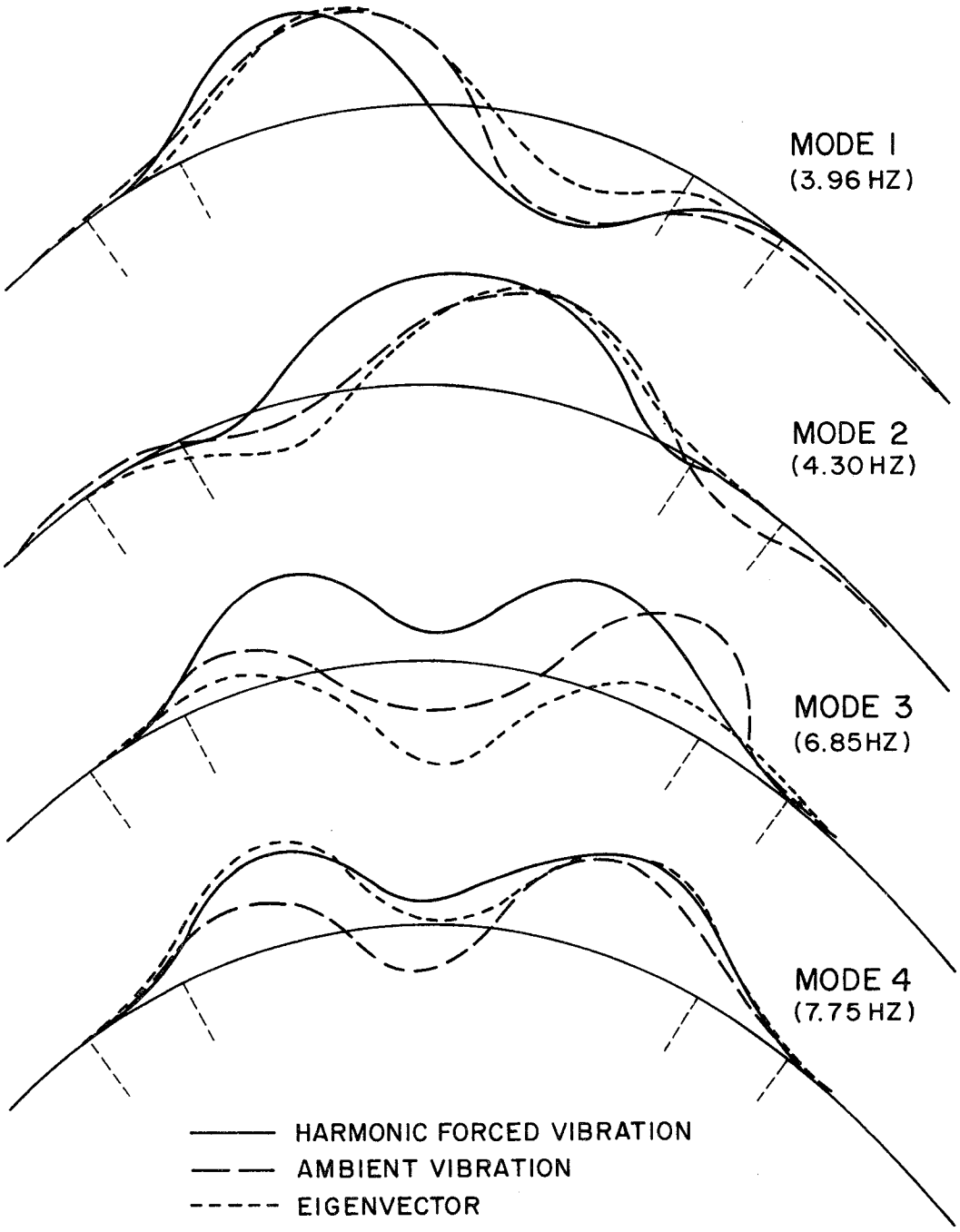

FIG. 4.4 CORRELATION OF RADIAL VIBRATION SHAPES AT CREST

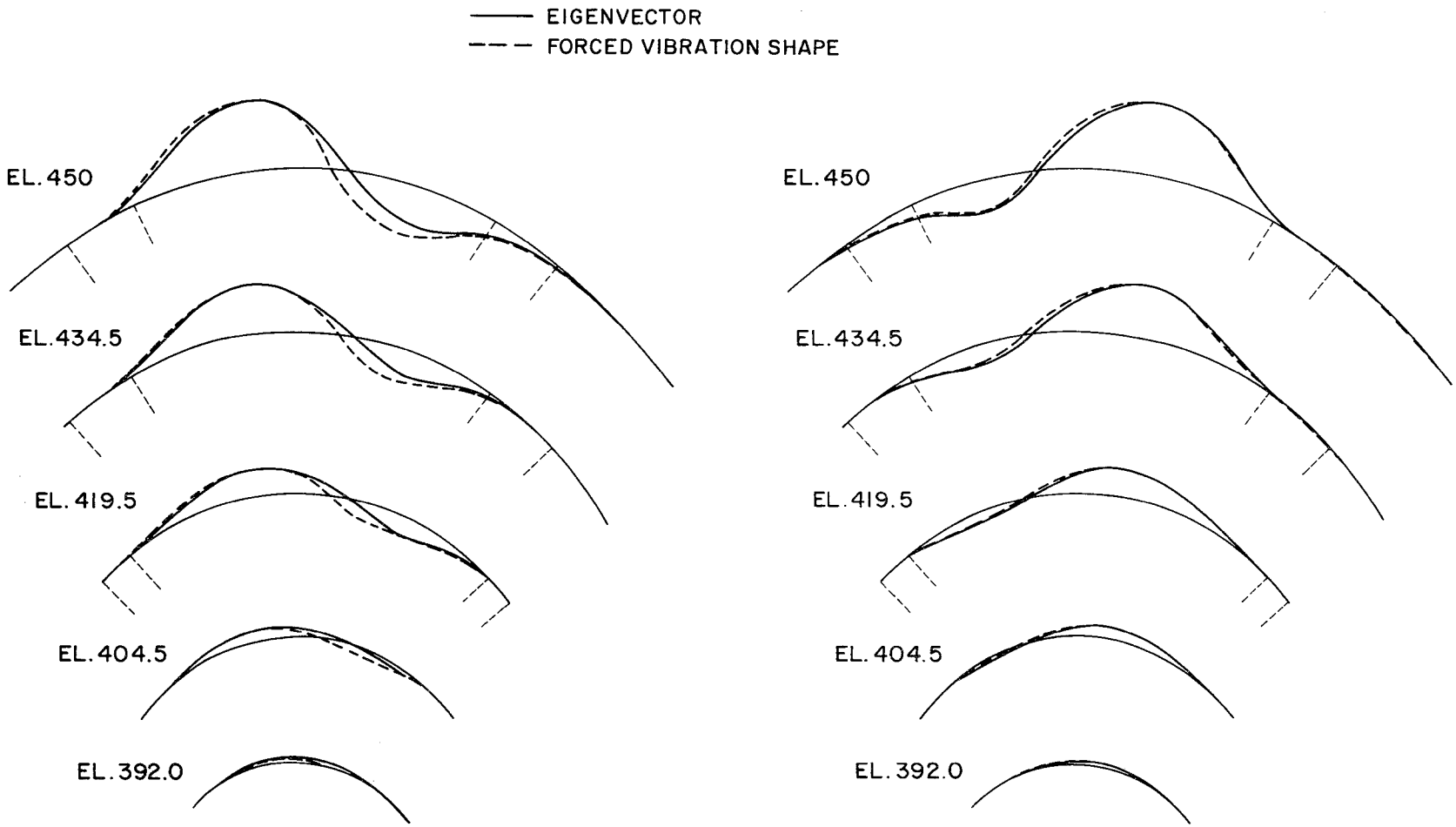

(a) MODE 1

(b) MODE 2

FIG. 4.5 CORRELATION OF CALCULATED RADIAL VIBRATION SHAPES

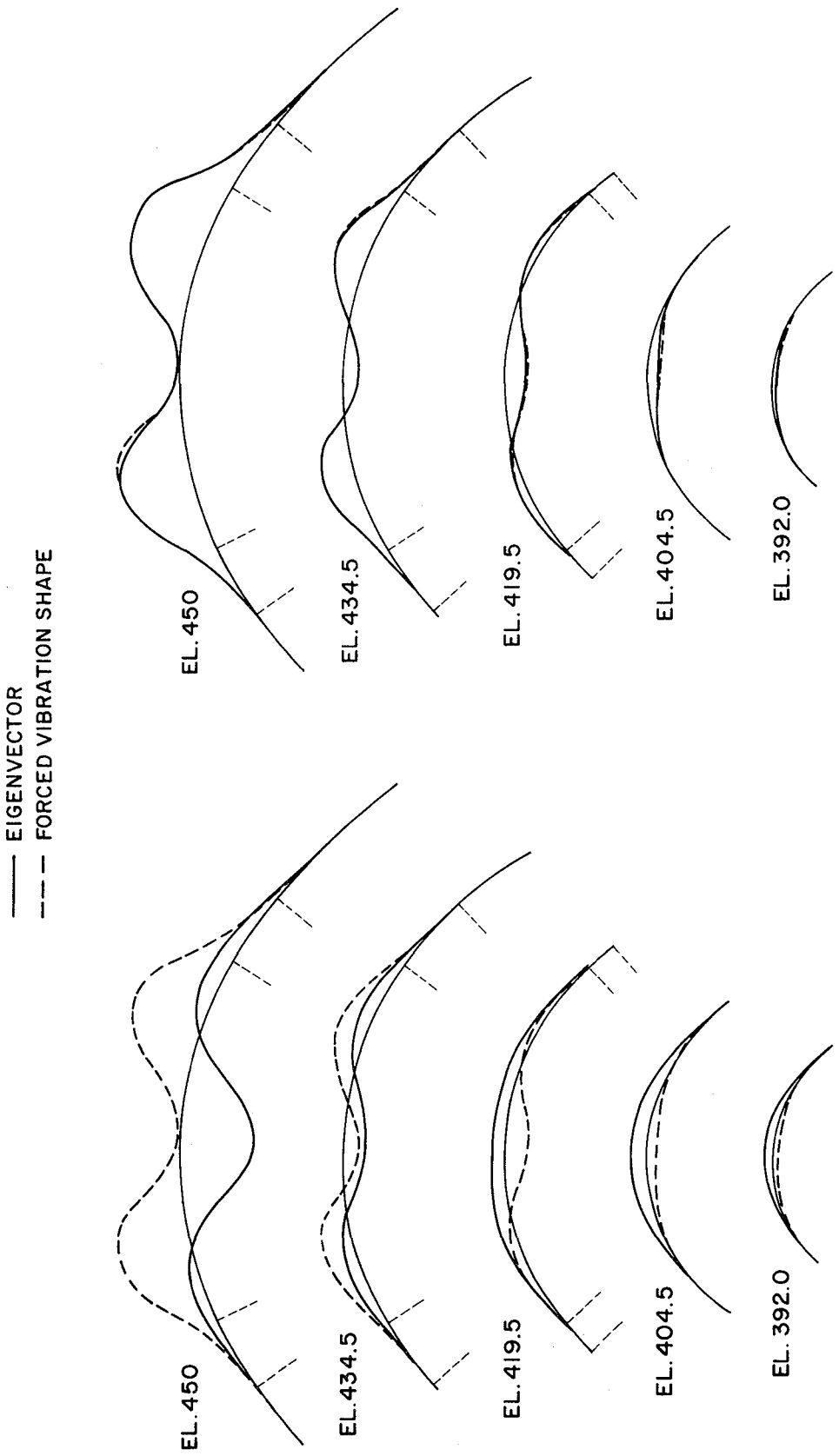
EIGENVECTOR
FORCED VIBRATION SHAPE
EL. 450
EL. 434.5
EL. 419.5
EL. 404.5
EL. 392.0
(c) MODE 3
(d) MODE 4

4.5 (Cont'd)

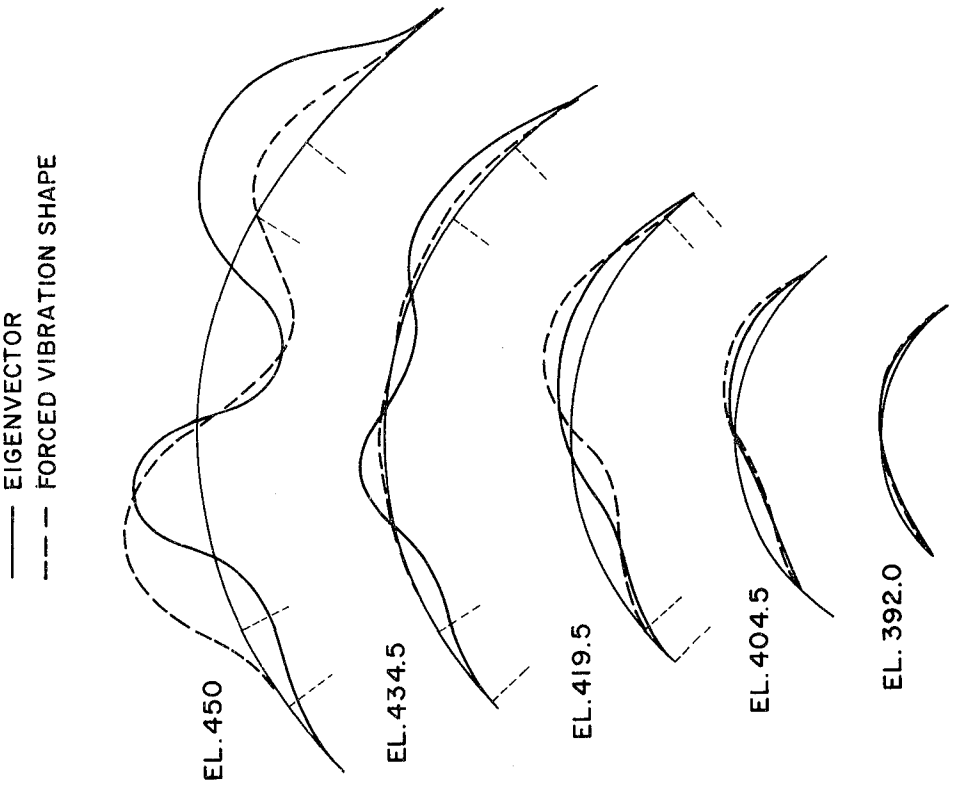

(e) MODE 5

FIG. 4.5 (Cont'd)

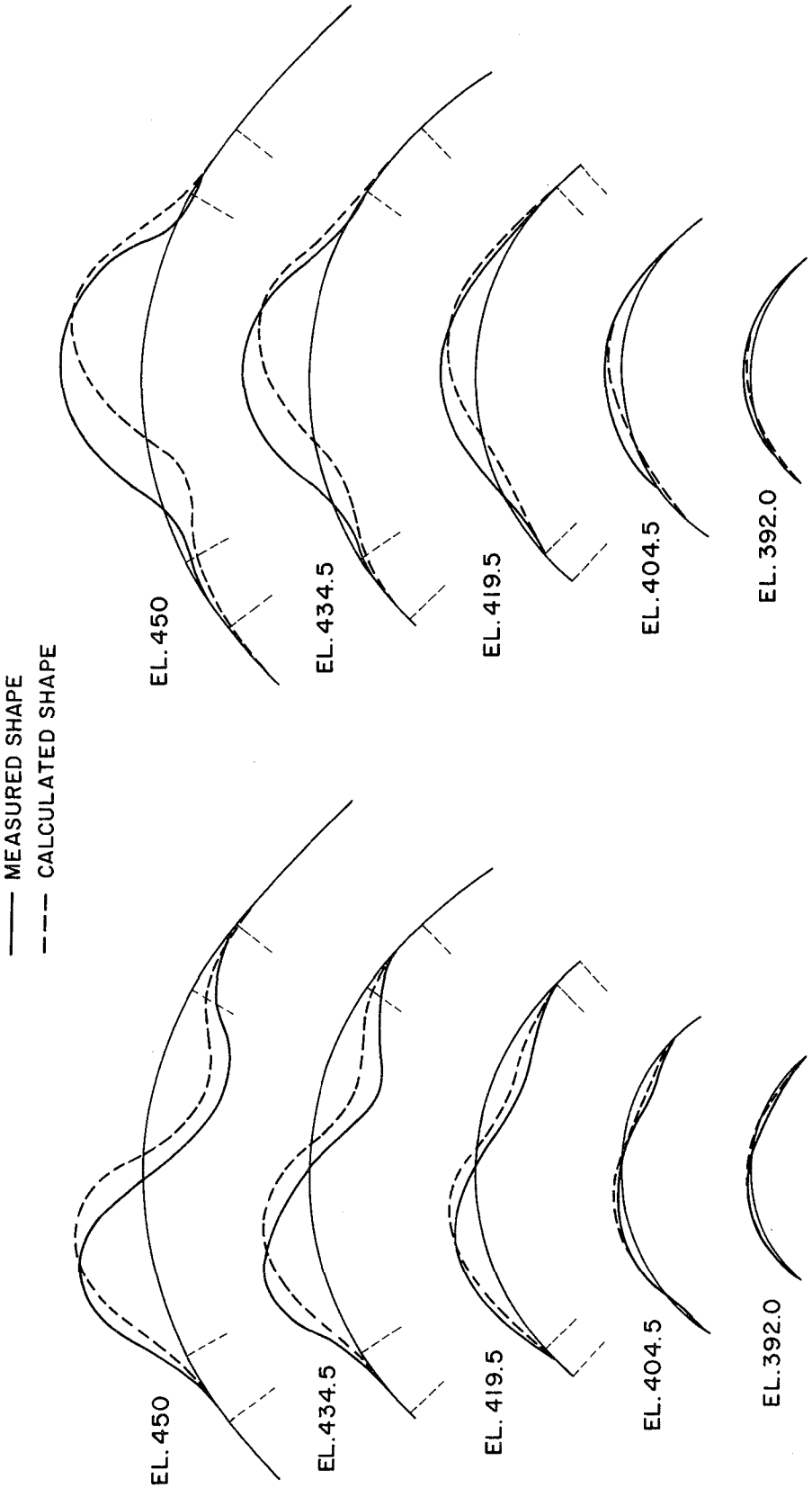

(a) FORCING FREQUENCY = 3.96 HZ

(b) FORCING FREQUENCY = 4.30 HZ

FIG. 4.6 CORRELATION OF CALCULATED AND MEASURED RADIAL FORCED VIBRATIONS

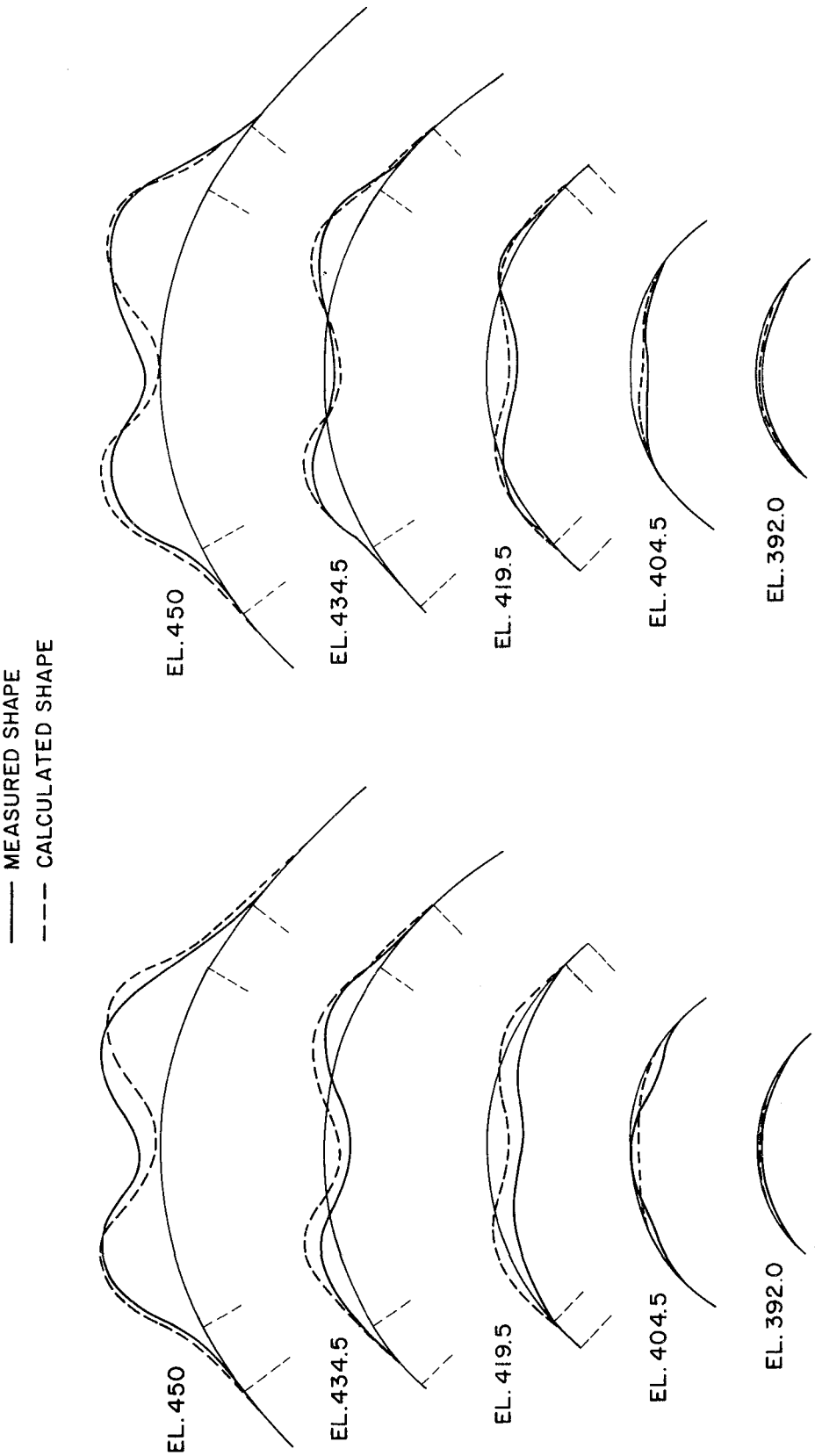

(c) FORCING FREQUENCY = 6.85 HZ

(d) FORCING FREQUENCY = 7.75 HZ

FIG. 4.6 (Cont'd)

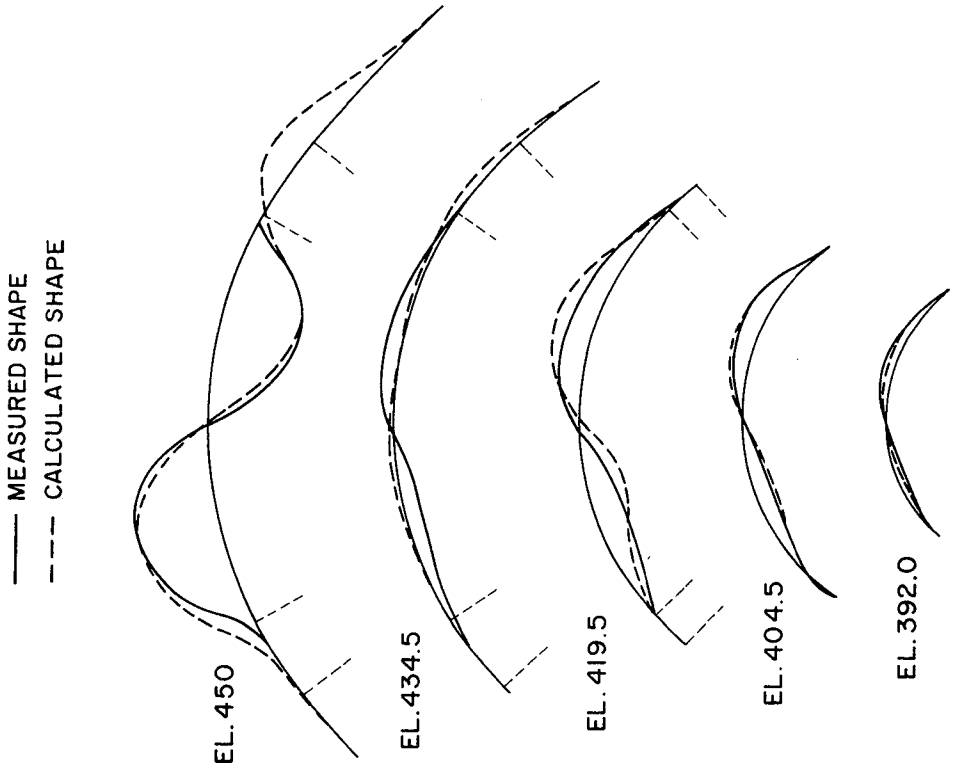

(e) FORCING FREQUENCY = 8.83 HZ

FIG. 4.6 (Cont'd)

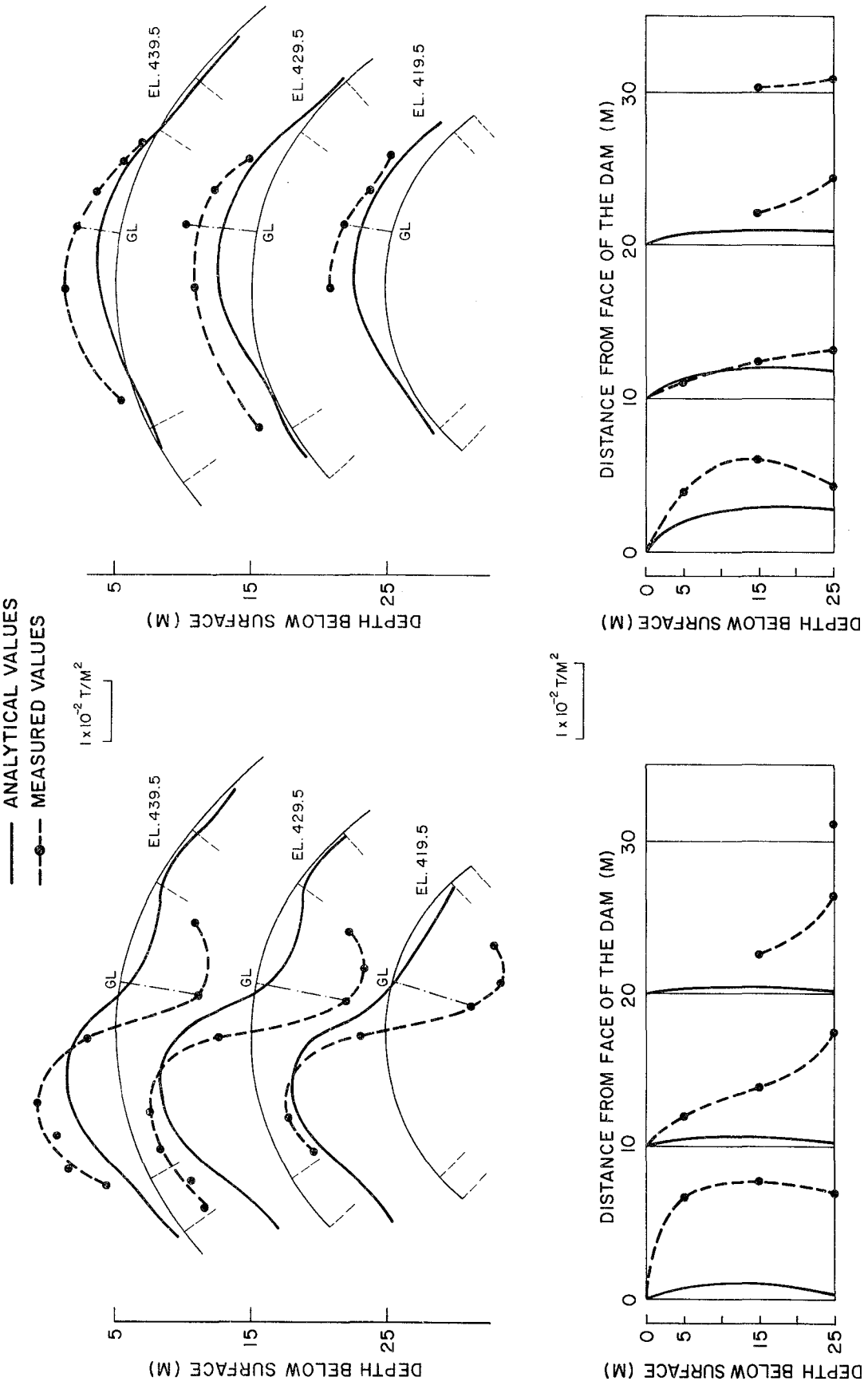

FIG. 4.7 HYDRODYNAMIC PRESSURES DUE TO EXCITATION AT 3.96 HZ

FIG. 4.8 HYDRODYNAMIC PRESSURES DUE TO EXCITATION AT 4.30 HZ

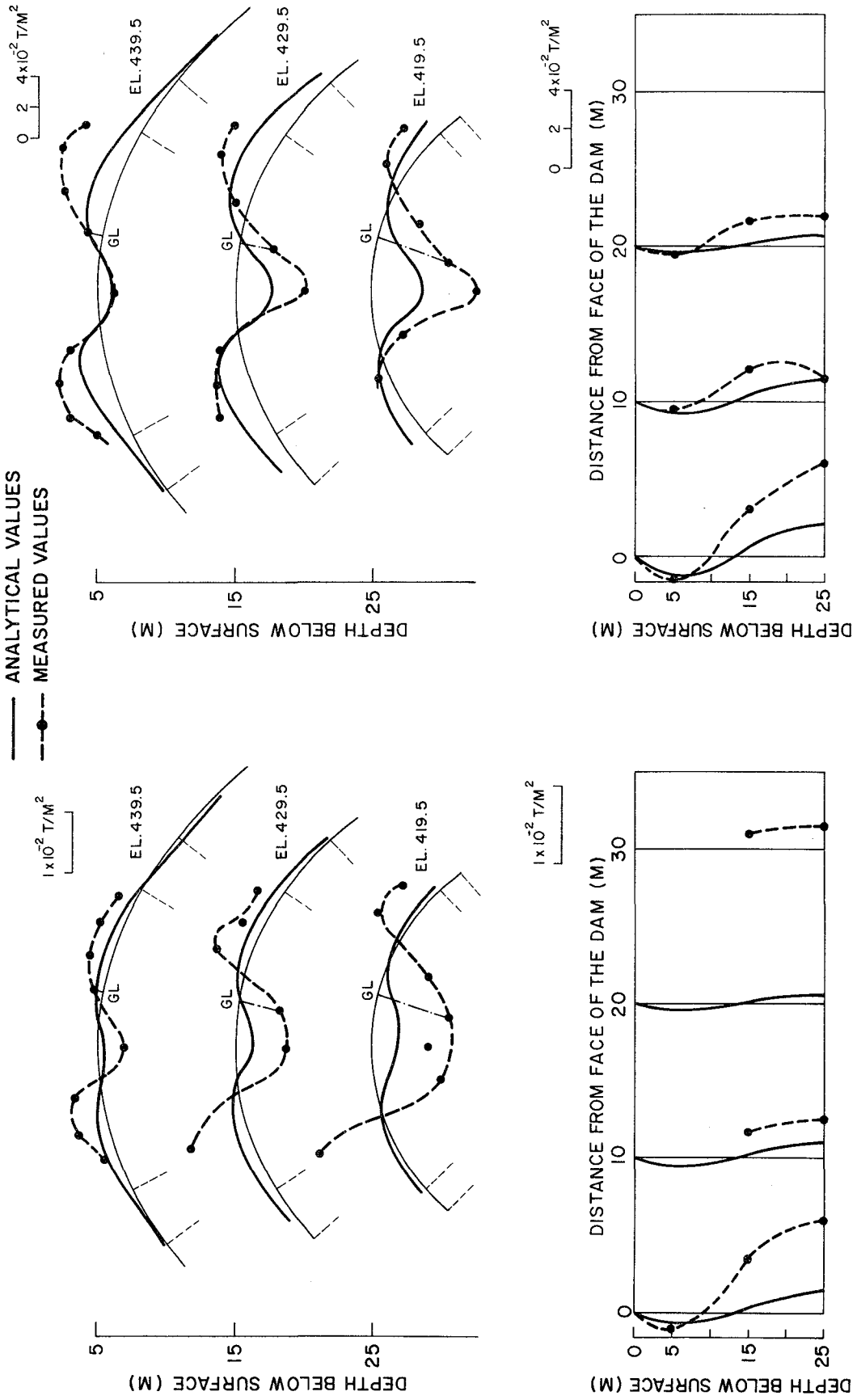

FIG. 4.10 HYDRODYNAMIC PRESSURES DUE TO EXCITATION AT 7.75 HZ

FIG. 4.9 HYDRODYNAMIC PRESSURES DUE TO EXCITATION AT 6.85 HZ

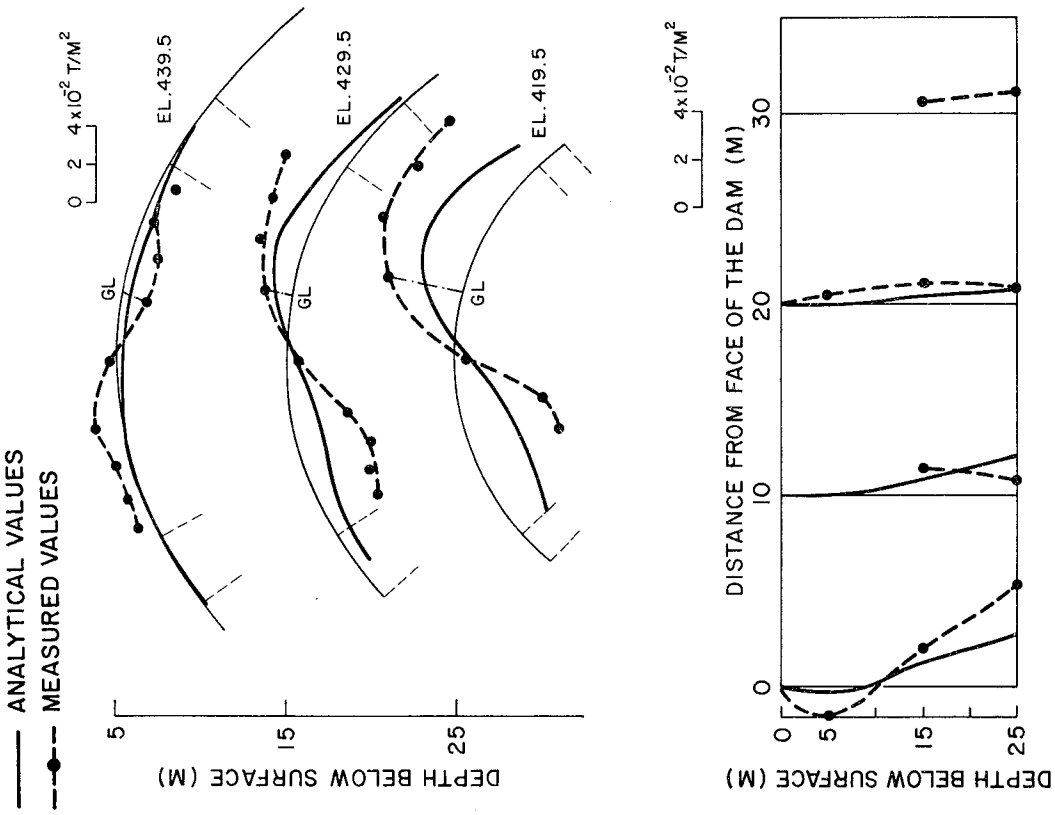

FIG. 4.11 HYDRODYNAMIC PRESSURES DUE TO EXCITATION AT 8.83 HZ

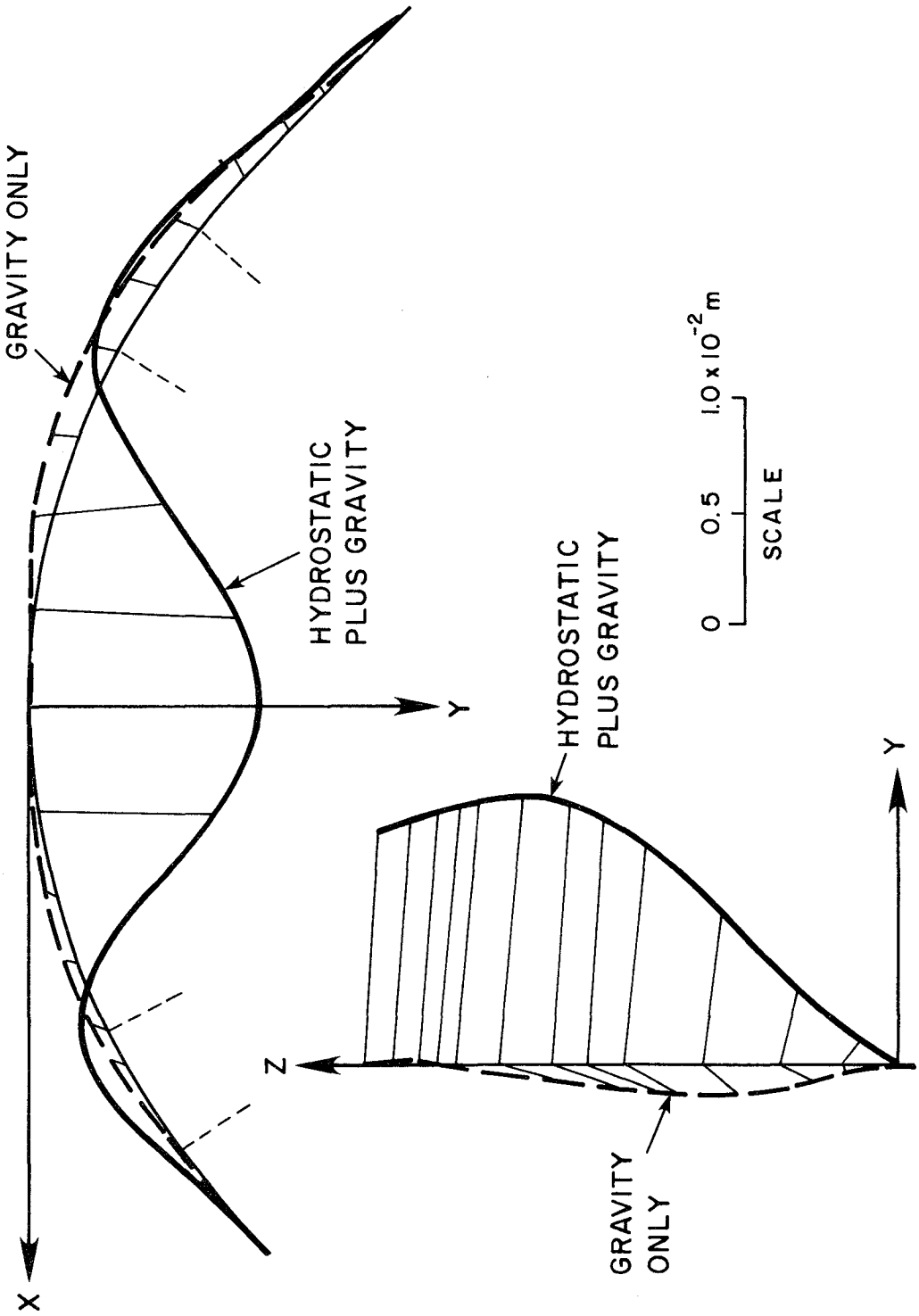

FIG. 5.1 CALCULATED STATIC DISPLACEMENTS DUE TO GRAVITY AND HYDROSTATIC LOADS

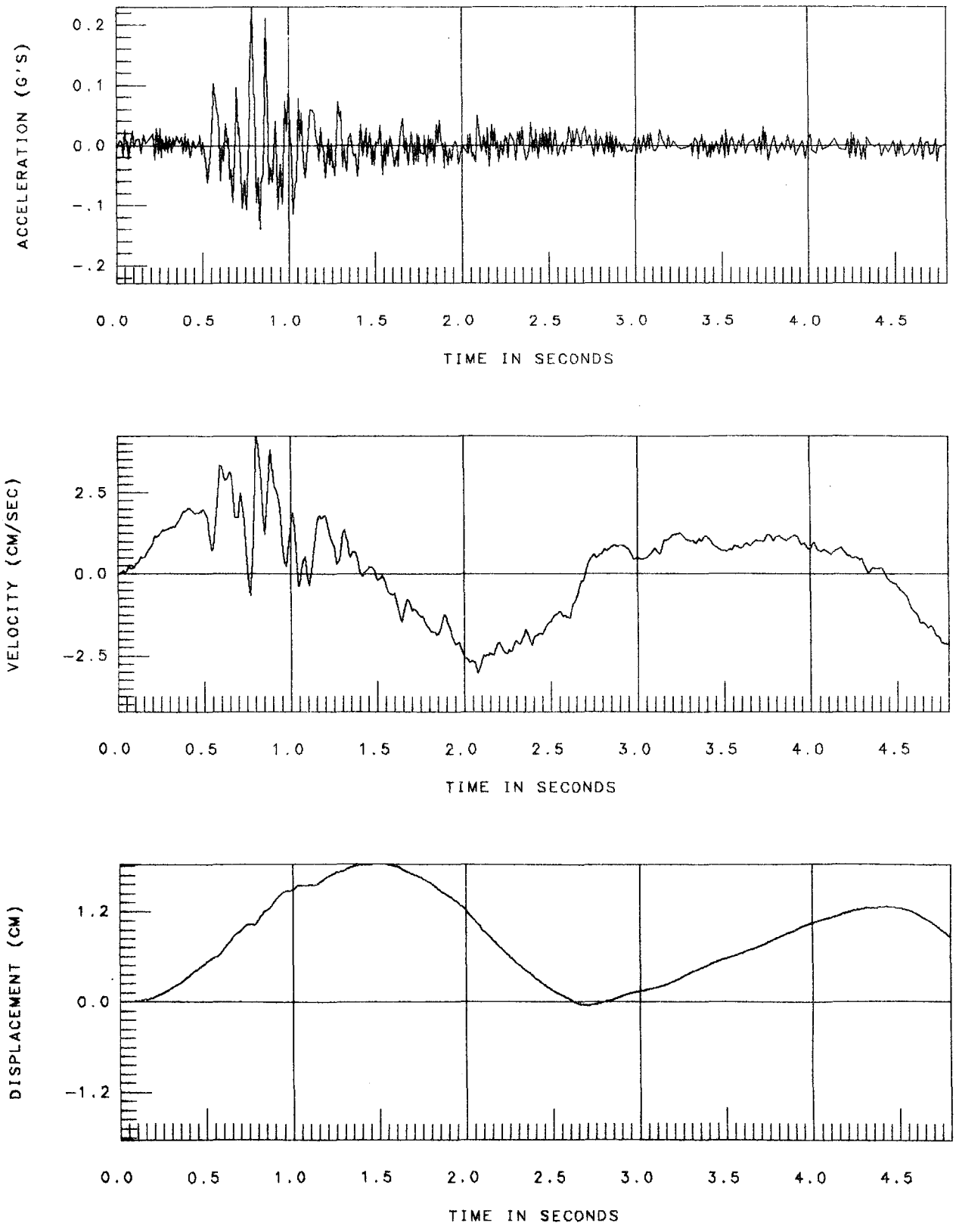

FIG. 5.2 HSIN FENG JIANG EARTHQUAKE MOTIONS (Magnified by 5)

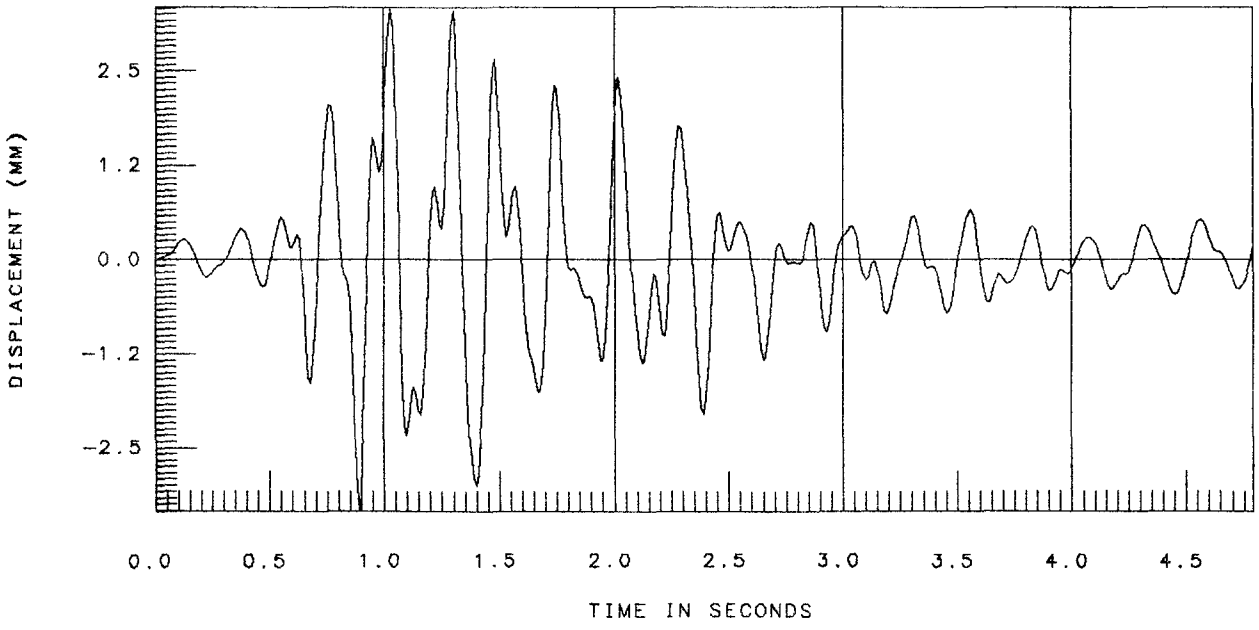

FIG. 5.3 EARTHQUAKE DISPLACEMENT RESPONSE AT MID-SECTION CREST

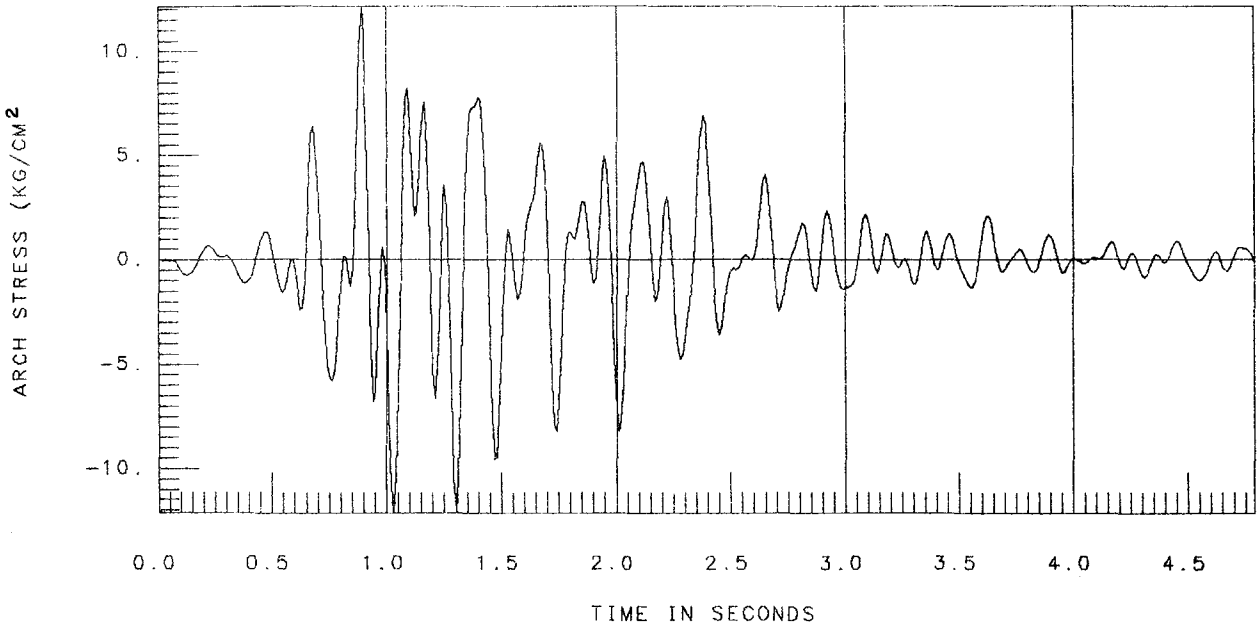

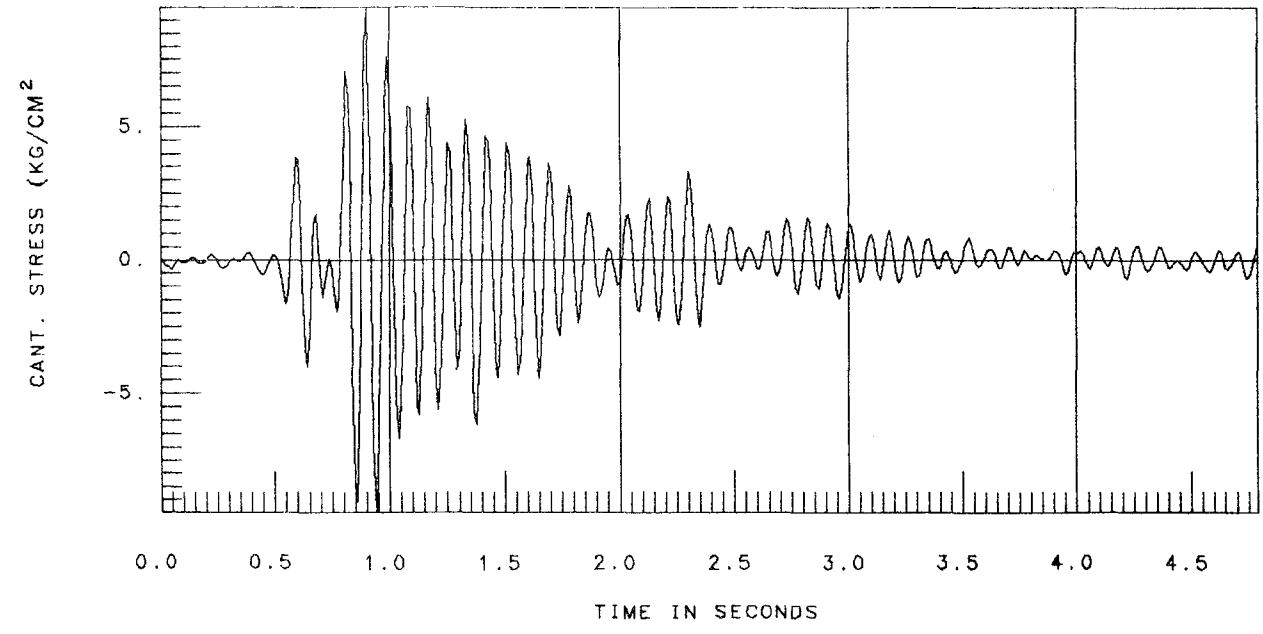

FIG. 5.4 CALCULATED DYNAMIC STRESS RESPONSE TO SEISMIC INPUT

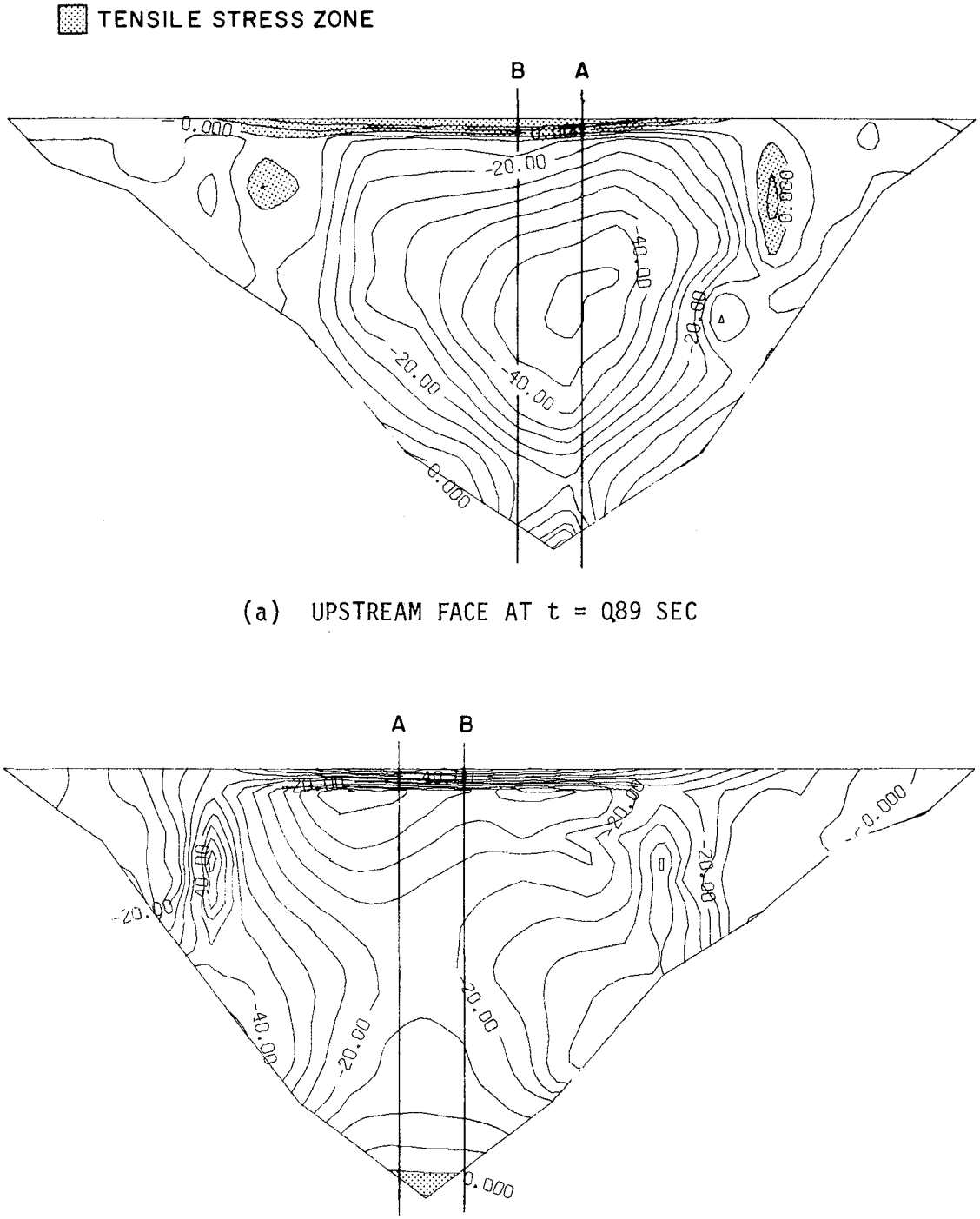

(a) UPSTREAM FACE AT t = Q89 SEC

(b) DOWNSTREAM FACE AT t = 0.89 SEC

FIG. 5.5 ARCH STRESSES DUE TO STATIC LOAD PLUS UPSTREAM-DOWNSTREAM EARTHQUAKE

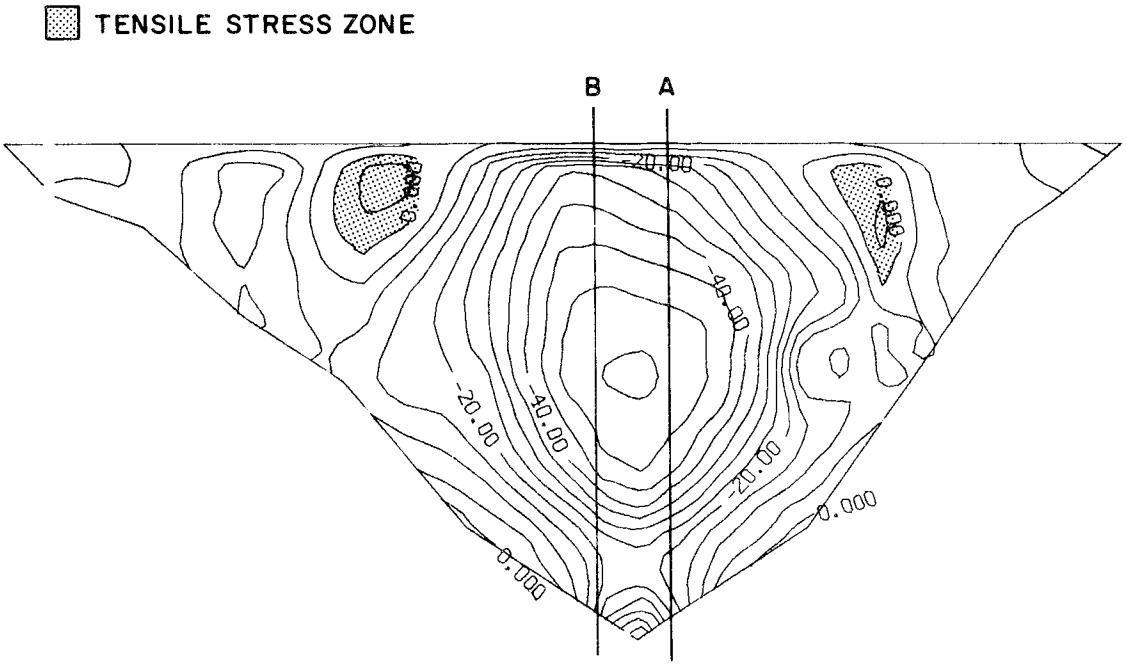

(c) UPSTREAM FACE AT t = 1.03 SEC

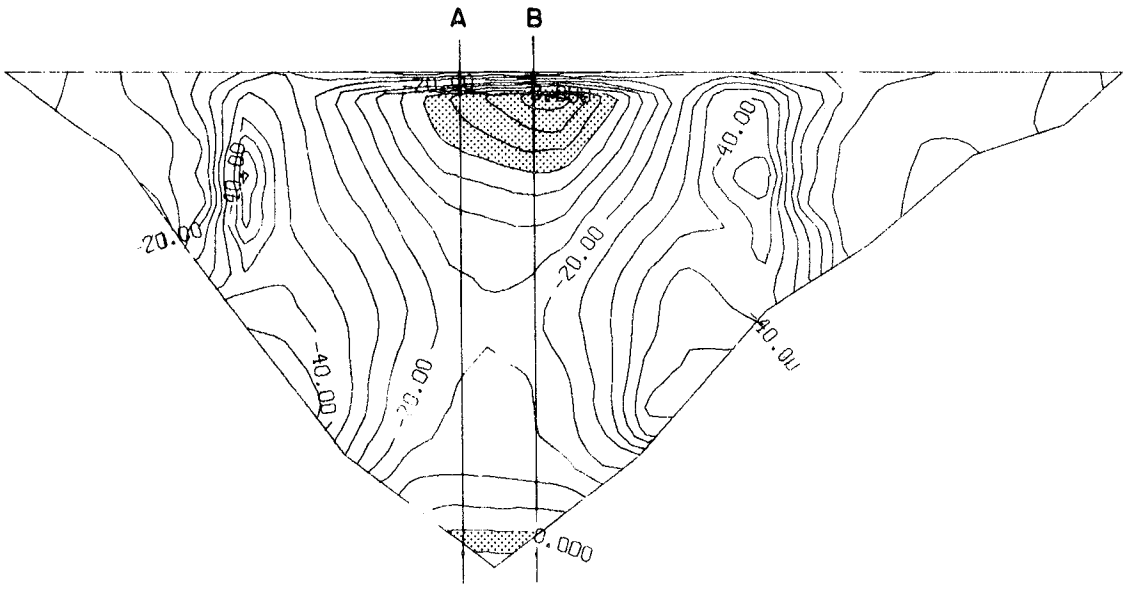

(d) DOWNSTREAM FACE AT t = 1.03 SEC

FIG. 5.5 (Cont'd)

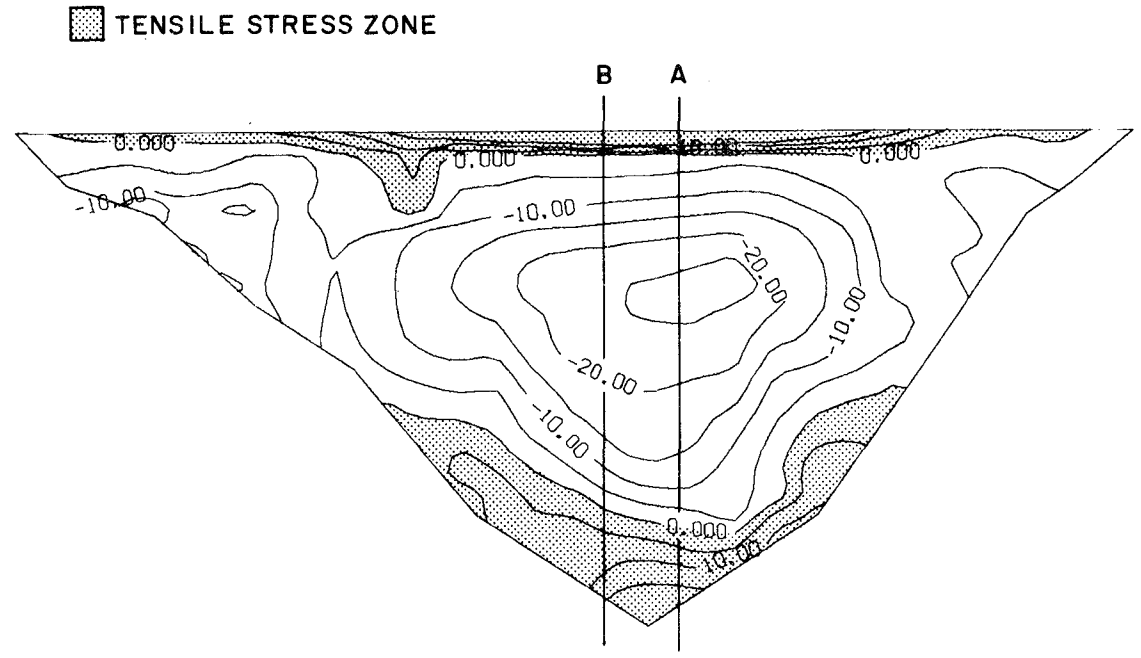

(a) UPSTREAM FACE AT t = 0.90 SEC

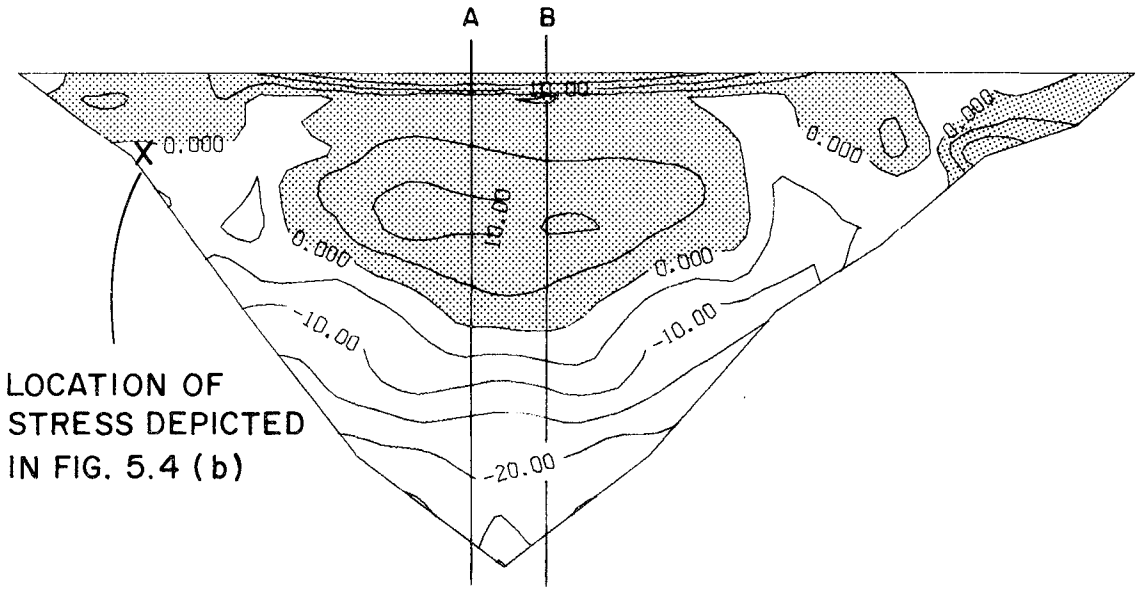

(b) DOWNSTREAM FACE AT t = 0.90 SEC

FIG. 5.6 CANTILEVER STRESSES DUE TO STATIC LOAD PLUS UPSTREAM-DOWNSTREAM EARTHQUAKE

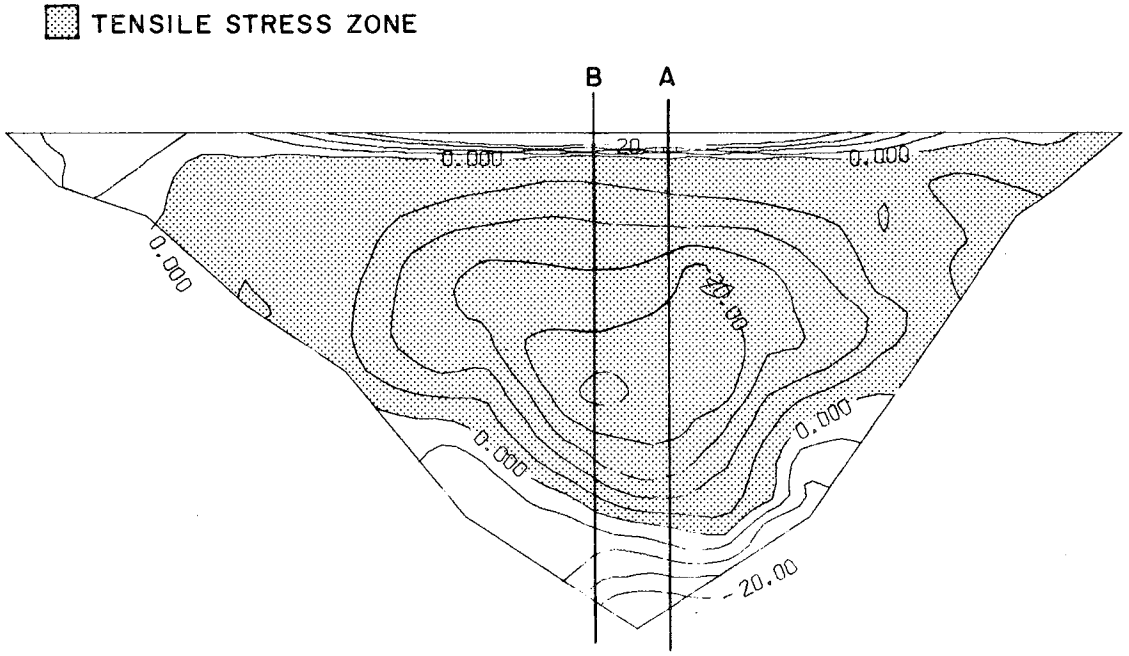

(c) UPSTREAM FACE AT t = 0.94 SEC

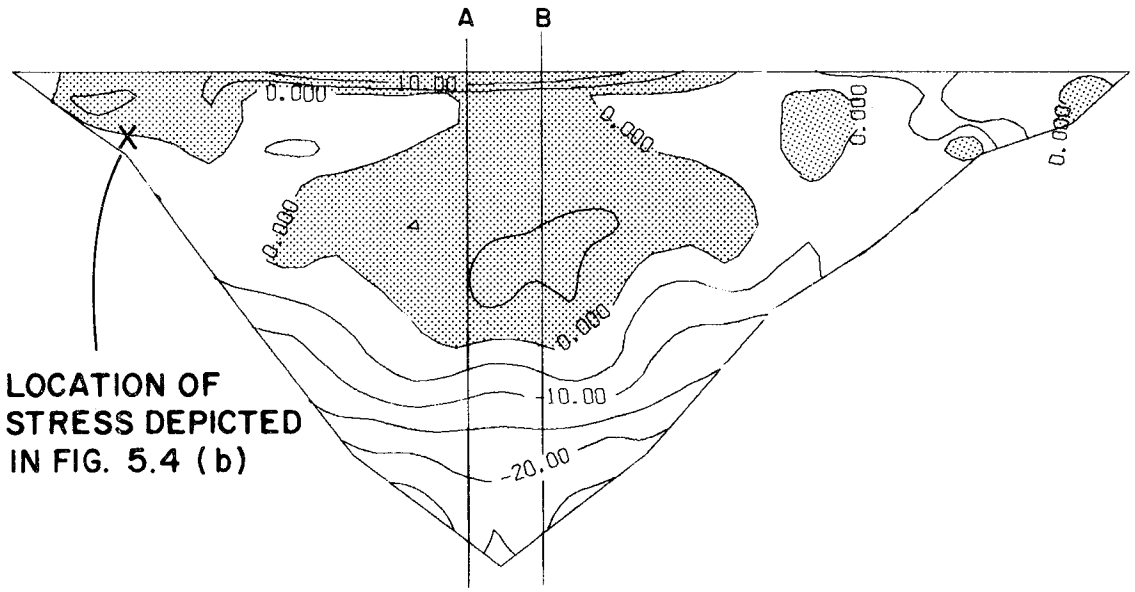

(d) DOWNSTREAM FACE AT t = 0.94 SEC

FIG. 5.6 (Cont'd)

EARTHQUAKE ENGINEERING RESEARCH CENTER REPORTS

NOTE: Numbers in parentheses are Accession Numbers assigned by the National Technical Information Service; these are followed by a price code. Copies of the reports may be ordered from the National Technical Information Service, 5285 Port Royal Road, Springfield, Virginia, 22161. Accession Numbers should be quoted on orders for reports (PB --- ---) and remittance must accompany each order. Reports without this information were not available at time of printing. The complete list of EERC reports (from EERC 67-1) is available upon request from the Earthquake Engineering Research Center, University of California, Berkeley, 47th Street and Hoffman Boulevard, Richmond, California 94804.

UCB/EERC-77/01 "PLUSH - A Computer Program for Probabilistic Finite Element Analysis of Seismic Soil-Structure Interaction," by M.P. Romo Organista, J. Lysmer and H.B. Seed - 1977 (PB81 177 651)A05

UCB/EERC-77/02 "Soil-Structure Interaction Effects at the Humboldt Bay Power Plant in the Ferndale Earthquake of June 7, 1975," by J.E. Valera, H.B. Seed, C.F. Tsai and J. Lysmer - 1977 (PB 265 795)A04

UCB/EERC-77/03 "Influence of Sample Disturbance on Sand Response to Cyclic Loading," by K. Mori, H.B. Seed and C.K. Chan - 1977 (PB 267 352)A04

UCB/EERC-77/04 "Seismological Studies of Strong Motion Records," by J. Shoja-Taheri - 1977 (PB 269 655)A10

UCB/EERC-77/05 Unassigned

UCB/EERC-77/06 "Developing Methodologies for Evaluating the Earthquake Safety of Existing Buildings," by No. 1 - B. Bresler; No. 2 - B. Bresler, T. Okada and D. Zisling; No. 3 - T. Okada and B. Bresler; No. 4 - V.V. Bertero and B. Bresler - 1977 (PB 267 354)A08

UCB/EERC-77/07 "A Literature Survey - Transverse Strength of Masonry Walls," by Y. Omote, R.L. Mayes, S.W. Chen and R.W. Clough - 1977 (PB 277 933)A07

UCB/EERC-77/08 "DRAIN-TABS: A Computer Program for Inelastic Earthquake Response of Three Dimensional Buildings," by R. Guendelman-Israel and G.H. Powell - 1977 (PB 270 693)A07

UCB/EERC-77/09 "SUBWALL: A Special Purpose Finite Element Computer Program for Practical Elastic Analysis and Design of Structural Walls with Substructure Option," by D.Q. Le, H. Peterson and E.P. Popov - 1977 (PB 270 567)A05

UCB/EERC-77/10 "Experimental Evaluation of Seismic Design Methods for Broad Cylindrical Tanks," by D.P. Clough (PB 272 280)A13

UCB/EERC-77/11 "Earthquake Engineering Research at Berkeley - 1976," - 1977 (PB 273 507)A09

UCB/EERC-77/12 "Automated Design of Earthquake Resistant Multistory Steel Building Frames," by N.D. Walker, Jr. - 1977 (PB 276 526)A09

UCB/EERC-77/13 "Concrete Confined by Rectangular Hoops Subjected to Axial Loads," by J. Vallenas, V.V. Bertero and E.P. Popov - 1977 (PB 275 165)A06

UCB/EERC-77/14 "Seismic Strain Induced in the Ground During Earthquakes," by Y. Sugimura - 1977 (PB 284 201)A04

UCB/EERC-77/15 Unassigned

UCB/EERC-77/16 "Computer Aided Optimum Design of Ductile Reinforced Concrete Moment Resisting Frames," by S.W. Zagajeski and V.V. Bertero - 1977 (PB 280 137)A07

UCB/EERC-77/17 "Earthquake Simulation Testing of a Stepping Frame with Energy-Absorbing Devices," by J.M. Kelly and D.F. Tsztoo - 1977 (PB 273 506)A04

UCB/EERC-77/18 "Inelastic Behavior of Eccentrically Braced Steel Frames under Cyclic Loadings," by C.W. Roeder and E.P. Popov - 1977 (PB 275 526)A15

UCB/EERC-77/19 "A Simplified Procedure for Estimating Earthquake-Induced Deformations in Dams and Embankments," by F.I. Makdisi and H.B. Seed - 1977 (PB 276 820)A04

UCB/EERC-77/20 "The Performance of Earth Dams during Earthquakes," by H.B. Seed, F.I. Makdisi and P. de Alba - 1977 (PB 276 821)A04

UCB/EERC-77/21 "Dynamic Plastic Analysis Using Stress Resultant Finite Element Formulation," by P. Lukkunapvasit and J.M. Kelly - 1977 (PB 275 453)A04

UCB/EERC-77/22 "Preliminary Experimental Study of Seismic Uplift of a Steel Frame," by R.W. Clough and A.A. Huckelbridge 1977 (PB 278 769)A08

UCB/EERC-77/23 "Earthquake Simulator Tests of a Nine-Story Steel Frame with Columns Allowed to Uplift," by A.A. Huckelbridge - 1977 (PB 277 944)A09

UCB/EERC-77/24 "Nonlinear Soil-Structure Interaction of Skew Highway Bridges," by M.-C. Chen and J. Penzien - 1977 (PB 276 176)A07

UCB/EERC-77/25 "Seismic Analysis of an Offshore Structure Supported on Pile Foundations," by D.D.-N. Liou and J. Penzien 1977 (PB 283 180)A06

UCB/EERC-77/26 "Dynamic Stiffness Matrices for Homogeneous Viscoelastic Half-Planes," by G. Dasgupta and A.K. Chopra - 1977 (PB 279 654)A06

UCB/EERC-77/27 "A Practical Soft Story Earthquake Isolation System," by J.M. Kelly, J.M. Eidinger and C.J. Derham - 1977 (PB 276 814)A07

UCB/EERC-77/28 "Seismic Safety of Existing Buildings and Incentives for Hazard Mitigation in San Francisco: An Exploratory Study," by A.J. Meltsner - 1977 (PB 281 970)A05

UCB/EERC-77/29 "Dynamic Analysis of Electrohydraulic Shaking Tables," by D. Rea, S. Abedi-Hayati and Y. Takahashi 1977 (PB 282 569)A04

UCB/EERC-77/30 "An Approach for Improving Seismic - Resistant Behavior of Reinforced Concrete Interior Joints," by B. Galunic, V.V. Bertero and E.P. Popov - 1977 (PB 290 870)A06

UCB/EERC-78/01 "The Development of Energy-Absorbing Devices for Aseismic Base Isolation Systems," by J.M. Kelly and D.F. Tsztoo - 1978 (PB 284 978)A04

UCB/EERC-78/02 "Effect of Tensile Prestrain on the Cyclic Response of Structural Steel Connections, by J.G. Bouwkamp and A. Mukhopadhyay - 1978

UCB/EERC-78/03 "Experimental Results of an Earthquake Isolation System using Natural Rubber Bearings," by J.M. Eidinger and J.M. Kelly - 1978 (PB 281 686)A04

UCB/EERC-78/04 "Seismic Behavior of Tall Liquid Storage Tanks," by A. Niwa - 1978 (PB 284 017)A14

UCB/EERC-78/05 "Hysteretic Behavior of Reinforced Concrete Columns Subjected to High Axial and Cyclic Shear Forces," by S.W. Zagajeski, V.V. Bertero and J.G. Bouwkamp - 1978 (PB 283 858)A13

UCB/EERC-78/06 "Three Dimensional Inelastic Frame Elements for the ANSR-I Program," by A. Riahi, D.G. Row and G.H. Powell - 1978 (PB 295 755)A04

UCB/EERC-78/07 "Studies of Structural Response to Earthquake Ground Motion," by O.A. Lopez and A.K. Chopra - 1978 (PB 282 790)A05

UCB/EERC-78/08 "A Laboratory Study of the Fluid-Structure Interaction of Submerged Tanks and Caissons in Earthquakes," by R.C. Byrd - 1978 (PB 284 957)A08

UCB/EERC-78/09 Unassigned

UCB/EERC-78/10 "Seismic Performance of Nonstructural and Secondary Structural Elements," by I. Sakamoto - 1978 (PB81 154 593)A05

UCB/EERC-78/11 "Mathematical Modelling of Hysteresis Loops for Reinforced Concrete Columns," by S. Nakata, T. Sproul and J. Penzien - 1978 (PB 298 274)A05

UCB/EERC-78/12 "Damageability in Existing Buildings," by T. Blejwas and B. Bresler - 1978 (PB 80 166 978)A05

UCB/EERC-78/13 "Dynamic Behavior of a Pedestal Base Multistory Building," by R.M. Stephen, E.L. Wilson, J.G. Bouwkamp and M. Button - 1978 (PB 286 650)A08

UCB/EERC-78/14 "Seismic Response of Bridges - Case Studies," by R.A. Imbsen, V. Nutt and J. Penzien - 1978 (PB 286 503)A10

UCB/EERC-78/15 "A Substructure Technique for Nonlinear Static and Dynamic Analysis," by D.G. Row and G.H. Powell - 1978 (PB 288 077)A10

UCB/EERC-78/16 "Seismic Risk Studies for San Francisco and for the Greater San Francisco Bay Area," by C.S. Oliveira - 1978 (PB 81 120 115)A07

UCB/EERC-78/17 "Strength of Timber Roof Connections Subjected to Cyclic Loads," by P. Gülkan, R.L. Mayes and R.W. Clough - 1978 (HUD-000 1491)A07

UCB/EERC-78/18 "Response of K-Braced Steel Frame Models to Lateral Loads," by J.G. Bouwkamp, R.M. Stephen and E.P. Popov - 1978

UCB/EERC-78/19 "Rational Design Methods for Light Equipment in Structures Subjected to Ground Motion," by J.L. Sackman and J.M. Kelly - 1978 (PB 292 357)A04

UCB/EERC-78/20 "Testing of a Wind Restraint for Aseismic Base Isolation," by J.M. Kelly and D.E. Chitty - 1978 (PB 292 833)A03

UCB/EERC-78/21 "APOLLO - A Computer Program for the Analysis of Pore Pressure Generation and Dissipation in Horizontal Sand Layers During Cyclic or Earthquake Loading," by P.P. Martin and H.B. Seed - 1978 (PB 292 835)A04

UCB/EERC-78/22 "Optimal Design of an Earthquake Isolation System," by M.A. Bhatti, K.S. Pister and E. Polak - 1978 (PB 294 735)A06

UCB/EERC-78/23 "MASH - A Computer Program for the Non-Linear Analysis of Vertically Propagating Shear Waves in Horizontally Layered Deposits," by P.P. Martin and H.B. Seed - 1978 (PB 293 101)A05

UCB/EERC-78/24 "Investigation of the Elastic Characteristics of a Three Story Steel Frame Using System Identification," by I. Kaya and H.D. McNiven - 1978 (PB 296 225)A06

UCB/EERC-78/25 "Investigation of the Nonlinear Characteristics of a Three-Story Steel Frame Using System Identification," by I. Kaya and H.D. McNiven - 1978 (PB 301 363)A05

UCB/EERC-78/26 "Studies of Strong Ground Motion in Taiwan," by Y.M. Hsiung, B.A. Bolt and J. Penzien - 1978 (PB 298 436)A06

UCB/EERC-78/27 "Cyclic Loading Tests of Masonry Single Piers: Volume 1 - Height to Width Ratio of 2," by P.A. Hidalgo, R.L. Mayes, H.D. McNiven and R.W. Clough - 1978 (PB 296 211)A07

UCB/EERC-78/28 "Cyclic Loading Tests of Masonry Single Piers: Volume 2 - Height to Width Ratio of 1," by S.-W.J. Chen, P.A. Hidalgo, R.L. Mayes, R.W. Clough and H.D. McNiven - 1978 (PB 296 212)A09

UCB/EERC-78/29 "Analytical Procedures in Soil Dynamics," by J. Lysmer - 1978 (PB 298 445)A06

UCB/EERC-79/01 "Hysteretic Behavior of Lightweight Reinforced Concrete Beam-Column Subassemblages," by B. Forzani, E.P. Popov and V.V. Bertero - April 1979(PB 298 267)A06

UCB/EERC-79/02 "The Development of a Mathematical Model to Predict the Flexural Response of Reinforced Concrete Beams to Cyclic Loads, Using System Identification," by J. Stanton & H. McNiven - Jan. 1979(PB 295 875)A10

UCB/EERC-79/03 "Linear and Nonlinear Earthquake Response of Simple Torsionally Coupled Systems," by C.L. Kan and A.K. Chopra - Feb. 1979(PB 298 262)A06

UCB/EERC-79/04 "A Mathematical Model of Masonry for Predicting its Linear Seismic Response Characteristics," by Y. Mengi and H.D. McNiven - Feb. 1979(PB 298 266)A06

UCB/EERC-79/05 "Mechanical Behavior of Lightweight Concrete Confined by Different Types of Lateral Reinforcement," by M.A. Manrique, V.V. Bertero and E.P. Popov - May 1979(PB 301 114)A06

UCB/EERC-79/06 "Static Tilt Tests of a Tall Cylindrical Liquid Storage Tank," by R.W. Clough and A. Niwa - Feb. 1979 (PB 301 167)A06

UCB/EERC-79/07 "The Design of Steel Energy Absorbing Restrainers and Their Incorporation into Nuclear Power Plants for Enhanced Safety: Volume 1 - Summary Report," by P.N. Spencer, V.F. Zackay, and E.R. Parker - Feb. 1979(UCB/EERC-79/07)A09

UCB/EERC-79/08 "The Design of Steel Energy Absorbing Restrainers and Their Incorporation into Nuclear Power Plants for Enhanced Safety: Volume 2 - The Development of Analyses for Reactor System Piping,""Simple Systems" by M.C. Lee, J. Penzien, A.K. Chopra and K, Suzuki "Complex Systems" by G.H. Powell, E.L. Wilson, R.W. Clough and D.G. Row - Feb. 1979(UCB/EERC-79/08)A10

UCB/EERC-79/09 "The Design of Steel Energy Absorbing Restrainers and Their Incorporation into Nuclear Power Plants for Enhanced Safety: Volume 3 - Evaluation of Commercial Steels," by W.S. Owen, R.M.N. Pelloux, R.O. Ritchie, M. Faral, T. Ohhashi, J. Toplosky, S.J. Hartman, V.F. Zackay and E.R. Parker - Feb. 1979(UCB/EERC-79/09)A04

UCB/EERC-79/10 "The Design of Steel Energy Absorbing Restrainers and Their Incorporation into Nuclear Power Plants for Enhanced Safety: Volume 4 - A Review of Energy-Absorbing Devices," by J.M. Kelly and M.S. Skinner - Feb. 1979(UCB/EERC-79/10)A04

UCB/EERC-79/11 "Conservatism In Summation Rules for Closely Spaced Modes," by J.M. Kelly and J.L. Sackman - May 1979(PB 301 328)A03

UCB/EERC-79/12 "Cyclic Loading Tests of Masonry Single Piers; Volume 3 - Height to Width Ratio of 0.5," by P.A. Hidalgo, R.L. Mayes, H.D. McNiven and R.W. Clough - May 1979(PB 301 321)A08

UCB/EERC-79/13 "Cyclic Behavior of Dense Course-Grained Materials in Relation to the Seismic Stability of Dams," by N.G. Banerjee, H.B. Seed and C.K. Chan - June 1979(PB 301 373)A13

UCB/EERC-79/14 "Seismic Behavior of Reinforced Concrete Interior Beam-Column Subassemblages," by S. Viwathanatepa, E.P. Popov and V.V. Bertero - June 1979(PB 301 326)A10

UCB/EERC-79/15 "Optimal Design of Localized Nonlinear Systems with Dual Performance Criteria Under Earthquake Excitations," by M.A. Bhatti - July 1979(PB 80 167 109)A06

UCB/EERC-79/16 "OPTDYN - A General Purpose Optimization Program for Problems with or without Dynamic Constraints," by M.A. Bhatti, E. Polak and K.S. Pister - July 1979(PB 80 167 091)A05

UCB/EERC-79/17 "ANSR-II, Analysis of Nonlinear Structural Response, Users Manual," by D.P. Mondkar and G.H. Powell July 1979(PB 80 113 301)A05

UCB/EERC-79/18 "Soil Structure Interaction in Different Seismic Environments," A. Gomez-Masso, J. Lysmer, J.-C. Chen and H.B. Seed - August 1979(PB 80 101 520)A04

UCB/EERC-79/19 "ARMA Models for Earthquake Ground Motions," by M.K. Chang, J.W. Kwiatkowski, R.F. Nau, R.M. Oliver and K.S. Pister - July 1979(PB 301 166)A05

UCB/EERC-79/20 "Hysteretic Behavior of Reinforced Concrete Structural Walls," by J.M. Vallenas, V.V. Bertero and E.P. Popov - August 1979(PB 80 165 905)A12

UCB/EERC-79/21 "Studies on High-Frequency Vibrations of Buildings - 1: The Column Effect," by J. Lubliner - August 1979 (PB 80 158 553)A03

UCB/EERC-79/22 "Effects of Generalized Loadings on Bond Reinforcing Bars Embedded in Confined Concrete Blocks," by S. Viwathanatepa, E.P. Popov and V.V. Bertero - August 1979(PB 81 124 018)A14

UCB/EERC-79/23 "Shaking Table Study of Single-Story Masonry Houses, Volume 1: Test Structures 1 and 2," by P. Gülkan, R.L. Mayes and R.W. Clough - Sept. 1979 (HUD-000 1763)A12

UCB/EERC-79/24 "Shaking Table Study of Single-Story Masonry Houses, Volume 2: Test Structures 3 and 4," by P. Gülkan, R.L. Mayes and R.W. Clough - Sept. 1979 (HUD-000 1836)A12

UCB/EERC-79/25 "Shaking Table Study of Single-Story Masonry Houses, Volume 3: Summary, Conclusions and Recommendations," by R.W. Clough, R.L. Mayes and P. Gülkan - Sept. 1979 (HUD-000 1837)A06

UCB/EERC-79/26 "Recommendations for a U.S.-Japan Cooperative Research Program Utilizing Large-Scale Testing Facilities," by U.S.-Japan Planning Group - Sept. 1979(PB 301 407)A06

UCB/EERC-79/27 "Earthquake-Induced Liquefaction Near Lake Amatitlan, Guatemala," by H.B. Seed, I. Arango, C.K. Chan, A. Gomez-Masso and R. Grant de Ascoli - Sept. 1979(NUREG-CR1341)A03

UCB/EERC-79/28 "Infill Panels: Their Influence on Seismic Response of Buildings," by J.W. Axley and V.V. Bertero Sept. 1979(PB 80 163 371)A10

UCB/EERC-79/29 "3D Truss Bar Element (Type 1) for the ANSR-II Program," by D.P. Mondkar and G.H. Powell - Nov. 1979 (PB 80 169 709)A02

UCB/EERC-79/30 "2D Beam-Column Element (Type 5 - Parallel Element Theory) for the ANSR-II Program," by D.G. Row, G.H. Powell and D.P. Mondkar - Dec. 1979(PB 80 167 224)A03

UCB/EERC-79/31 "3D Beam-Column Element (Type 2 - Parallel Element Theory) for the ANSR-II Program," by A. Riahi, G.H. Powell and D.P. Mondkar - Dec. 1979(PB 80 167 216)A03

UCB/EERC-79/32 "On Response of Structures to Stationary Excitation," by A. Der Kiureghian - Dec. 1979(PB 80166 929)A03

UCB/EERC-79/33 "Undisturbed Sampling and Cyclic Load Testing of Sands," by S. Singh, H.B. Seed and C.K. Chan Dec. 1979(ADA 087 298)A07

UCB/EERC-79/34 "Interaction Effects of Simultaneous Torsional and Compressional Cyclic Loading of Sand," by P.M. Griffin and W.N. Houston - Dec. 1979(ADA 092 352)A15

UCB/EERC-80/01 "Earthquake Response of Concrete Gravity Dams Including Hydrodynamic and Foundation Interaction Effects," by A.K. Chopra, P. Chakrabarti and S. Gupta - Jan. 1980(AD-A087297)A10

UCB/EERC-80/02 "Rocking Response of Rigid Blocks to Earthquakes," by C.S. Yim, A.K. Chopra and J. Penzien - Jan. 1980 (PB80 166 002)A04

UCB/EERC-80/03 "Optimum Inelastic Design of Seismic-Resistant Reinforced Concrete Frame Structures," by S.W. Zagajeski and V.V. Bertero - Jan. 1980(PB80 164 635)A06

UCB/EERC-80/04 "Effects of Amount and Arrangement of Wall-Panel Reinforcement on Hysteretic Behavior of Reinforced Concrete Walls," by R. Iliya and V.V. Bertero - Feb. 1980(PB81 122 525)A09

UCB/EERC-80/05 "Shaking Table Research on Concrete Dam Models," by A. Niwa and R.W. Clough - Sept. 1980(PB81 122 368)A06

UCB/EERC-80/06 "The Design of Steel Energy-Absorbing Restrainers and their Incorporation into Nuclear Power Plants for Enhanced Safety (Vol 1A): Piping with Energy Absorbing Restrainers: Parameter Study on Small Systems," by G.H. Powell, C. Oughourlian and J. Simons - June 1980

UCB/EERC-80/07 "Inelastic Torsional Response of Structures Subjected to Earthquake Ground Motions," by Y. Yamazaki April 1980(PB81 122 327)A08

UCB/EERC-80/08 "Study of X-Braced Steel Frame Structures Under Earthquake Simulation," by Y. Ghanaat - April 1980 (PB81 122 335)A11

UCB/EERC-80/09 "Hybrid Modelling of Soil-Structure Interaction," by S. Gupta, T.W. Lin, J. Penzien and C.S. Yeh May 1980(PB81 122 319)A07

UCB/EERC-80/10 "General Applicability of a Nonlinear Model of a One Story Steel Frame," by B.I. Sveinsson and H.D. McNiven - May 1980(PB81 124 877)A06

UCB/EERC-80/11 "A Green-Function Method for Wave Interaction with a Submerged Body," by W. Kioka - April 1980 (PB81 122 269)A07

UCB/EERC-80/12 "Hydrodynamic Pressure and Added Mass for Axisymmetric Bodies," by F. Nilrat - May 1980(PB81 122 343)A08

UCB/EERC-80/13 "Treatment of Non-Linear Drag Forces Acting on Offshore Platforms," by B.V. Dao and J. Penzien May 1980(PB81 153 413)A07

UCB/EERC-80/14 "2D Plane/Axisymmetric Solid Element (Type 3 - Elastic or Elastic-Perfectly Plastic) for the ANSR-II Program," by D.P. Mondkar and G.H. Powell - July 1980(PB81 122 350)A03

UCB/EERC-80/15 "A Response Spectrum Method for Random Vibrations," by A. Der Kiureghian - June 1980(PB81 122 301)A03

UCB/EERC-80/16 "Cyclic Inelastic Buckling of Tubular Steel Braces," by V.A. Zayas, E.P. Popov and S.A. Mahin June 1980(PB81 124 885)A10

UCB/EERC-80/17 "Dynamic Response of Simple Arch Dams Including Hydrodynamic Interaction," by C.S. Porter and A.K. Chopra - July 1980(PB81 124 000)A13

UCB/EERC-80/18 "Experimental Testing of a Friction Damped Aseismic Base Isolation System with Fail-Safe Characteristics," by J.M. Kelly, K.E. Beucke and M.S. Skinner - July 1980(PB81 148 595)A04

UCB/EERC-80/19 "The Design of Steel Energy-Absorbing Restrainers and their Incorporation into Nuclear Power Plants for Enhanced Safety (Vol 1B): Stochastic Seismic Analyses of Nuclear Power Plant Structures and Piping Systems Subjected to Multiple Support Excitations," by M.C. Lee and J. Penzien - June 1980

UCB/EERC-80/20 "The Design of Steel Energy-Absorbing Restrainers and their Incorporation into Nuclear Power Plants for Enhanced Safety (Vol 1C): Numerical Method for Dynamic Substructure Analysis," by J.M. Dickens and E.L. Wilson - June 1980

UCB/EERC-80/21 "The Design of Steel Energy-Absorbing Restrainers and their Incorporation into Nuclear Power Plants for Enhanced Safety (Vol 2): Development and Testing of Restraints for Nuclear Piping Systems," by J.M. Kelly and M.S. Skinner - June 1980

UCB/EERC-80/22 "3D Solid Element (Type 4-Elastic or Elastic-Perfectly-Plastic) for the ANSR-II Program," by D.P. Mondkar and G.H. Powell - July 1980(PB81 123 242)A03

UCB/EERC-80/23 "Gap-Friction Element (Type 5) for the ANSR-II Program," by D.P. Mondkar and G.H. Powell - July 1980 (PB81 122 285)A03

UCB/EERC-80/24 "U-Bar Restraint Element (Type 11) for the ANSR-II Program," by C. Oughourlian and G.H. Powell July 1980(PB81 122 293)A03

UCB/EERC-80/25 "Testing of a Natural Rubber Base Isolation System by an Explosively Simulated Earthquake," by J.M. Kelly - August 1980(PB81 201 360)A04

UCB/EERC-80/26 "Input Identification from Structural Vibrational Response," by Y. Hu - August 1980(PB81 152 308)A05

UCB/EERC-80/27 "Cyclic Inelastic Behavior of Steel Offshore Structures," by V.A. Zayas, S.A. Mahin and E.P. Popov August 1980(PB81 196 180)A15

UCB/EERC-80/28 "Shaking Table Testing of a Reinforced Concrete Frame with Biaxial Response," by M.G. Oliva October 1980(PB81 154 304)A10

UCB/EERC-80/29 "Dynamic Properties of a Twelve-Story Prefabricated Panel Building," by J.G. Bouwkamp, J.P. Kollegger and R.M. Stephen - October 1980(PB82 117 128)A06

UCB/EERC-80/30 "Dynamic Properties of an Eight-Story Prefabricated Panel Building," by J.G. Bouwkamp, J.P. Kollegger and R.M. Stephen - October 1980(PB81 200 313)A05

UCB/EERC-80/31 "Predictive Dynamic Response of Panel Type Structures Under Earthquakes," by J.P. Kollegger and J.G. Bouwkamp - October 1980(PB81 152 316)A04

UCB/EERC-80/32 "The Design of Steel Energy-Absorbing Restrainers and their Incorporation into Nuclear Power Plants for Enhanced Safety (Vol 3): Testing of Commercial Steels in Low-Cycle Torsional Fatigue," by P. Spencer, E.R. Parker, E. Jongewaard and M. Drory

UCB/EERC-80/33 "The Design of Steel Energy-Absorbing Restrainers and their Incorporation into Nuclear Power Plants for Enhanced Safety (Vol 4): Shaking Table Tests of Piping Systems with Energy-Absorbing Restrainers," by S.F. Stiemer and W.G. Godden - Sept. 1980

UCB/EERC-80/34 "The Design of Steel Energy-Absorbing Restrainers and their Incorporation into Nuclear Power Plants for Enhanced Safety (Vol 5): Summary Report," by P. Spencer

UCB/EERC-80/35 "Experimental Testing of an Energy-Absorbing Base Isolation System," by J.M. Kelly, M.S. Skinner and K.E. Beucke - October 1980(PB81 154 072)A04

UCB/EERC-80/36 "Simulating and Analyzing Artificial Non-Stationary Earthquake Ground Motions," by R.F. Nau, R.M. Oliver and K.S. Pister - October 1980(PB81 153 397)A04

UCB/EERC-80/37 "Earthquake Engineering at Berkeley - 1980," - Sept. 1980(PB81 205 874)A09

UCB/EERC-80/38 "Inelastic Seismic Analysis of Large Panel Buildings," by V. Schricker and G.H. Powell - Sept. 1980 (PB81 154 338)A13

UCB/EERC-80/39 "Dynamic Response of Embankment, Concrete-Gravity and Arch Dams Including Hydrodynamic Interaction," by J.F. Hall and A.K. Chopra - October 1980(PB81 152 324)A11

UCB/EERC-80/40 "Inelastic Buckling of Steel Struts Under Cyclic Load Reversal," by R.G. Black, W.A. Wenger and E.P. Popov - October 1980(PB81 154 312)A08

UCB/EERC-80/41 "Influence of Site Characteristics on Building Damage During the October 3, 1974 Lima Earthquake," by P. Repetto, I. Arango and H.B. Seed - Sept. 1980(PB81 161 739)A05

UCB/EERC-80/42 "Evaluation of a Shaking Table Test Program on Response Behavior of a Two Story Reinforced Concrete Frame," by J.M. Blondet, R.W. Clough and S.A. Mahin

UCB/EERC-80/43 "Modelling of Soil-Structure Interaction by Finite and Infinite Elements," by F. Medina - December 1980(PB81 229 270)A04

UCB/EERC-81/01 "Control of Seismic Response of Piping Systems and Other Structures by Base Isolation," edited by J.M. Kelly - January 1981 (PB81 200 735)A05

UCB/EERC-81/02 "OPTNSR - An Interactive Software System for Optimal Design of Statically and Dynamically Loaded Structures with Nonlinear Response," by M.A. Bhatti, V. Ciampi and K.S. Pister - January 1981 (PB81 218 851)A09

UCB/EERC-81/03 "Analysis of Local Variations in Free Field Seismic Ground Motions," by J.-C. Chen, J. Lysmer and H.B. Seed - January 1981 (AD-A099508)A13

UCB/EERC-81/04 "Inelastic Structural Modeling of Braced Offshore Platforms for Seismic Loading," by V.A. Zayas, P.-S.B. Shing, S.A. Mahin and E.P. Popov - January 1981(PB82 138 777)A07

UCB/EERC-81/05 "Dynamic Response of Light Equipment in Structures," by A. Der Kiureghian, J.L. Sackman and B. Nour-Omid - April 1981 (PB81 218 497)A04

UCB/EERC-81/06 "Preliminary Experimental Investigation of a Broad Base Liquid Storage Tank," by J.G. Bouwkamp, J.P. Kollegger and R.M. Stephen - May 1981(PB82 140 385)A03

UCB/EERC-81/07 "The Seismic Resistant Design of Reinforced Concrete Coupled Structural Walls," by A.E. Aktan and V.V. Bertero - June 1981(PB82 113 358)A11

UCB/EERC-81/08 "The Undrained Shearing Resistance of Cohesive Soils at Large Deformations," by M.R. Pyles and H.B. Seed - August 1981

UCB/EERC-81/09 "Experimental Behavior of a Spatial Piping System with Steel Energy Absorbers Subjected to a Simulated Differential Seismic Input," by S.F. Stiemer, W.G. Godden and J.M. Kelly - July 1981

UCB/EERC-81/10 "Evaluation of Seismic Design Provisions for Masonry in the United States," by B.I. Sveinsson, R.L. Mayes and H.D. McNiven - August 1981 (PB82 166 075)A08

UCB/EERC-81/11 "Two-Dimensional Hybrid Modelling of Soil-Structure Interaction," by T.-J. Tzong, S. Gupta and J. Penzien - August 1981(PB82 142 118)A04

UCB/EERC-81/12 "Studies on Effects of Infills in Seismic Resistant R/C Construction," by S. Brokken and V.V. Bertero - September 1981 (PB82 166 190)A09

UCB/EERC-81/13 "Linear Models to Predict the Nonlinear Seismic Behavior of a One-Story Steel Frame," by H. Valdimarsson, A.H. Shah and H.D. McNiven - September 1981(PB82 138 793)A07

UCB/EERC-81/14 "TLUSH: A Computer Program for the Three-Dimensional Dynamic Analysis of Earth Dams," by T. Kagawa, L.H. Mejia, H.B. Seed and J. Lysmer - September 1981(PB82 139 940)A06

UCB/EERC-81/15 "Three Dimensional Dynamic Response Analysis of Earth Dams," by L.H. Mejia and H.B. Seed - September 1981 (PB82 137 274)A12

UCB/EERC-81/16 "Experimental Study of Lead and Elastomeric Dampers for Base Isolation Systems," by J.M. Kelly and S.B. Hodder - October 1981 (PB82 166 182)A05

UCB/EERC-81/17 "The Influence of Base Isolation on the Seismic Response of Light Secondary Equipment," by J.M. Kelly - April 1981 (PB82 255 266)A04

UCB/EERC-81/18 "Studies on Evaluation of Shaking Table Response Analysis Procedures," by J. Marcial Blondet - November 1981 (PB82 197 278)A10

UCB/EERC-81/19 "DELIGHT.STRUCT: A Computer-Aided Design Environment for Structural Engineering," by R.J. Balling, K.S. Pister and E. Polak - December 1981 (PB82 218 496)A07

UCB/EERC-81/20 "Optimal Design of Seismic-Resistant Planar Steel Frames," by R.J. Balling, V. Ciampi, K.S. Pister and E. Polak - December 1981 (PB82 220 179)A07

UCB/EERC-82/01 "Dynamic Behavior of Ground for Seismic Analysis of Lifeline Systems," by T. Sato and A. Der Kiureghian - January 1982 (PB82 218 926)A05

UCB/EERC-82/02 "Shaking Table Tests of a Tubular Steel Frame Model," by Y. Ghanaat and R. W. Clough - January 1982 (PB82 220 161)A07

UCB/EERC-82/03 "Behavior of a Piping System under Seismic Excitation: Experimental Investigations of a Spatial Piping System supported by Mechanical Shock Arrestors and Steel Energy Absorbing Devices under Seismic Excitation," by S. Schneider, H.-M. Lee and W. G. Godden - May 1982 (PB83 172 544)A09

UCB/EERC-82/04 "New Approaches for the Dynamic Analysis of Large Structural Systems," by E. L. Wilson - June 1982 (PB83 148 080)A05

UCB/EERC-82/05 "Model Study of Effects of Damage on the Vibration Properties of Steel Offshore Platforms," by F. Shahrivar and J. G. Bouwkamp - June 1982 (PB83 148 742)A10

UCB/EERC-82/06 "States of the Art and Practice in the Optimum Seismic Design and Analytical Response Prediction of R/C Frame-Wall Structures," by A. E. Aktan and V. V. Bertero - July 1982 (PB83 147 736)A05

UCB/EERC-82/07 "Further Study of the Earthquake Response of a Broad Cylindrical Liquid-Storage Tank Model," by G. C. Manos and R. W. Clough - July 1982 (PB83 147 744)A11

UCB/EERC-82/08 "An Evaluation of the Design and Analytical Seismic Response of a Seven Story Reinforced Concrete Frame - Wall Structure," by F. A. Charney and V. V. Bertero - July 1982(PB83 157 628)A09

UCB/EERC-82/09 "Fluid-Structure Interactions: Added Mass Computations for Incompressible Fluid," by J. S.-H. Kuo - August 1982 (PB83 156 281)A07

UCB/EERC-82/10 "Joint-Opening Nonlinear Mechanism: Interface Smeared Crack Model," by J. S.-H. Kuo - August 1982 (PB83 149 195)A05

UCB/EERC-82/11 "Dynamic Response Analysis of Techi Dam," by R. W. Clough, R. M. Stephen and J. S.-H. Kuo - August 1982 (PB83 147 496)A06

UCB/EERC-82/12 "Prediction of the Seismic Responses of R/C Frame-Coupled Wall Structures," by A. E. Aktan, V. V. Bertero and M. Piazza - August 1982 (PB83 149 203)A09

UCB/EERC-82/13 "Preliminary Report on the SMART 1 Strong Motion Array in Taiwan," by B. A. Bolt, C. H. Loh, J. Penzien, Y. B. Tsai and Y. T. Yeh - August 1982 (PB83 159 400)A10

UCB/EERC-82/14 "Shaking-Table Studies of an Eccentrically X-Braced Steel Structure," by M. S. Yang - September 1982 (PB83 260 778)A12

UCB/EERC-82/15 "The Performance of Stairways in Earthquakes," by C. Roha, J. W. Axley and V. V. Bertero - September 1982 (PB83 157 693)A07

UCB/EERC-82/16 "The Behavior of Submerged Multiple Bodies in Earthquakes," by W.-G. Liao - Sept. 1982 (PB83 158 709)A07

UCB/EERC-82/17 "Effects of Concrete Types and Loading Conditions on Local Bond-Slip Relationships," by A. D. Cowell, E. P. Popov and V. V. Bertero - September 1982 (PB83 153 577)A04

UCB/EERC-82/18 "Mechanical Behavior of Shear Wall Vertical Boundary Members: An Experimental Investigation," by M. T. Wagner and V. V. Bertero - October 1982 (PB83 159 764)A05

UCB/EERC-82/19 "Experimental Studies of Multi-support Seismic Loading on Piping Systems," by J. M. Kelly and A. D. Cowell - November 1982

UCB/EERC-82/20 "Generalized Plastic Hinge Concepts for 3D Beam-Column Elements," by P. F.-S. Chen and G. H. Powell - November 1982 (PB83 247 981)A13

UCB/EERC-82/21 "ANSR-III: General Purpose Computer Program for Nonlinear Structural Analysis," by C. V. Oughourlian and G. H. Powell - November 1982 (PB83 251 330)A12

UCB/EERC-82/22 "Solution Strategies for Statically Loaded Nonlinear Structures," by J. W. Simons and G. H. Powell - November 1982 (PB83 197 970)A06

UCB/EERC-82/23 "Analytical Model of Deformed Bar Anchorages under Generalized Excitations," by V. Ciampi, R. Eligehausen, V. V. Bertero and E. P. Popov - November 1982 (PB83 169 532)A06

UCB/EERC-82/24 "A Mathematical Model for the Response of Masonry Walls to Dynamic Excitations," by H. Sucuoğlu, Y. Mengi and H. D. McNiven - November 1982 (PB83 169 011)A07

UCB/EERC-82/25 "Earthquake Response Considerations of Broad Liquid Storage Tanks," by F. J. Cambra - November 1982 (PB83 251 215)A09

UCB/EERC-82/26 "Computational Models for Cyclic Plasticity, Rate Dependence and Creep," by B. Mosaddad and G. H. Powell - November 1982 (PB83 245 829)A08

UCB/EERC-82/27 "Inelastic Analysis of Piping and Tubular Structures," by M. Mahasuverachai and G. H. Powell - November 1982 (PB83 249 987)A07

UCB/EERC-83/01 "The Economic Feasibility of Seismic Rehabilitation of Buildings by Base Isolation," by J. M. Kelly - January 1983 (PB83 197 988)A05

UCB/EERC-83/02 "Seismic Moment Connections for Moment-Resisting Steel Frames," by E. P. Popov - January 1983 (PB83 195 412)A04

UCB/EERC-83/03 "Design of Links and Beam-to-Column Connections for Eccentrically Braced Steel Frames," by E. P. Popov and J. O. Malley - January 1983 (PB83 194 811)A04

UCB/EERC-83/04 "Numerical Techniques for the Evaluation of Soil-Structure Interaction Effects in the Time Domain," by E. Bayo and E. L. Wilson - February 1983 (PB83 245 605)A09

UCB/EERC-83/05 "A Transducer for Measuring the Internal Forces in the Columns of a Frame-Wall Reinforced Concrete Structure," by R. Sause and V. V. Bertero - May 1983 (PB84 119 494)A06

UCB/EERC-83/06 "Dynamic Interactions between Floating Ice and Offshore Structures," by P. Croteau - May 1983 (PB84 119 486)A16

UCB/EERC-83/07 "Dynamic Analysis of Multiply Tuned and Arbitrarily Supported Secondary Systems," by T. Igusa and A. Der Kiureghian - June 1983 (PB84 118 272)A11

UCB/EERC-83/08 "A Laboratory Study of Submerged Multi-body Systems in Earthquakes," by G. R. Ansari - June 1983 (PB83 261 842)A17

UCB/EERC-83/09 "Effects of Transient Foundation Uplift on Earthquake Response of Structures," by C.-S. Yim and A. K. Chopra - June 1983 (PB83 261 396)A07

UCB/EERC-83/10 "Optimal Design of Friction-Braced Frames under Seismic Loading," by M. A. Austin and K. S. Pister - June 1983 (PB84 119 288)A06

UCB/EERC-83/11 "Shaking Table Study of Single-Story Masonry Houses: Dynamic Performance under Three Component Seismic Input and Recommendations," by G. C. Manos, R. W. Clough and R. L. Mayes - June 1983

UCB/EERC-83/12 "Experimental Error Propagation in Pseudodynamic Testing," by P. B. Shing and S. A. Mahin - June 1983 (PB84 119 270)A09

UCB/EERC-83/13 "Experimental and Analytical Predictions of the Mechanical Characteristics of a 1/5-scale Model of a 7-story R/C Frame-Wall Building Structure," by A. E. Aktan, V. V. Bertero, A. A. Chowdhury and T. Nagashima - August 1983 (PB84 119 213)A07

UCB/EERC-83/14 "Shaking Table Tests of Large-Panel Precast Concrete Building System Assemblages," by M. G. Oliva and R. W. Clough - August 1983

UCB/EERC-83/15 "Seismic Behavior of Active Beam Links in Eccentrically Braced Frames," by K. D. Hjelmstad and E. P. Popov - July 1983 (PB84 119 676)A09

UCB/EERC-83/16 "System Identification of Structures with Joint Rotation," by J. S. Dimsdale and H. D. McNiven - July 1983

UCB/EERC-83/17 "Construction of Inelastic Response Spectra for Single-Degree-of-Freedom Systems," by S. Mahin and J. Lin - July 1983

UCB/EERC-83/18 "Interactive Computer Analysis Methods for Predicting the Inelastic Cyclic Behaviour of Structural Sections," by S. Kaba and S. Mahin - July 1983 (PB84 192 012) A06

UCB/EERC-83/19 "Effects of Bond Deterioration on Hysteretic Behavior of Reinforced Concrete Joints," by F.C. Filippou, E.P. Popov and V.V. Bertero - August 1983 (PB84 192 020) A10

UCB/EERC-83/20 "Analytical and Experimental Correlation of Large-Panel Precast Building System Performance," by M.G. Oliva, R.W. Clough, M. Velkov, P. Gavrilovic and J. Petrovski - November 1983

UCB/EERC-83/21 "Mechanical Characteristics of Materials Used in a 1/5 Scale Model of a 7-Story Reinforced Concrete Test Structure," by V.V. Bertero, A.E. Aktan, H.G. Harris and A.A. Chowdhury - September 1983 (PB84 193 697) A05

UCB/EERC-83/22 "Hybrid Modelling of Soil-Structure Interaction in Layered Media," by T.-J. Tzong and J. Penzien - October 1983 (PB84 192 178) A08

UCB/EERC-83/23 "Local Bond Stress-Slip Relationships of Deformed Bars under Generalized Excitations," by R. Eligehausen, E.P. Popov and V.V. Bertero - October 1983 (PB84 192 848) A09

UCB/EERC-83/24 "Design Considerations for Shear Links in Eccentrically Braced Frames," by J.O. Malley and E.P. Popov - November 1983 (PB84 192 186) A07

UCB/EERC-84/01 "Pseudodynamic Test Method for Seismic Performance Evaluation: Theory and Implementation," by P.-S. B. Shing and S. A. Mahin - January 1984 (PB84 190 644) A08

UCB/EERC-84/02 "Dynamic Response Behavior of Xiang Hong Dian Dam," by R.W. Clough, K.-T. Chang, H.-Q. Chen, R.M. Stephen, G.-L. Wang, and Y. Ghanaat - April 1984

UCB/EERC-84/03 "Refined Modelling of Reinforced Concrete Columns for Seismic Analysis," by S.A. Kaba and S.A. Mahin - April, 1984

UCB/EERC-84/04 "A New Floor Response Spectrum Method for Seismic Analysis of Multiply Supported Secondary Systems," by A. Asfura and A. Der Kiureghian - June 1984

UCB/EERC-84/05 "Earthquake Simulation Tests and Associated Studies of a 1/5th-scale Model of a 7-Story R/C Frame-Wall Test Structure," by V.V. Bertero, A.E. Aktan, F.A. Charney and R. Sause - June 1984

UCB/EERC-84/06 "R/C Structural Walls: Seismic Design for Shear," by A.E. Aktan and V.V. Bertero

UCB/EERC-84/07 "Behavior of Interior and Exterior Flat-Plate Connections subjected to Inelastic Load Reversals," by H.L. Zee and J.P. Moehle

UCB/EERC-84/08 "Experimental Study of the Seismic Behavior of a two-story Flat-Plate Structure," by J.W. Diebold and J.P. Moehle

UCB/EERC-84/09 "Phenomenological Modeling of Steel Braces under Cyclic Loading," by K. Ikeda, S.A. Mahin and S.N. Dermitzakis - May 1984

UCB/EERC-84/10 "Earthquake Analysis and Response of Concrete Gravity Dams," by G. Fenves and A.K. Chopra - August 1984

UCB/EERC-84/11 "EAGD-84: A Computer Program for Earthquake Analysis of Concrete Gravity Dams," by G. Fenves and A.K. Chopra - August 1984

UCB/EERC-84/12 "A Refined Physical Theory Model for Predicting the Seismic Behavior of Braced Steel Frames," by K. Ikeda and S.A. Mahin - July 1984

UCB/EERC-84/13 "Earthquake Engineering Research at Berkeley - 1984" - August 1984

UCB/EERC-84/14 "Moduli and Damping Factors for Dynamic Analyses of Cohesionless Soils," by H.B. Seed, R.T. Wong, I.M. Idriss and K. Tokimatsu - September 1984

UCB/EERC-84/15 "The Influence of SPT Procedures in Soil Liquefaction Resistance Evaluations," by H. B. Seed, K. Tokimatsu, L. F. Harder and R. M. Chung - October 1984

UCB/EERC-84/16 "Simplified Procedures for the Evaluation of Settlements in Sands Due to Earthquake Shaking," by K. Tokimatsu and H. B. Seed - October 1984

UCB/EERC-84/17 "Evaluation and Improvement of Energy Absorption Characteristics of Bridges under Seismic Conditions," by R. A. Imbsen and J. Penzien - November 1984

UCB/EERC-84/18 "Structure-Foundation Interactions under Dynamic Loads," by W. D. Liu and J. Penzien - November 1984

UCB/EERC-84/19 "Seismic Modelling of Deep Foundations," by C.-H. Chen and J. Penzien - November 1984

UCB/EERC-84/20 "Dynamic Response Behavior of Quan Shui Dam," by R. W. Clough, K.-T. Chang, H.-Q. Chen, R. M. Stephen, Y. Ghanaat, and J.-H. Qi - November 1984